Universitat Autònoma de Barcelona

LASER COOKING SYSTEM APPLIED TO A 3D FOOD PRINTING DEVICE

Alvar Gràcia Julià

Universitat Autònoma de Barcelona

Departament de Ciència Animal i dels Aliments

Facultat de Veterinària

LASER COOKING SYSTEM APPLIED TO A 3D FOOD PRINTING DEVICE

Memòria presentada per a optar al grau de
Doctor en Ciència dels Aliments

Doctorand:

Alvar Gràcia Julià
Departament de Ciència Animal i dels Aliments
Universitat Autònoma de Barcelona

Directora i tutora:

Dra. Marta Capellas Puig
Departament de Ciència Animal i dels Aliments
Universitat Autònoma de Barcelona

Director:

Dr. Joaquim Rigola Serrano
Departament de Màquines i Motors Tèrmics
Universitat Politècnica de Catalunya

Bellaterra (Cerdanyola del Vallès), febrer del 2019

Aquesta tesi s'ha realitzat mitjançant l'ajut concedit per l'Agència de Gestió d'Ajuts Universitaris i de Recerca de la Generalitat de Catalunya, en el marc del programa de Doctorat Industrial entre la Universitat Autònoma de Barcelona i l'empresa 2 Vegan Natural Machines (2013-DI-063).

Als meus pares, Jesús i Joana

A la Bea i als nostres fills Maria i Gerard

"Lo que está abajo es como lo que está arriba, y lo que está arriba es como lo que está abajo, para que se obren los milagros de una sola cosa"

"Separa la Tierra del Fuego, y lo sutil de lo grueso, suavemente y con todo cuidado"

Hermes

Au som deu malh, que i a ua lutz,
Qu'i cau guardar los uelhs dessús,
Que'ns cau traucar tot lo segàs,
Tà ns'arrapar, sonque las mans,
Après lo malh, un aute malh,
Après la lutz, ua auta lutz,
Haut, Peiròt, vam caminar,
De cap tà l'immortèla

Nadau

AGRAÏMENTS

Després de 5 anys de doctorat i de grans dosis de paciència per part de la Marta Capellas, de tots els meus companys de Natural Machines i de la família, he pogut completar la present tesi, que desitjo pugui contribuir a establir la cocció per làser com un nou sistema per a cuinar aliments de manera eficient i segura.

En primer lloc, vull agrair tot el suport demostrat des del principi i fins el darrer moment per la Marta Capellas, que m'ha acompanyat en aquesta aventura de la cocció per làser. Gràcies per la teva direcció i contribució científica, sempre has estat al meu costat en tot moment. Gràcies per la teva perfecció i la voluntat de fer la feina ben feta. Ja t'ho han dit abans, ets una gran directora de tesi!

Desitjaria agrair al Quim Rigola el seu consell i dedicació en la modelització matemàtica de la cocció làser, que ens ha permès anar més enllà del laboratori, i desenvolupar una eina de simulació capaç d'establir les temperatures de cocció en diferents aliments...sense usar el termòmetre. Gràcies sempre per la teva bona disposició, criteri científic i bon humor!

Gràcies a la Begoña Miñarro que em va acompanyar en els primers passos de la tesi i que, juntament amb la Marta i l'equip de Natural Machines, van demanar l'ajut a l'AGAUR pel programa de doctorat industrial. I el més important, van creure en mi com a candidat.

Vull agrair especialment al Dr. Eugenio Schillacci per tota la seva contribució en el disseny i validació de la modelització de la transferència del calor del sistema làser. Gràcies per la teva valuosa dedicació!

Gràcies als responsables de Natural Machines, Emilio Sepúlveda i Lynette Kucsma, per l'oportunitat de realitzar aquest doctorat industrial, pels mitjans que m'han proveït per a dur-lo a terme i, sobretot, per la gran satisfacció d'incorporar a curt termini la cocció per làser en la Foodini. Aquesta perspectiva és l'objectiu que justifica un doctorat industrial. I, més enllà del doctorat, gràcies també per permetre continuar formant part del projecte de NM!

He de donar les gràcies a tots els meus col·legues de NM: Enric, Víctor, Joan, Xavi, Adri, Alba, Naoufal, Pere, Rosa, Armando, Marta...gràcies a tots per la vostra

col·laboració i pels grans moments viscuts en el muntatge de l'equip làser de Foodini. NM, Foodini i la impressió 3D d'aliments tenen un gran equip!

Gràcies al Víctor Socias i a l'Albert Gil per obrir-me les portes de Laser Project i dur a terme les primers proves de cocció làser amb els seus equips Epilog. Amb la seva generositat i bones vibracions es va iniciar l'èxit d'aquest projecte.

Gràcies a la Dra. Montserrat Serra Milà per col·laborar en aquest projecte mitjançant els tests que es van realitzar amb els equips de Làser Mèdic - Clínica Tres Torres.

Gràcies a tots aquells que m'han ajudat durant les llargues hores del treball experimental al laboratori, al Marc, la Camila, la Rocío, la Pamela, la Dolo, l'Anthea, la Mirte i la Judit. Sempre recordaré la vostra inestimable companyia i afany.

Gràcies també a la Montse, pels seus bons consells sobre la cocció de carn i hamburgueses.

Gràcies a la Sònia, per la seva gran estima i recolzament en el laboratori durant tots aquest anys.

Gràcies a l'Alícia i a la Idoia, per la seva amistat i suport.

Gràcies a tots els doctorands que m'han precedit i m'han acompanyat, a la Sonia, a l'Advelí, al Jezer, a la Carol, a la Maria, a l'Alfons, al Johnny, a l'Ulises, al Daniel, a la Cris, a l'Òscar, a l'Arnau, a l'Ashraf, la Noemí, ...sempre us recordaré.

Gràcies també a tots els professors i tècnics del departament. Gràcies per les converses al passadís, pel bon humor, gràcies pels milers de "bon dia", "bon cap de setmana", "bones vacances"... i gràcies per fer que el dia a dia sigui més fàcil amb vosaltres.

Gràcies a la Bibi pel seus bons consells i exemple de treball.

Gràcies al Joan Miquel i al Ramon per les grans converses a la planta, durant el temps que vaig estar treballant amb el primer sistema làser, i de totes les bones hamburgueses que es van cuinar i menjar.

Gràcies també a l'equip de l'AGAUR per la seva col·laboració durant la tesi, amb tots els retards i les dificultats que es succeeixen en el mon de la innovació tecnològica. El resultat final, amb una nova aplicació industrial, ha valgut la pena.

I per últim, recordar i agrair el suport a tota la meva família i amics. Als meus pares Jesús i Joana, i als meus germans Jesús, Lluís i Sergi que sempre pregunten "per quan la tesi?"...i com a enginyer o tecnòleg sempre responia "...aviat, aviat". Gràcies per existir! Doncs finalment ja la tenim aquí.

I l'agraïment més important de tots, per tot el seu amor, alegria , innocència i comprensió , a la Bea i als meus fills Maria i Gerard. Aquest treball també està dedicat a vosaltres tres. Bea, gràcies per tot el teu temps i pel recolzament durant les absències d'aquests darrers temps, que segur ens faran guanyar noves vivències, gràcies per escoltar-me i per estimar-me. I gràcies a la Maria per animar-me a passar-m'ho bé i gaudir "amb les meves cosetes i amb les meves maquinetes". I a tu Gerard per tots els teus somriures i per recordar-me cada dia que el més important es tornar a casa.

I per últims recordar a aquells amics que ja no estan aquí, aquells que han marxat durant el període de la tesi, al Roque i al Pablo. Amics, ens retrobem a on sempre neix el sol.

Patents related to this thesis:

- **Patent**

Title: Apparatus and method for heating and cooking food using laser beams and electromagnetic radiation.

Inventors: Alvar Gracia, Emilio Sepulveda.

Assignee: Natural Machines, Inc.

Priority date: 29/09/2014

Applications: EP3200612A4, US20170245682A1, JP2017532520A, CN107427044A, CA2961394A1, WO2016053681A1.

Abstract

An innovative cooking system based on infrared radiation (IR) using a CO_2 laser (CO_2 IR Laser) has been developed considering that water absorbance of electromagnetic infrared radiation at CO_2 laser wavelength is very high. The new cooking system has been adapted into a 3D food printer and has been designed with the following requirements: 1) ability to cook in a delimited area; 2) control of the cooking temperature; 3) physical dimensions that fit inside the 3D Food Printer; 4) energy consumption below the power supply limits; 5) software-controlled system; 6) versatility to cook while printing the food or to cook once the food is printed. In the present study, two CO_2 IR Laser cooking systems have been used and tested. The first CO_2 IR Laser cooking system studied was a laser engraver and cutter equipment in which specific conditions were applied to cook beef burgers, mashed potatoes bites and pizza dough. After, a new cooking system adapted to the 3D food printer was developed, consisting of a CO_2 laser lamp, a system of galvo mirrors that direct the laser beam to the cooking area, and a software that allowed controlling the position and the frequency of movement of galvanometers. With this new system, a chosen area could be homogenously cooked, due to the rapid movement of the galvo mirrors. The food products cooked inside the 3D food printer were: beef burgers; vegetarian patties prepared with legumes, vegetables and egg as main ingredients; and pizza dough. To demonstrate that cooking had been achieved, food products were cooked with the CO_2 IR laser systems and different traditional cooking systems (flat and barbeque grills; IR, convection, desk and microwave ovens). Microbiological, physico-chemical and sensory characteristics of the cooked foods were evaluated. The formation of polycyclic aromatic hydrocarbons was analyzed in beef burgers and pizzas to evaluate toxicological safety, and the thermal effect in the count reduction or survival of *Salmonella* Typhimurium, *Salmonella* Senftenberg and *Escherichia coli* O157:H7 inoculated in beef burgers and vegetarian patties was studied. Microbiological and toxicological analyses showed that food products cooked with the new CO_2 IR Laser system were as safe as food cooked with traditional methods. Sensory analyses showed that consumers had the same, or even higher, level of preference for foods cooked with CO_2 IR laser system in comparison with foods cooked with traditional methods. In addition, a numerical model based on computational fluid dynamics was developed to simulate the cooking process of beef burgers and vegetarian patties, and it was validated with experimental data of temperature evolution during the cooking process. The

numerical results for temperature evolution given by the model coincide with the experimental data, except for the first minutes of cooking. The numerical simulation model is a powerful tool to optimize the cooking process of the CO_2 IR Laser system. Based on the results obtained, future work will be carried out including cooking experimental studies with foods containing a significantly different composition; the simulation of the cooking process with different parametric conditions; and nutritional studies.

Resumen

Se ha desarrollado un sistema innovador de cocción de alimentos basado en el calentamiento por radiación infrarroja (IR) mediante un láser de CO_2 (IR Láser CO_2) teniendo en cuenta que el agua posee una elevada capacidad de absorción electromagnética en la longitud de onda del IR Láser CO_2. El sistema de cocción se ha adaptado en una impresora 3D de alimentos y se ha diseñado con los siguientes requerimientos: 1) cocción en un área delimitada; 2) capacidad de control de la temperatura de cocción; 3) las dimensiones físicas de la lámpara de CO_2 deben adaptarse a la impresora 3D de alimentos; 4) el consumo de energía debe ser compatible con la capacidad de la impresora 3D de alimentos; 5) el sistema debe ser controlado por software; 6) versatilidad para cocinar mientras se imprime el alimento o después de la impresión. En el presente estudio se han usado dos sistemas de cocción por IR Láser CO_2. Primero se usó una grabadora y cortadora con IR Láser CO_2 en la que se establecieron unas condiciones específicas que permitieron la cocción de hamburguesas de ternera, puré de patatas y masas de pizza. Después se desarrolló un nuevo sistema de cocción integrado en la impresora 3D de alimentos formado por una lámpara láser de CO_2, un sistema de galvos para dirigir el haz láser a la zona de cocción y un software que permitía controlar la posición y frecuencia del movimiento de los galvanómetros. Con este nuevo sistema se podía cocinar de manera homogénea un área determinada, debido al rápido movimiento de los espejos de los galvos. Se cocinaron los siguientes alimentos en el interior de la impresora 3D de alimentos: hamburguesas de carne de ternera; preparados vegetales tipo hamburguesas formuladas con legumbres, hortalizas y huevo como ingredientes principales; y bases de pizza. Para demostrar que la cocción fue adecuada y suficiente, la cocción mediante IR Láser CO_2 se comparó con diferentes sistemas de cocción tradicionales (plancha, barbacoa y hornos IR, de convección, de suela refractaria y microondas) y se evaluaron las características microbiológicas, físico-químicas y sensoriales de los alimentos cocidos. Se analizó la formación de hidrocarburos aromáticos policíclicos con el fin de evaluar la seguridad toxicológica, y se estudió el efecto térmico en la eliminación de *Salmonella* Typhimurium, *Salmonella* Senftenberg y *Escherichia coli* O157:H7 inoculadas en las hamburguesas de ternera y en los preparados vegetales. Los análisis microbiológicos y toxicológicos demostraron que los alimentos cocinados con el nuevo sistema IR Láser CO_2 son tan seguros como los cocinados con los métodos convencionales. Los análisis sensoriales indicaron que la preferencia de los consumidores

por los alimentos cocidos con IR Láser CO_2 fue igual o superior a la preferencia por los alimentos cocidos con los sistemas convencionales. Además, se desarrolló un modelo numérico basado en la dinámica computacional de fluidos para simular el proceso de cocción de las hamburguesas de ternera y los preparados vegetales y se validó con los resultados experimentales de aumento de temperatura durante el proceso de cocción. Los resultados numéricos de la evolución de la temperatura coincidieron con los datos experimentales, excepto durante los primeros minutos de la cocción. El modelo de simulación numérico se considera una potente herramienta para optimizar el proceso de cocción del sistema IR Láser CO_2. A partir de los resultados obtenidos se abren nuevas vías de trabajo, que incluyen estudios de cocción con alimentos de composición sensiblemente diferente a los probados hasta el momento; la simulación del proceso de cocción con diferentes parámetros y estrategias de cocción; y la realización de estudios nutricionales.

TABLE OF CONTENTS

Abbreviation Key

3D	3 dimensional
3DFP	3D FOOD PRINTING
IR	Infrared
BBQ	Barbeque
BGBL	Brilliant Green Bile Lactose
CFD	Computational Fluid Dynamics
CV	Control Volume
FDA	Food and Drug Administration
FIR	Far Infrared
FSAI	Food Safety Authority of Ireland
IR	Infrared
MIR	Mid Infrared
MPN	Most Probable Number
NIR	Near Infrared
NM	Natural Machines
PAHs	Polycyclic Aromatic Hydrocarbons
TSA	Tryptone Soya Agar
TSB	Tryptone Soya Broth
TPA	Texture Profile Analysis
UI/UX	User Interface/ User Experience
VRBA	Violet Red Bile Agar

CHAPTER 1

INTEREST OF THE STUDY, OBJECTIVES AND WORKING PLAN

1.1. Initial statement

2 Vegan Natural Machines (NM) is a company founded in October 2012 in Barcelona (Spain). NM defines itself as the maker of Foodini, a 3D food printing (3DFP) kitchen appliance that enables consumers to print food ingredients into precise portions and shapes. NM claims to be the first international designer and manufacturer of a 3D food printer that can be used for different food matrices (www.naturalmachines.com).

In 2014, NM in collaboration with the Department of Animal and Food Science of the Autonomous University of Barcelona (UAB, *Universitat Autònoma de Barcelona*) decided to apply for an industrial doctorate funded by the Catalan Government through the Agency of Management for University and Research Grants (AGAUR, *Agència de Gestió d'Ajuts Universitaris i de Recerca*). The initial aim of the industrial doctorate was to design food formulations with different ingredients for 3DFP. Once the thesis started in March 2014, the topic rapidly changed towards a cooking system development applied to a 3D food printer.

1.2. Interest of the study

Currently, the main commercial target of 3D food printers is focused into professional market (business to business, B2B). To access to consumer market (business to consumer, B2C), NM decided to increase the capabilities of the 3D food printer Foodini with the integration of an innovative cooking system. The ability of cooking has been identified by NM as the key factor that must be fully developed to become a main actor in the incipient 3DFP consumer market.

Cooking inside Foodini has several limitations that hinder the application of standard current cooking systems. In the inner chamber of Foodini, where 3D printing occurs, there are placed several elements such as capsule holders, mechanics of the extrusion system, different electronic-based control systems, 3D scanner, IR detection appliance, etc. Since this chamber is like an open environment where different systems interact, heating the whole area up to cooking temperatures (above 100°C) could deteriorate irreversibly some heat-sensitive elements. Standard cooking methods based on conduction, convection or radiation systems would require isolated chambers which cannot be adapted inside 3D Food Printer Foodini. Thus, a cooking system inside 3D food printer must guarantee that

electronic systems and internal materials and mechanisms are not affected during heating process. A new solution which would allow cooking in this specific environment had to be searched, tested and developed.

Previously to the design of the working plan, the requirements that a cooking method should have inside Foodini were identified:

i) ability to cook in a delimited area
ii) control of the cooking temperature
iii) physical dimensions that fit inside Foodini
iv) energy consumption below the power supply limits (≤ 1000 W)
v) software-controlled system
vi) versatility to cook while printing the food or to cook once the food is printed

A system which could be adapted to these conditions would be a laser-based method, specifically, a CO_2 IR laser. CO_2 laser wavelength (9.4 μm to 10.6 μm) is placed in the IR light spectra, then being another IR radiation cooking system with the advantage that a laser allows to control the energy in a delimited area, without damaging internal parts of Foodini. CO_2 IR laser beam could allow a cooking process focused on food. Moreover, water absorbance of electromagnetic IR radiation at 10.6 μm is very high.

As stated in the literature review, CO_2 laser equipments are a consolidated technology widely used in several industrial applications. It means that there are several manufacturers of CO_2 lasers and mirrors reflection systems, spare parts are easily accessible, and there is a high range of CO_2 lasers lamps with different radiation power, energy consumption and physical dimensions.

Considering all these statements, the following objectives are proposed in order to study the cooking effect of CO_2 IR lasers.

1.3. Objectives

1.3.1. General Objective

The general objective of the present work is to study the cooking effect of CO_2 IR lasers on different food matrices and design an innovative cooking system inside a 3D food printer.

1.3.2. Specific objectives

To achieve the general objective, specific objectives are defined:

- To study the cooking effect of different commercial available lasers. To accomplish this goal, physico-chemical, microbiological, toxicological and sensory characteristics of several food products cooked with IR laser and standard cooking methods are compared.
- To develop an innovative laser cooking method based on CO_2 IR lamp to cook inside 3D food printer Foodini, and to study and define the cooking conditions for this new integrated system.
- To develop a heat transfer numerical model for CO_2 IR laser radiation cooking system based on ray tracing method.

1.4. Working plan

Considering the requirements mentioned above, exploratory tests were carried out with three types of commercial equipment based on different IR laser wavelenghts. From this point, two main experimental studies were developed. The first experiment was carried out using a commercial laser cutter and engraver equipment (Epilog). Specific cooking conditions were stablished for beef burgers, pizza dough and mashed potatoes, and several parameters were measured to characterize laser cooking. The second experiment was designed to cook inside 3D Food Printer using an innovative engineering solution developed by Natural Machines. Beef burgers, vegetarian patties and pizza dough were cooked and analyzed. In the third study, the heat transfer inside beef burger and vegetarian patties, cooked by laser radiation, was mathematically modelized by ray tracing method.

Three studies were carried out to address the specific objectives:

Study 1: Cooking experiments with CO_2 IR laser Epilog equipment for beef burgers, pizza dough and mashed potatoes.

Study 2: Cooking experiments using a new CO_2 IR laser system integrated in 3D Foodini food printer for beef burgers, vegetarian patties and pizza dough.

Study 3: Numerical modeling by ray tracing method of the heat transfer inside beef burgers and vegetarian patties cooked by IR laser raditon.

The experimental design of the assays performed in the different works is schematically represented as follows:

- Fig. 2.1. Global working plan procedure.
- Fig. 2.2. Exploratory tests with IR lasers of several wavelenghts.
- Fig. 2.3. Cooking experiments with CO_2 IR laser Epilog equipment.
- Fig. 2.4. Analyses performed in cooking experiments with CO_2 IR laser Epilog equipment and beef burguer.
- Fig. 2.5. Analyses performed in cooking experiments with CO_2 IR laser Epilog equipment and pizza dough.

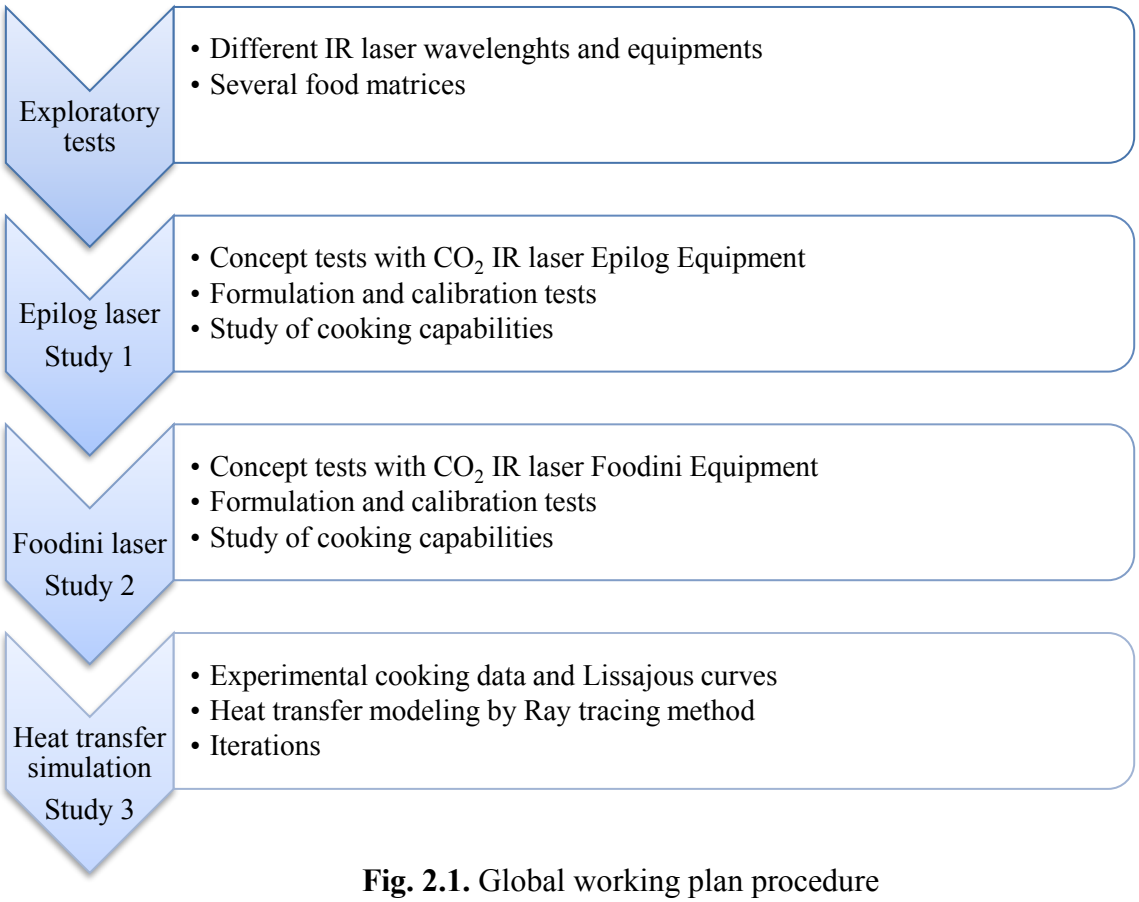

Fig. 2.1. Global working plan procedure

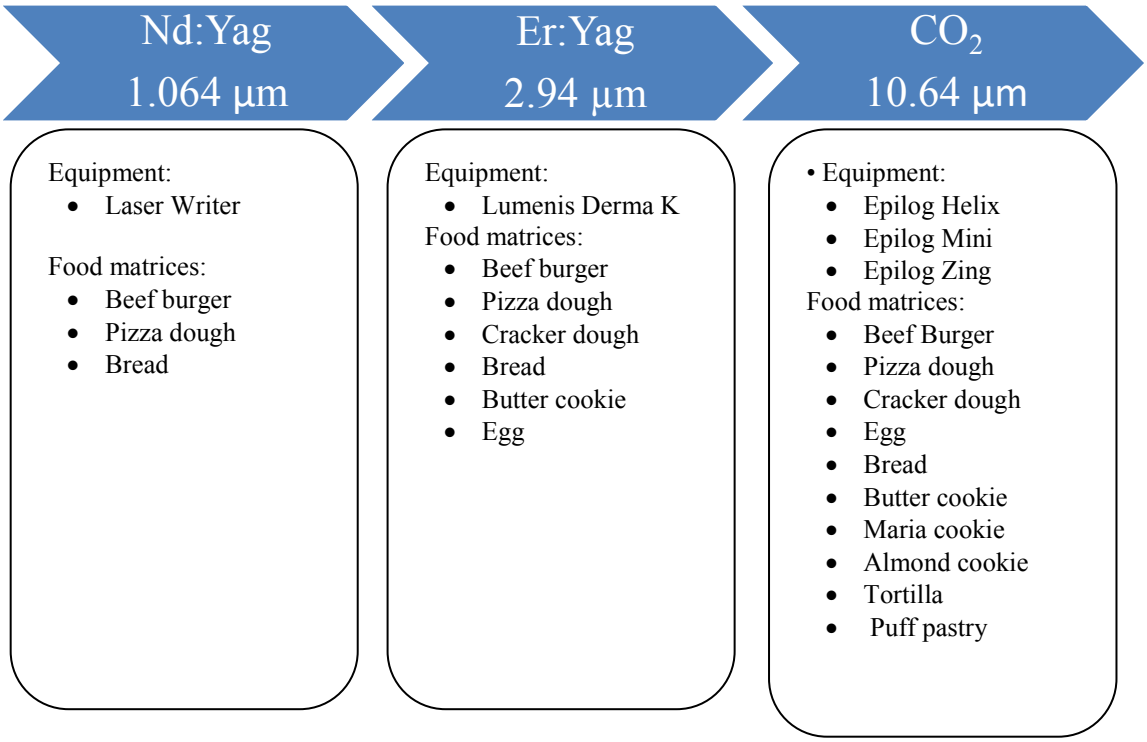

Fig. 2.2. Exporatory tests with IR lasers of several wavelenghts

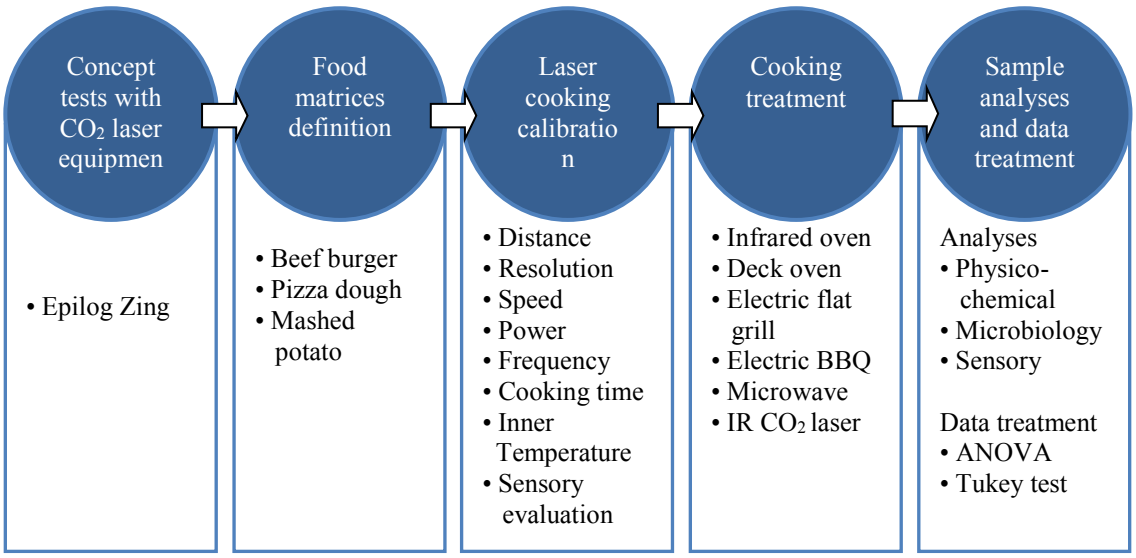

Fig. 2.3. Cooking experiments with CO_2 IR laser Epilog equipment

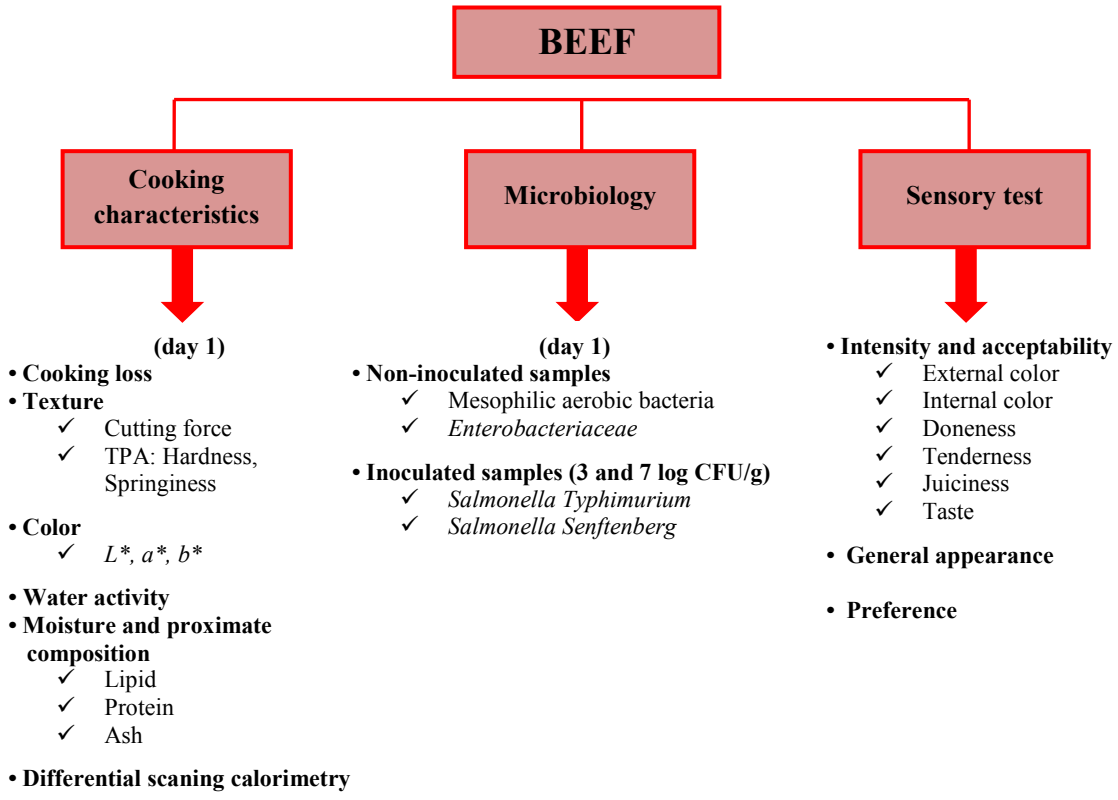

Fig. 2.4. Analyses performed in cooking experiments with CO_2 IR laser Epilog equipment and beef burguer

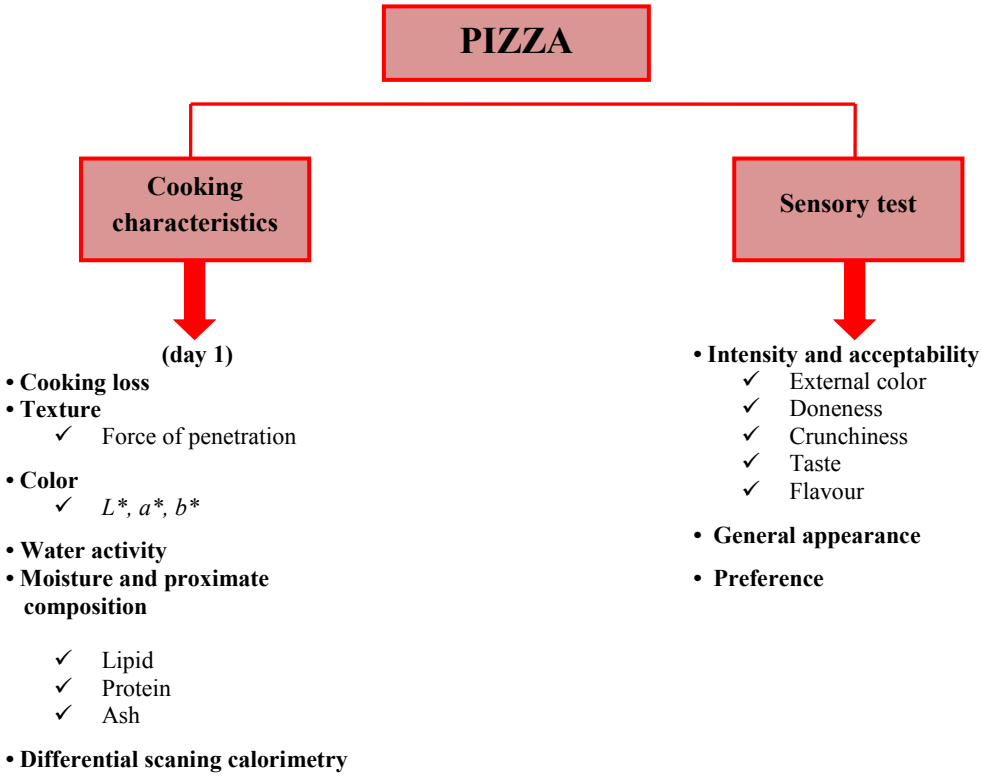

Fig. 2.5. Analyses performed in cooking experiments with CO_2 IR laser Epilog equipment and pizza dough

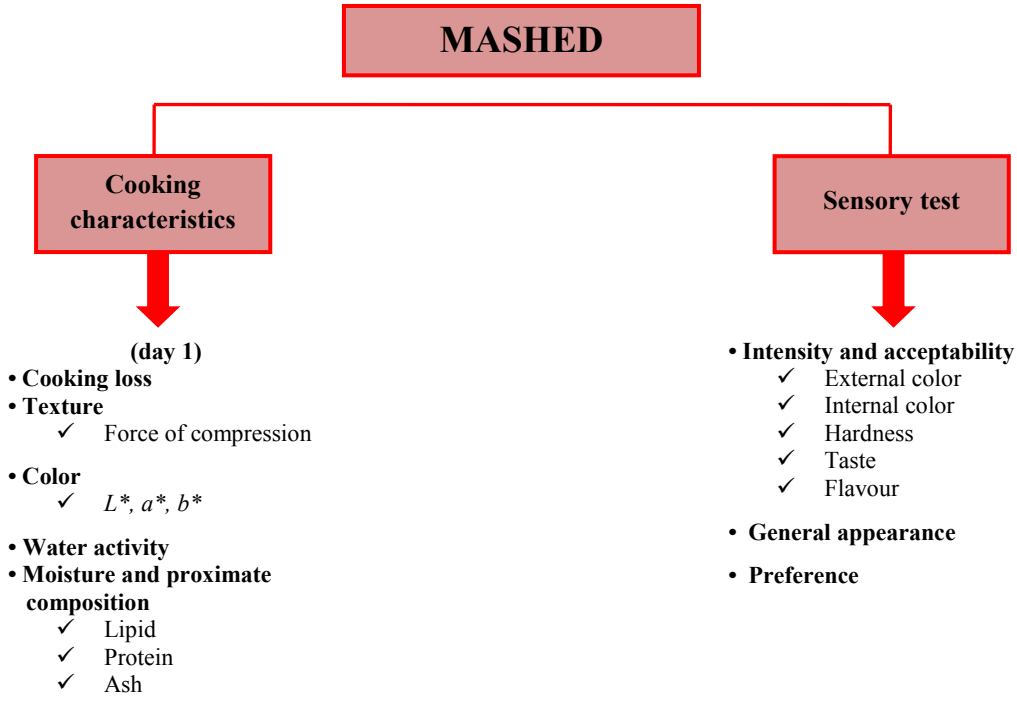

Fig. 2.6. Analyses performed in cooking experiments with CO_2 IR laser Epilog equipment and mashed potatoes

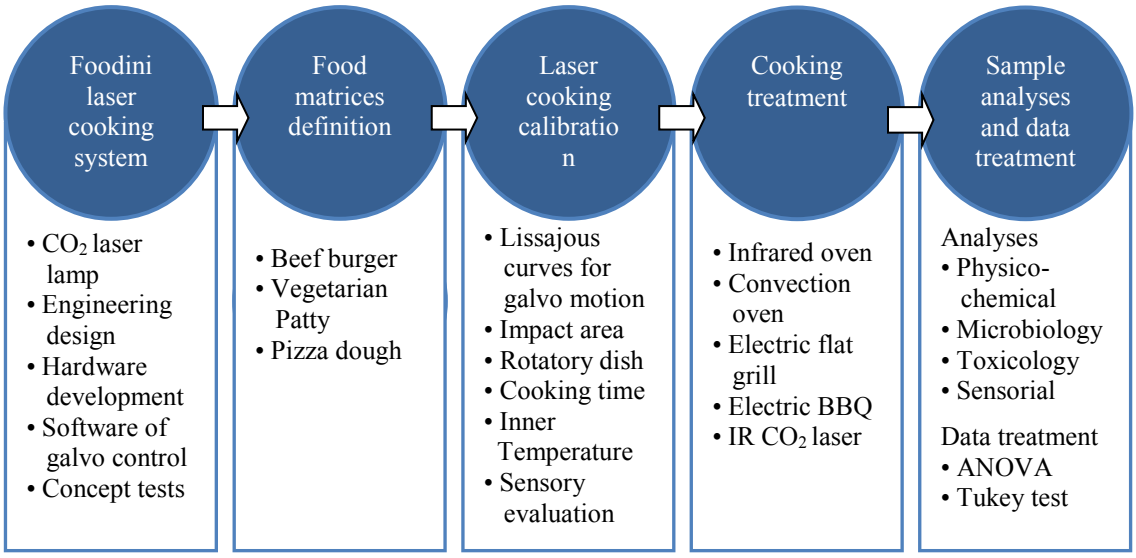

Fig. 2.7. Cooking experiments with CO_2 IR laser Foodini system

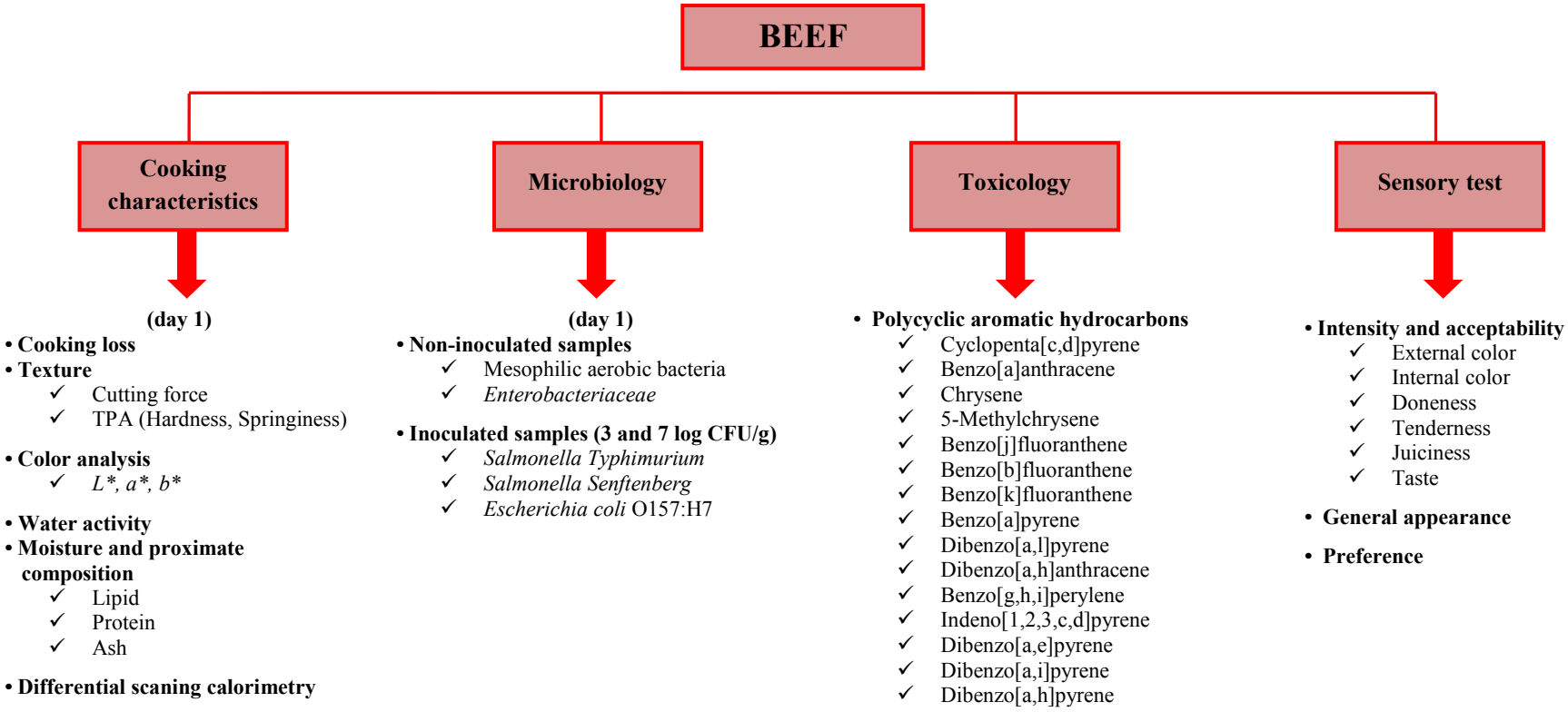

Fig. 2.8. Analyses performed in cooking experiments with CO_2 IR laser Foodini system and beef burgers

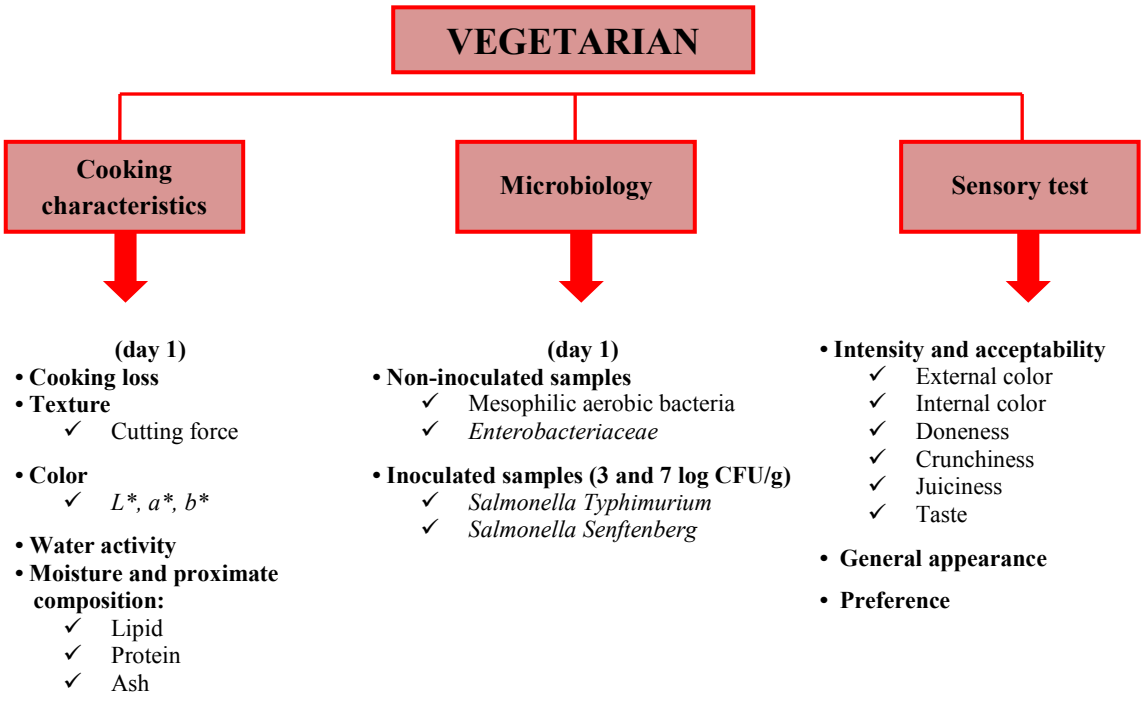

Fig. 2.9. Analyses performed in cooking experiments with CO_2 IR laser Foodini system and vegetarian patties

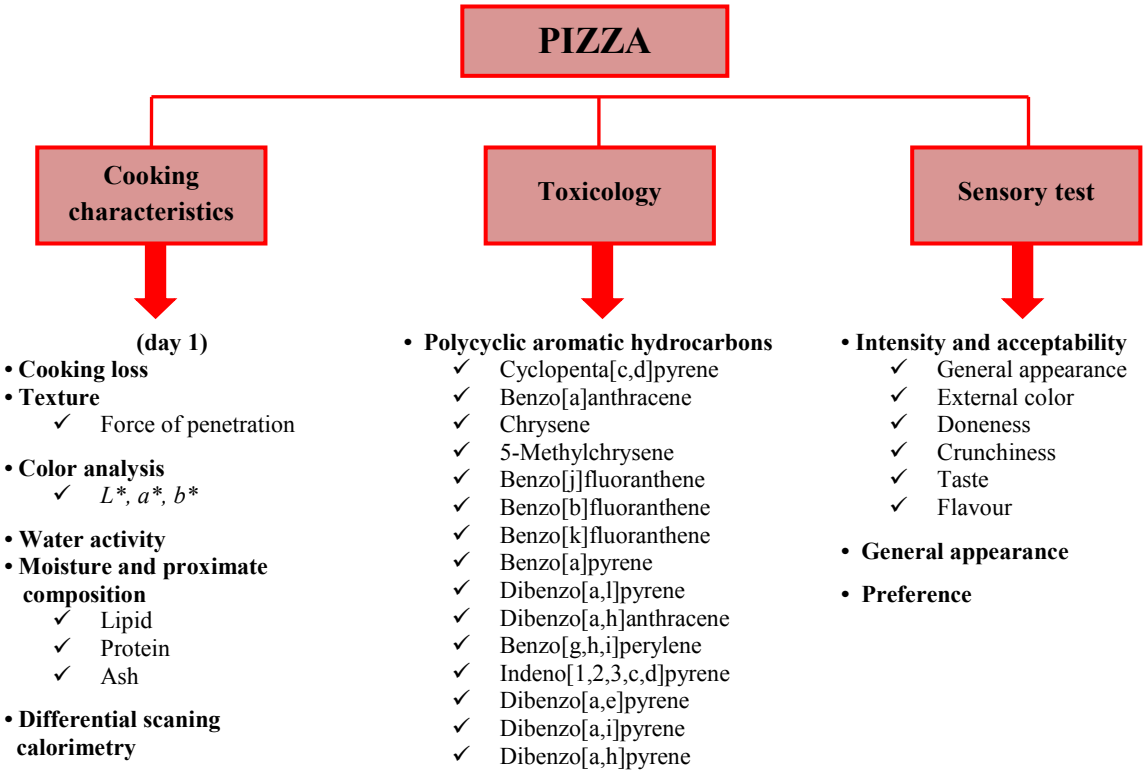

Fig. 2.10. Analyses performed in cooking experiments with CO_2 IR laser Foodini system and pizza dough

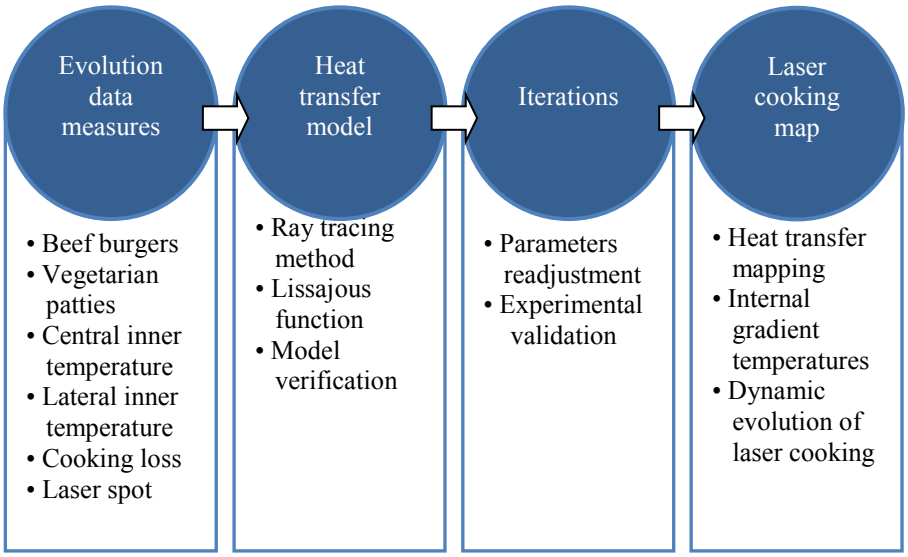

Fig. 2.11. Numerical modeling of heat transfer in beef burgers and vegetarian patties cooked with CO_2 IR laser Foodini system.

CHAPTER 2

INTRODUCTION

2. Introduction

1.1. General aspects about cooking

Cooking is a complex process where different physico-chemical, sensory and microbiological changes occur in food mainly due to heat application. Toxicological food safety can be also be influenced by cooking (for example, by formation of benzopyrenes or acrylamides). Changes induced by cooking can be generated by different processes including chemical reactions between molecules of food components, water evaporation, fat melting, loss of lipid-soluble and/or water-soluble proteins, loss of volatile aromatic lipid compounds, thermal inactivation of pathogens, etc.

Food components are mainly water, carbohydrates, fats, proteins, minerals and vitamins. Food components are highly influenced by the cooking process.

Water is present in most of food materials. Cooking can change the water concentration in food products mainly by evaporation and also by dripping. Water loss induces changes in the texture and sensory attributes, such as, juiciness, crunchiness, etc., thus, increasing the acceptability of cooked food. High water losses (for example in bakery products) induces a reduction in the water activity, increasing the shelf-life of products by lowering the water availability for microbial growth.

Carbohydrates include sugars, starches and fibers. The interaction between heat and the different types of carbohydrates is very complex and wide. For example, when heated, starch follows gelatinization which highly influences textural properties of food, and heating sugars and proteins generates the Maillard reaction, a basic flavor-enhancing and browning technique, and also acrylamide a potential carcinogenic compound.

Fat includes a wide range of vegetable oils and triglycerides and lipids from animal origin. Fats can reach temperatures higher than the boiling point of water, and are used to conduct high heat flux to other ingredients, for example in frying or deep frying treatments. Fats are often used as ingredients to improve texture or as flavor-enhancers.

Proteins are large biomolecules consisting of one or more long chains of amino acid residues or polypeptides present mainly in food of animal origin (*e. g.* meat, fish, milk, eggs) and vegetable products (*e. g.* legumes, seeds, mushrooms). For example, when

heated, proteins become denatured (unfolded) and, depending on the type of protein, can form aggregates which can lead to the formation of gels (like egg albumen) or structural networks (like gluten).

Vitamins and minerals are essential micronutrients. Minerals and vitamins in food products and vegetables may be decomposed or eluted by cooking process. On the other hand, bioavailability of some vitamins (thiamin, vitamin B6, niacin, folate, carotenoids) is increased with cooking by being free from the food microstructure.

Concerning microbiology, cooking processes increases shelf-life of products and guarantee food safety since prevents many foodborne illnesses related with pathogenic microorganisms present in raw food. Cooking would kill or inactivate harmful organisms, such as bacteria, viruses and parasites. The pasteurization or sterilization effect of cooking depends on combination of temperature and time applied for each type of pathogen.

Concerning toxicological facts, known potential carcinogenic products like polycyclic aromatic hydrocarbons (PAHs) or acrylamides are formed at high cooking temperatures (above 200°C). Grilling, barbecuing and smoking meat and fish could increase levels of PAHs. Intake of PAHs also could come from cereals, oils and fats treated at high temperature. Moreover, toasting, grilling or broiling starchy foods, until a toasted crust is formed, generates significant concentrations of acrylamide. These effects are driven by the characteristics of each cooking method and the composition of food ingredients (www.efsa.europa.eu).

Traditional cooking methods include baking, roasting, frying, grilling, barbecuing, smoking, boiling, steaming and braising. More recent cooking methods have been industrially developed, for example, microwaving or infrared (IR) cooking. Each method affects differently the physico-chemical characteristics of foods.

Since the present study is based on an IR system using CO_2 wavelength lamps, main characteristics of IR cooking and its effect on food components and matrices are described in the next section.

1.2. IR heating and cooking processes

Heat transfer occurs through one of these three methods: conduction, convection, and radiation. In conventional heating, which is usually carried out by an electric resistive system or by combustion of fuels, heat is generated outside the food to be cooked, and the heating energy is conveyed to the food matrix by convection of hot air or by thermal conduction. Electromagnetic methods include ohmic and inductive heating, radio frequency heating, microwave dielectric heating and IR heating. (Koutchma, 2017).

IR heating provides significant advantages over conventional heating methods, including reduced heating time, uniform heating, reduced quality losses, versatile, simple, compact equipment, significant energy saving and provides a high degree of process control. IR heating has a higher thermal efficiency, faster heating rate and a shorter response time in comparison to conventional heating systems. Moreover, IR systems give the possibility of selective heating (Krishnamurty *et al.*, 2008). Because of these benefits, IR radiation has been widely applied to various thermal preservations operations in the food industry mainly dehydration and pasteurization, and also for blanching and sterilization (Koutchma, 2017). IR radiation is also used for different cooking methods, such as roasting, baking, frying, and broiling.

IR radiation transfers thermal energy in the form of electromagnetic waves. IR radiation can be classified into 3 regions: near IR (NIR), mid-IR (MIR) and far-IR (FIR), corresponding to the spectral ranges of 0.75 to 1.4, 1.4 to 3, and 3 to 1000 μm, respectively (Sakai and Hanzawa, 1994). In general, FIR radiation, like the CO_2 laser wavelength (10.6 μm) used in the present work, is advantageous for food processing because most food components absorb radiative energy in the FIR region (Sandu, 1986). In a food product exposed to IR radiation (wavelength of 0.78 to 1000 μm), the heat energy delivered on the surface can be absorbed by different food components.

1.2.1 Interaction of IR radiation with Food Components

The wavelength at which the maximum radiation occurs is determined by the IR emitter material and by the temperature of the IR heating elements (Koutchma, 2017). As food is exposed to IR light, the radiation is absorbed, reflected or scattered, but does not behave as a black-body (which does reflect or scatter IR light) (Birth, 1978). For materials with

a rough surface, for example, at NIR wavelength region ($\lambda < 1.25$ μm), approximately 50% of the radiation is reflected, whereas less than 10% radiation is reflected at the FIR wavelength region (Skjoldebrand, 2001). Most organic materials reflect 4% of the total reflection on the surface, and the rest of the reflection occurs when radiation enters the food material and scatters (Dagerskog, 1979).

Absorption intensities at different wavelengths differ by food components. When radiant electromagnetic energy impinges upon a food surface, it may induce changes in the electronic, vibrational and rotational states of atoms and molecules. The type of mechanisms for energy absorption determined by the wavelength range of the incident radiative energy can be categorized: (1) changes in the electronic state correspond to the wavelength range 0.2 to 0.7 μm (ultraviolet and visible rays), (2) changes in the vibrational state correspond to wavelength range 2.5 to 1000 μm (FIR), and (3) changes in the rotational state correspond to wavelengths above 1000 μm (microwaves) (Decareau, 1985). In general, food substances absorb FIR energy most efficiently through the mechanism of changes in the molecular vibrational state, which can lead to radiative heating. The IR absorption spectra of food mixtures are originated by the mechanical vibrations of molecules or molecular aggregates, due to a very complex phenomenon of reciprocal overlapping (Halford, 1957).

Water and organic compounds such as proteins, lipids and starches, which are the main components of food, absorb FIR energy at wavelengths greater than 2.5 μm (Sakai and Hanzawa, 1994). Sandu (1986) reported that most foods have high transmissivities (low absorptivities) at $\lambda < 2.5$ μm. Amino acids, polypeptides, and proteins reveal two strong absorption bands localized at 3 to 4 and 6 to 9 μm. On the other hand, lipids show strong absorption phenomena over the entire IR radiation spectrum with three stronger absorption bands situated at 3 to 4, 6, and 9 to 10 μm. Carbohydrates yield two strong absorption bands around at 3 and 7 to 10 μm (Sandu, 1986; Rosenthal, 1992). Hence, the absorbance of IR radiation on food components is very important for the design of an IR cooking system and optimization of a thermal process.

Water effect on absorption of incident radiation is predominant over all the wavelengths. Figure 1.1. (Kebes, 2008) depicts the water absorption spectrum for a wide range of wavelengths: ultraviolet, visible, IR and microwaves.

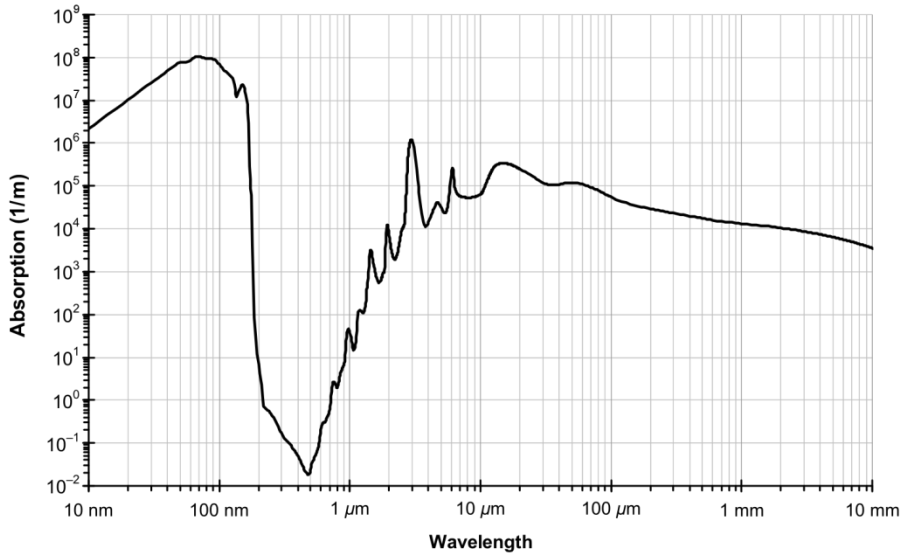

Figure 1.1. Absorption spectrum of liquid water for a given wavelength range

High water absorption of FIR has a low penetration depth inside a food material which contains water (Vogel, 2003). This is, the higher the absorption of IR radiation, the shorter its penetration depth. Sakai and Hanzawa (1994) reported that penetration depth of the FIR energy did not affect the temperature distribution inside the food. Moreover, they indicated that FIR energy penetrates very little, almost all the energy being converted to heat at the surface of the food, which is consistent with the study of Hashimoto *et al.* (1993) that evaluated FIR heating technique as a surface heating method.

1.2.2. Applications of IR heating in food processing and cooking operations

1.2.2.1. Drying and dehydration

The use of IR radiation technology for dehydrating foods has numerous advantages including reduction in drying time, increased energy efficiency, uniform temperature in the product while drying, better-quality of finished products, reduced necessity for air flow across the product, high degree of process control parameters, space saving, and clean working environment (Dostie *et al.*, 1989; Navari *et al*., 1992; Sakai and Hanzawa, 1994; Mongpreneet *et al.*, 2002). Theoretical calculations showed that intermittent IR drying with energy input of 10 W/m^2 becomes equivalent to convective drying in which the heat transfer coefficient would be as high as 200 W/(m^{2}K) (Krishnamurty, 2008).

FIR drying operations have been successfully applied for drying of fruit and vegetable products such as potatoes (Masamura *et al.,* 1988; Afzal and Abe, 1998), sweet potatoes (Sawai *et al.*, 2004), onions (Mongpreneet *et al.*, 2002; Sharma *et al.*, 2005), kiwifruit (Fenton and Kennedy, 1998), and apples (Nowak and Levicki, 2004; Togrul, 2005). Drying of seaweed, vegetables, fish flakes, and pasta is also done in tunnel IR dryers (Hagen and Drawert, 1986).

IR drying is a fast process and produces heating inside the material being dried, although its penetrating capacity is limited (Hashimoto *et al.*, 1990; Sakai *et al.*, 1993). Prolonged exposure of a biological material to IR heat results in swelling and ultimately fracturing and cracking on the surface of the material (Jones, 1992; Fasina *et al.*, 1997). However, a combination of intermittent IR heating and continuous convection drying of thick porous material results in better product quality and energy efficiency (Hashinomoto *et al.*, 1993). Then, IR radiation can be considered a surface treatment similar to other radiation technologies. Application of combined electromagnetic radiation and conventional convective heating is considered to be more efficient than radiation or convective heating alone, as it gives a synergistic effect (Koutchma, 2017).

1.2.2.2 Enzyme inactivation

FIR has been successfully used to inactivate enzymes in order to preserve the colors of carrots. Galindo *et al.* (2005) investigated the application of IR heating of carrot slices prior to freezing as compared to blanching (hot water and steam) in terms of carrot cell and tissue damage. Carrot slices heated by FIR radiation contained damaged cells only in the first half millimeter from the surface and exhibited the texture characteristic of the raw tissue.

1.2.2.3 Pathogen inactivation

IR heating can be used to inactivate bacteria, spores, yeasts and molds in both liquid and solid foods. Efficacy of microbial inactivation by IR heating depends on the following parameters: temperature of food sample, IR power level, peak wavelength (bandwidth of IR heating source), sample depth, , moisture content, type and physiological state of microorganism (exponential or stationary growth phase), and type of food material. Pathogen inactivation inside a food matrix during a cooking process is mainly achieved

by thermal mechanisms which damage their intracellular components such as DNA, RNA, ribosomes, cell envelope and/or cell proteins (Krishnamurty *et al.*, 2009). Tanaka *et al.*, (2007) demonstrated that IR heating can be used for surface pasteurization of strawberries without deteriorating their quality. In their studiy, IR heating raised the internal temperature of strawberries below 50 ◦ C while the surface temperature was high enough to effectively inactivate microorganisms.

According to the results of a USDA study (Huang and Sites, 2008), IR surface pasteurization was effective to inactivate *L. monocytogenes* in hot dogs. The hotdogs were surface inoculated with a cocktail of four strains of *L. monocytogenes* to average initial inoculums of 7.32 log CFU/g. On the average, 1.0, 2.1, 3.0 and 5.3 log reduction was observed after the surface temperature of hotdogs was increased to 70, 75, 80 and 85°C, respectively. Holding the sample temperature led to additional bacterial inactivation. With a 3-min holding at 80°C or 2 min at 85°C, at total of 6.4 or 6.7.logs of *L. monocytogenes* were inactivated. Since post-process contamination of ready-to-eat meats primarily occurs on the surface, IR radiation can be used as effective post-lethality treatment applied for meat processing to ensure final microbial safety (Krishnamurty *et al.*, 2008).

1.2.2.4. IR cooking processes

The usefulness and versatility of IR heating has also been demonstrated in various food processing applications: roasting, frying, broiling, heating, cooking meat and meat products, soy beans, cereal grains, cocoa beans, and nuts.

The two main conventional types of IR radiators used for process heating are electric and gas-fired heaters. Temperature ranges applied are: 343 to 1100°C for gas and electric IR, and 1100 to 2200°C for electric IR only. IR temperatures are normally used in the range of 650 to 1200°C to prevent charring of products. The spectral region suitable for industrial process heating ranges from 1.17 to 5.4 μm, which corresponds to 260 to 2200°C (Sheridan and Shilton, 1999). Proper emitter and process parameters, have to be selected for a particular product and process. Electrical IR heaters can be easily installed and produce a prompt heating rate. For the food heating sector, IR modules are manufactured in stainless steel and fitted with a wire mesh for mechanical protection. IR

emitters can be switched on and off in 1-2 s providing control from any unexpected or unwanted conveyor belt stoppage. Halogen lamps can also generate IR heating in the wavelength range of 0.7 to 5 μm. Some halogen ovens feature built-in microwave and convection oven options. Koutchma (2017) consider that the combinations of IR heating with microwave and with other conductive and convective heating technologies hold a great potential in optimizing energy usage and have a high applicability in food processing.

1.2.2.4.1. IR cooking of meat

When a sample of meat product is cooked by IR radiation, heat transfer from source to sample, depends on a number of factors: temperature difference between the heater source and sample surface, source emissivity and wavelength, sample surface absorptivity, reflection and radiation penetration depth (Sheridan *et al.*, 2002).

Baghe-Khandan & Okos (1981) found that thermal conductivity of lean beef increased with temperature up to 70°C, followed by a decrease during the denaturation of proteins and subsequent loss of water. After protein denaturation, the thermal conductivity of beef again increased with temperature. In the case of meat/fat mixtures, thermal conductivity also increases with temperature. According to Sheridan and Shilton (1999) the increase in thermal conductivity is due to the movement of water and melted fat within the meat product. Although the thermal conductivity of fat is low, it starts to melt at temperature around 40°C and the movement of the melted fat would carry heat into the interior of the product. Hence, Heat transfer within a beef patty sample is mainly due to conduction and diffusion of water and fat.

As the cooking progresses, the moisture content of the surface approaches to zero and the fat fraction of this zone decreases as some melted fat falls as drip. The surface zone is an area of high IR radiation absorption/transmission and high heat transfer by conduction/convection, at the outer of which the surface crust forms (Skjoldebrand, 1979; Luikov,1975). Skoldejbrand & Olson (1980) defined crust as the portion of the meat product that has exceeded 100°C during cooking. Initially this happens at the surface, but as cooking proceeds the >100°C zone moves towards the center. Yildiz *et al.* (2016) did not attain 100°C in the surface of meatballs cooked with a FIR source. Sheridan and

Shilton (1999) cooked hamburger patties with a MIR and FIR sources. In the case of MIR source, the samples attained and exceed this temperature and crust was formed.

Moreover, as the water content of the surface is reduced, the surface contains more air-filled interstices that have an insulating effect. Perez and Calvelo (1984) found that the thermal conductivity of a crust fell from a value of 0.49 W/m·K for raw meat, almost to 0.14 W/m·K, for a cooked meat with low residual water content.

The effects of IR cooking on the characteristics of meat products have been studied by several authors. The quality of beef produced by IR dehydration was similar to conventionally heated beef as indicated by surface appearance and taste tests (Burgheimer *et al.*, 1971).

Muriana *et al.* (2004) showed that deli turkey treated with IR heating had a more appealing brown color and roasted appearance, in addition to the pasteurizing effect on the surface.

Khan and Vandermey (1985) prepared ground beef patties by IR broiling in a conveyorized broiler. The cooking time was reduced compared to conventional gas heating. In addition, it was found that IR-broiled ground beef patties did not undergo any adverse effects on cooking conditions and quality (number of samples cooked/min, % shrinkage, cooking time) compared with conventional gas broiling method. Sensory evaluation of ground beef patties treated by IR heating and gas broiling in terms of flavor, texture, juiciness and overall acceptability showed no significant difference between both treatments. However, the general appearance was rated better in gas-broiled patties than in IR-broiled patties.

Sheridan and Shilton (1999) evaluated the efficacy of cooking beef burger patties using IR sources at a maximum wavelength of 2.7 μm (MIR) and at a maximum wavelength of 4.0 μm (FIR). They observed that the target core temperatures were achieved more rapidly as the fat content of samples increased. Moreover, with FIR radiation source, the target core temperature of beef patty was achieved at lower surface temperature, with less surface drying and charring. This study also concludes that FIR radiation heaters are more energy efficient for meat cooking in comparison with MIR heaters. In a later study, the same authors studied the effect on the yield of beef burger patties cooked with FIR. They

observed that water-based cooking loss was mostly due to vaporization whereas fat-based cooking loss was almost exclusively due to drip. Moreover, they observed that the surface zone was less thick in low-fat burgers than in high-fat burgers and suggested that greater surface water availability in low-fat burgers would kept temperature close to 100°C for longer and delay crust formation (Sheridan and Shilton, 2002).

1.2.2.4.2. IR cooking of vegetables and legumes

The effect of IR cooking has been studied on several plant foods different points of view. Hashimoto *et al.* (1990, 1994) studied the penetration of FIR energy into sweet potato and found that FIR radiation absorbed by the vegetable model was decreased to 1% of the initial values at a depth of 0.26 to 0.36 mm below the surface, whereas NIR showed a similar reduction at a depth of 0.38 to 2.54 mm. Chua and Chou (2005) studied the application of IR radiation in potato and carrot by slowly increasing the power, with short cooling between power levels, finding that it resulted in less color degradation than with intermittent IR heating. Reductions in overall color change of 37.6 and 18.1% were obtained for potato and carrot, respectively. Galindo *et al.* (2005) also studied the effect of IR heating on carrots. IR treatment caused less damage to the tissue than blanching, as observed by lower relative electrolyte leakage values and microscopic observations, while effectively inactivated the enzymes on carrot surface. Moreover, IR-treated carrots had higher tissue strength than those blanched with mild hot water.

Mongpreneet *et al.* (2002) found that chlorophyll content of dehydrated onions treated by IR increased with an increase in irradiation power. Gabel *et al*. (2006) observed that pungency of onions decreased with reduction in moisture after an IR radiation treatment. Regarding the effect IR treatment duration, they concluded that long IR heat treatments may darken the color of onion due to browning.

Abdul-Kadir *et al.* (1990) evaluated the effect of IR heating on pinto beans (*Phaseolus vulgaris*) heated to 99 and 107 °C. IR-heating improved rehydration rate and degree of swelling of pinto beans; however, cooking time of pinto beans significantly increased. McCurdy (1992) observed that bitterness and protein solubility of peas were reduced after IR heat treatment. Arntfield *et al.* (2001) found that IR heat-treated lentils were darker than raw lentils. Moreover, cell walls of lentils were less susceptible to fracture after IR

heat treatment, although they had a more open microstructure that enhanced their rehydration characteristics.

1.2.2.4.3. IR cooking of bread

Some authors have compared the use of different wavelengths or IR radiation to cook doughs. Sakai and Hanzawa (1994) discussed the effects of NIR and FIR heaters on crust formation and color development at the surfaces of white bread and wheat flour. NIR heater led to a greater heat penetration into food samples, resulting in formation of relatively wet crust layers, compared to dry layers formed by FIR heaters. However, the rate of color development caused by FIR heaters was greater than the caused by NIR heaters, due to a more rapid heating rate on the surface. Nevertheless, Lentz *et al.* (1995) stated that, for bread dough, unless the emitting wavelength is restricted to the wavelength best absorbed, heating will be very inefficient, resulting in excessing heating of the surface and poor heating of the interior. Excessive surface heating, in the absence of corresponding heat removal to the interior, will give rise to crust formation, inhibiting heat transfer.

Olsson *et al.* (2005) studied the effect of IR heating followed by air jet impingement on crust formation of par-baked baguettes. Combination of IR heating and jet impingement resulted in rapid drying and enhanced color development, compared to conventional oven treatment. Though the water loss rate increased due to the high heat transfer rate, the total water loss was reduced because of shorter heating time and, in general, IR treatment time enabled the formation of a thinner crust.

According to Koutchma (2017), further studies have to be done to obtain a detailed insight into the theoretical explanation of IR effects, especially regarding its interaction with food components, changes in taste and flavor compounds and living organisms.

1.2.3. IR heat transfer modeling

IR heat transfer modeling inside food has been widely researched due to the complexity of optical characteristics, radiative energy extinction and combined conductive and/or convective heat transfer phenomena.

In general, numerical methods applied to solve the set of equations are: finite elements, finite difference, and the control volume method (Turner and Perre, 1996). Diffusion characteristics in relation with radiation intensity and thickness of a given food volume have been studied using the finite element method to explain the phenomenon of heat transfer inside food systems under FIR radiation.

Dagerskog (1979) created a model that successfully predicted the experimentally measured temperature distribution of beef slices during IR frying. The model was based on combined IR radiation and convection heating. Heat conduction equation was solved numerically using the finite difference method. The infinitesimal differentials were replaced by differences of finite size and the degree of accuracy of the representation was determined by the step size of these differences.

Sakai and Hanzawa (1994) assumed that most FIR radiation energy would be absorbed at the surface of a food system due to the predominant energy absorption of water. Then, energy would be transported by heat conduction inside the food sample. Based on this assumption, a governing equation and boundary conditions to explain heat transfer derived from energy balance in a food system were solved using Galerkin's finite element method. The measured temperature distribution in samples was in good agreement with model predictions, permitting control of the surface temperature to retain food properties without overtreatment.

Abe and Afzal (1997) investigated four mathematical drying models: exponential model, Page model, diffusion model based on spherical grain shape, and an approximation of the diffusion model to address the thin-layer IR drying characteristics of rough rice. They found the Page model as most satisfactory for describing thin-layer IR radiation drying of rough rice. Das *et al.* (2004) also reported that the Page model adequately fitted the experimental drying data while studying the drying characteristics of high-moisture paddy rice.

Afzal and Abe (1998) studied the effect of radiation intensity and thickness of slab on the moisture diffusion characteristics of potato during FIR drying applying a model fitting procedure to the experimental drying data to determine the diffusion coefficients. The diffusivity was found to vary with radiation intensity and the thickness of slab. The radiation energy driving internal moisture movement during FIR drying of a potato,

induced the activation energy for diffusion inversely proportional to thickness of the given volume of the sample (Afzal and Abe, 1998).

Ranjan *et al.* (2002) developed a 3-dimensional control volume formulation for the solution of a set of 3-way coupled heat, moisture transfer, and pressure equations with an IR source term. The solution procedure uses a fully implicit time-stepping scheme to simulate the drying of potato during IR heating in 3-dimensional Cartesian coordinates. Simulation indicated that the 3-way coupled model predicted the temperature and moisture contents better than the 2-way coupled heat and mass transfer model. The overall predictions agreed well with the available experimental data and demonstrated a good potential for application in grain and food drying.

The variation of moisture ratio with time during IR drying of apple could be described by the model developed by Midilli *et al.* (2002). Sixty-six different model equations relating the temperature and time dependence of IR drying of apple were derived, having the highest efficiency the model derived from modified Page II. Moreover, a single equation was derived to predict the moisture ratio change during IR drying (0 to 240 min) of apple in the temperature range of 50 to 80°C. Togrul (2005) investigated IR drying of apple, including combined effects of drying time and temperature to create new suitable models. Ten different drying models (Newton, Page, modified Page, Wang and Singh, Henderson and Pabis, logarithmic, diffusion approach, simplified Ficks diffusion [SFFD] equation, modified Page equation-II, and Midilli equation) were developed and validated.

FIR radiation simulations with convection–diffusion air flow and heat transfer simulations were combined to investigate the suitability of IR radiation for surface decontamination in strawberries (Tanaka *et al.*, 2007). The model was a powerful tool to evaluate in a fast and comprehensive way complex heating configurations including radiation, convection, and conduction phenomena. Computations were validated against measurements with a thermographic camera. FIR heating obtained more uniform surface heating than air convection heating, with a maximum temperature well below the critical limit of about 50 °C.

Shilton *et al.* (2002) developed a model based on heat and mass transfer during the cooking of beef patties by long wavelength FIR source. A one-dimensional model based on an infinite slab was described and the model was solved using the finite difference

technique. The results obtained from the model were compared to experimental results over a range of fat content from 0% to 30%. Heat transfer results for the 0% fat content, using a conduction model, showed very good agreement with the experimental data. By including a term to account for internal fat and moisture convection in the beef patties during cooking, the heat transfer process could be predicted for fat contents ranging from 10% to 30% fat. A diffusion coefficient based on temperature and moisture was applied for the prediction of the evaporative mass losses. The model showed a very good agreement with the experimental data.

Sargolzaei et *al.* (2010) developed a model for an unsteady-state heat transfer in hamburger cooking process using one dimensional finite difference and three dimensional computational fluid dynamic (CFD) models. A double-side cooking system was designed to study the effect of pressure and oven temperature on the cooking process. Applying pressure to hamburger increased the contact area of hamburger with the heating plate increased the heat transfer rate to the hamburger, caused weight loss due to water evaporation and decreased cooking time. CFD predicted results fitted better the experimental results than the finite difference ones.

1.2.4. Selective heating by IR radiation

In practice, IR sources emit radiation covering a wide range of wavelengths. Nevertheless, there are systems which can control or filter radiation within a specific spectral range using optical band pass filters. This controlled radiation can stimulate the maximum optical response of the target (*e.g.*, food component, microorganism) when the emission band of IR and the peak absorbance band of the target material are identical. IR radiation for selective heating of foods could be very useful for a wide range of potential process applications. Hence, it is considered a challenge to control or filter the spectral distribution to obtain a specific bandwidth and IR sources that emit with a specific wavelength should be considered for optimization of the heating process.

There is not much literature on selective heating using IR radiation in foods. Few attempts have been made to study selective IR bandwidth or wavelength in the food industry. Jun (2002) developed a novel selective FIR heating system for soy protein and glucose. The system used band pass filter that selected the specific wavelengths that were emitted according to the specific absorptivity of each food powder. Soy protein was heated about

6°C higher than glucose after 5 min of heating, exhibiting a reverse phenomenon when heating without the filter. Moreover, they demonstrated that the selective IR heating caused a higher lethality of fungal spores in corn meal than pulsed UV heating.

1.2.4.1. IR Lasers

IR lasers could be considered like a very precise selective IR heating system because they work with a single wavelength. Table 1.1 describes commercially available laser sources that emit at IR wavelengths close to strong absorption bands of water.

Table 1.1. Commercially available lasers sources with IR emission wavelength close to high water absorption wavelength.

Type of laser	Wavelenght of interest	Pump source	Application
Er:YAG	2.94 μm	Flashlamp, laser diode	Periodontal scaling, dental treatment, skin resurfacing
He-Ne	3.3913 μm	Electrical discharge	Interferometry, holography, spectroscopy, barc ode scanning, alignment, optical demonstrations.
CO	2.6 to 4 μm, 4.8 to 8.3 μm	Electrical discharge	Material processing (engraving, welding, etc.), photoacoustic spectroscopy.
CO_2	10.6 μm	Transverse (high power), longitudinal (low power) electrical discharge	Material processing (cutting, welding, etc.), surgery, dental treatmment, military lasers.

Table adapted from: https://en.wikipedia.org

As depicted in Figure 1.1, for IR spectrum, three strong absorption peaks appear at 3 μm, 6 μm and ~10.5 μm. For Er:Yag laser wavelength, there is a very short penetration depth in water-rich matrices (~0.001 mm), whereas for CO_2 lasers penetration depth increases ten times (~0.01 mm) (Vogel, 2003). For medical applications, Er:Yag and CO_2 lasers are considered the most commercially available efficient ones. CO_2 lasers are widely used in comparison with Er:Yag lasers, because the later require complex power supplies, cooling systems, and beam delivery devices that are expensive and have high maintenance costs (https://www.aesculight.com). In the case of diode lasers in the visible range wavelength (455 – 980 nm), absorption depth increases substantially (>5 mm) whereas water energy absorbance is very low (Pope and Fry, 1997).

1.2.4.1.2. CO2 laser

The CO_2 laser is a molecular gas laser based on a gas mixture as the gain medium, which contains carbon dioxide (CO_2), helium (He), nitrogen (N_2), and possibly some hydrogen (H_2), water vapor and/or xenon (Xe). Such a laser is electrically pumped via a gas discharge, which can be operated with DC current, with AC current (e.g. 20–50 kHz) or in the radio frequency domain. N_2 molecules are excited by the discharge into a metastable vibrational level and transfer their excitation energy to the CO_2 molecules when colliding with them. Other constituents such as H_2 or water vapor can help (particularly in sealed-tube lasers) to reoxidize CO formed in the discharge to CO_2 (Patel, 1964).

CO_2 lasers have a wide range of commercially available powers, combined with a reasonable cost and a large variety of specialized equipment and, moreover, they are also quite efficient: the ratio of output power to pump power can be as large as 20%. The CO_2 laser produces a beam of IR light with the principal wavelength bands centering between 9.4 and 10.6 μm (www.laserproject.es).

CO_2 lasers are frequently used in industrial applications for cutting and welding, whereas lower power level lasers are used for engraving and marking of different material. CO2 lasers are also used in the additive manufacturing process of selective laser sintering. (https://www.rp-photonics.com)

CO_2 laser (10.6 μm) is considered the most suitable for soft tissue procedures in human and animal medical treatments, as compared to other laser wavelengths. Soft tissue treatments include cutting and hemostasis which are achieved photo-thermally heating). The advantages of using CO_2 lasers include less bleeding, shorter surgery time, less risk of infection, and less post operations swelling. Medical areas of application include gynecology, dentistry, oral and maxillofacial surgery, and many others. CO_2 lasers have become versatile and useful in surgical procedures since water, which is present in a high concentration in most biological tissues, highly absorbs their frequency radiation (Fisher, 1993; Vogel, 2003).

1.2.4.1.3. Laser Cooking

Several patents have described systems to use lasers in conjunction with cooking or as a cooking system:

- Kiyoshi (1998) patented a laser cooking device system, and described how to improve thermal efficiency by using laser beams as a cooking means. This system device did not heat the food directly with a laser and it employed a laser oscillator to heat the bottom of a cooker.

- Hideki (2002) patented a food cooking apparatus System. They described a microwave oven with a semiconductor laser irradiation unit which irradiated a laser beam having a specific wavelength (0.8 μm and 1.5 μm) onto foodstuffs accommodated in a cooking chamber.

- Muchnik (2008) patented an apparatus and method for cooking food directly with a CO_2 laser. The laser beam was directed at a beam splitter, which split the laser beam in half; mirrors were used to focus the beam to either side of the food. The split beam reached a higher temperature than most types of lasers.

- Singh (2013), described a method and apparatus for plasma assisted laser cooking of food products. This system applied energy with a laser emitter very close to the food product. The application of the energy could be controlled according to a profile to generate plasma inside and around the food product during cooking, and it could be adjusted according to the feedback from the controlled application of energy to the food product.

Recently, Butingler *et al.* (2018) studied the gelatinization of starch in dough using a blue diode laser, which operates at 445 nm, by adjusting the water content of the dough (50-70%) and the exposure pattern of the laser. They applied a ring-shaped cooking pattern of 5mm diameter, 120 repetitions, 4000mm/min speed, and 2W laser power. Their results showed that high internal temperatures were achieved in laser-treated dough samples with greater water content: dough with 70% water content (106.7°C) was >20% warmer than dough with 50% water content (87°C). The correlation between dough temperature and the amount of water content was attributed to the low absorbance of water at 445 nm, resulting in greater heat penetration depth in the dough with the highest amount of water (70%). Surface burning was observed on the dryer dough (50% water) that also limited the depth penetration of laser. The authors concluded that further processing with an IR laser is required to achieve optimal browning.

CO_2 IR laser cooking could be considered an innovative IR-based cooking technique and, to the best of our knowledge, a specific cooking system based on CO_2 wavelength sources and their effects on physico-chemical, microbiological, toxicological and sensory aspects for different food matrices have not been studied or reported yet.

CHAPTER 3

MATERIALS AND METHODS

3.1. Formulation and preparation of samples

3.1.1. Beef Burgers

Ingredients used for burger preparations were: raw minced beef meat 98.26% (w/w) (Bon Area, Grup Alimentari Guissona, Guissona, Spain), iodized refined salt 1.5% (w/w) (Sal Costa, Barcelona, Spain) and ground black pepper 0.24% (w/w) (Jesús Navarro S.A., Novelda, Spain). Ingredients were manually mixed and molded using a 78 mm diameter circular mold, with 11±1 mm height. Each burger weighted 50±1 g. Once prepared, burgers were kept at 4°C in plastic containers in order to avoid bacterial growth and to standardize initial cooking temperature. Burgers were cooked the same day of preparation.

3.1.2. Mashed potatoes bites

Ingredients used for mashed potatoes were: water 56.99% (w/w), half-skimmed milk 28.16% (w/w) (ATO Natura, Llet ATO S.L., Barcelona), dehydrated mashed potatoes 14.62% (w/w) (Maggi®, Nestlé España, S.A., Esplugues de Llobregat, Spain), and iodized refined salt 0,23% (w/w) (Sal Costa). Ingredients were mixed together using a mixer (Thermomix 21/2-1, Vorwerk Elektrowerke GmbH & Co., Wuppertal, Germany). Each sample weighed 11±1 g and was prepared using a 47 mm diameter circular mold, with 5 mm height. Once prepared, they were immediately cooked.

3.1.3. Pizza dough

Ready-to-use fresh pizza doughs (Finissima and Tradizionale, Buitoni®, Nestlé España, S.A.) were used. Samples were prepared using circular molds as cutters. Finissima pizza dough samples were prepared using a 60 mm diameter circular mold and their average height was 3 ± 1 mm. Tradizionale pizza dough samples were cut using a 100 mm diameter circular mold and their average height was 5 ± 1 mm. Pizza dough samples were immediately cooked after preparation.

3.1.4. Vegetarian patties

Ingredients used for vegetarian patties preparations with egg were: cooked chickpeas (Acico S.A., Elorrio, Spain), cooked brown lentils (Acico S.A.), fresh red onions (Hortus

Abatis®, Torribas S.A., Barcelona), fresh carrots (Hortícola Esma S.L., Elorrio), fresh eggs (Liderou S.L., Maià de Montcal, Spain), corn flour (Maizena, Unilever España, S.A., Viladecans, Spain), Original type dehydrated mashed potato (Maggi®), sunflower refined oil (Borgesol, Borges Branded Foods S.L.U., Tàrrega, Spain), iodized refined salt (Sal Costa), ground cumin, ground sweet paprika, oregano, ground nutmeg (Ducros, McCormick España, S.A., Sabadell, Spain) and ground black pepper (Jesús Navarro S.A.). Formulation is described in table 3.1 Patties mix was prepared using a mixer (Thermomix 21/2-1). First, chickpeas, brown lentils, carrots and red onions were grounded together inside the mixer. The rest of ingredients were added and mixed to obtain a homogeneous mix which was molded using a 78 mm diameter circular mold, with 11±1 mm height. Each vegetarian patty weighed 50±1 g. Once prepared, patties were kept at 4°C in plastic containers in order to avoid bacterial growth and to standardize initial cooking temperature. Patties were cooked the same day of preparation.

Table 3.1. Percentage of ingredients of vegetarian patties

Ingredients	Percentage (%)
Cooked chickpeas	30.0
Cooked brown lentils	30.0
Fresh red onions	7.5
Fresh carrots	7.5
Fresh eggs	9.0
Corn flour	6.0
Dehydrated mashed potato	6.0
Sunflower oil	2.0
Iodized salt	1.4
Ground cumin	0.3
Ground sweet paprika	0.1
Oregano	0.1
Ground nutmeg	0.1
Ground black pepper	0.1

3.2. Cooking procedure

As previously mentioned in the working plan, three food matrices were cooked and analyzed in each experimental study. Two experimental studies were carried out based on the CO_2 IR laser cooking system applied: Epilog Equipment study and Foodini Equipment study. Food matrices were also cooked with different standard cooking systems in order to compare analytical results between methods. Table 3.2 summarizes food matrices and cooking methods for each study.

Table 3.2. Food samples and cooking methods applied for each experimental study.

First Study - Epilog Equipment		**Second Study - Foodini Equipment**	
Food sample	**Cooking methods**	**Food sample**	**Cooking methods**
Beef burgers	CO_2 IR laser Epilog	Beef Burgers	CO_2 IR laser Foodini
	Infrared oven		Infrared oven
	Electric BBQ grill		Electric BBQ grill
	Electric Flat grill		Electric Flat grill
Mashed potatoes bites	CO_2 IR laser Epilog	Vegetarian patties	CO_2 IR laser Foodini
	Infrared oven		Infrared oven
	Microwave		Electric BBQ grill
			Electric Flat grill
Pizza dough	CO_2 IR laser Epilog	Pizza dough	CO_2 IR laser Foodini
	Infrared oven		Infrared oven
	Deck oven		Convection oven

3.2.1. Definition of cooking conditions

Beef burgers and vegetarian patties were cooked to a minimum internal end point temperature of 72°C (FSAI, 2018; AMSA, 2016; www.fda.gov), which was recorded at the geometrical center of each burger by using a penetration probe-type thermocouple (0900 0530, Instrumentos Testo S.A., Cabrils, Spain). This reference temperature (72°C) was used to set up the cooking time and conditions of the different cooking methods used.

Cooking conditions for pizza dough and mashed potatoes bites were chosen to obtain an optimum organoleptical result for each cooking system.

3.2.2. Infrared laser cooking

3.2.2.1. Epilog equipment

First experiment with laser cooking was carried out using an IR laser engraver equipment, based on an air-cooled CO_2 laser lamp (Epilog Zing 24, 1200 W, EPILOG LASER, Golden, Colorado, USA) (figure 3.1). Beef burgers, mashed potatoes bites and pizza dough were placed over a crystal microwave plate (28 cm diameter) placed at the bottom of the laser engraver. Laser beam impacted perpendicularly on the sample surface.

Figure 3.1. Epilog Zing laser equipment

Specific cooking conditions applied for each food matrix are described as follows:

3.2.2.1.1. Beef burgers

Two cooking time conditions were applied: 1) 12 min and 15 s per side and 2) 14 min and 15 s per side. Burger sides were cooked consecutively. The area of cooking was a full black square of 83x83 mm. Operation conditions given by Epilog software were: Engraver mode (Raster); 500 dpi resolution; 100% power; 5000 Hz frequency; 29% speed equivalent to 205,3 mm/s (this corresponds to time condition 1 and it will be named from now as IR Laser 29) and 25% speed equivalent to 176,98 mm/sec (this corresponds to time condition 2 and it will be named from now as IR Laser 25). Beef burgers were cooked from upper pole to lower pole (as shown in figure 3.2).

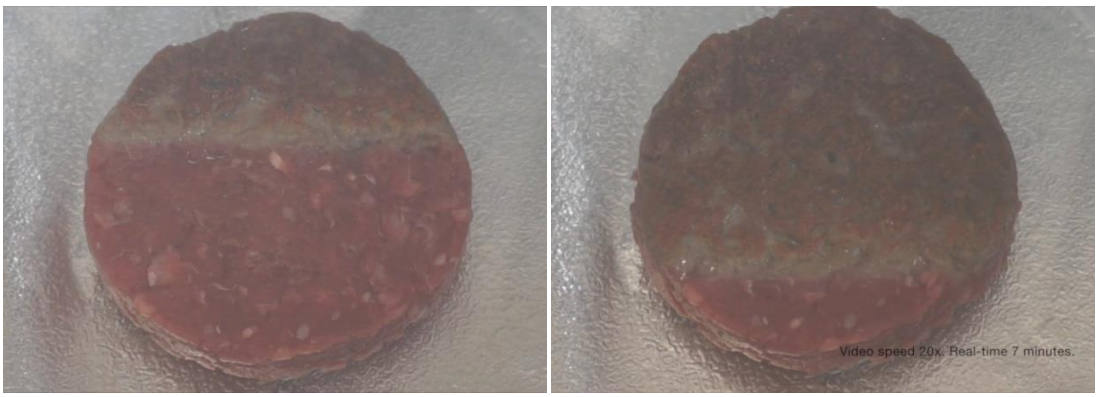

Figure 3.2. Cooking stages of Beef Burger using CO_2 IR laser Epilog Equipment

3.2.2.1.2. Pizza dough

Cooking time per side was 8 min and 51 s. Pizza sides were cooked consecutively. The area of cooking was a full black circle of 70 mm diameter. Operation conditions given by Epilog software were: Engraver mode (Raster); 500 dpi resolution; 27% power; 5000 Hz frequency; 20% speed. This cooking time condition will be named from now as IR Laser 20. Pizza dough was cooked from upper pole to lower pole (figure 3.3).

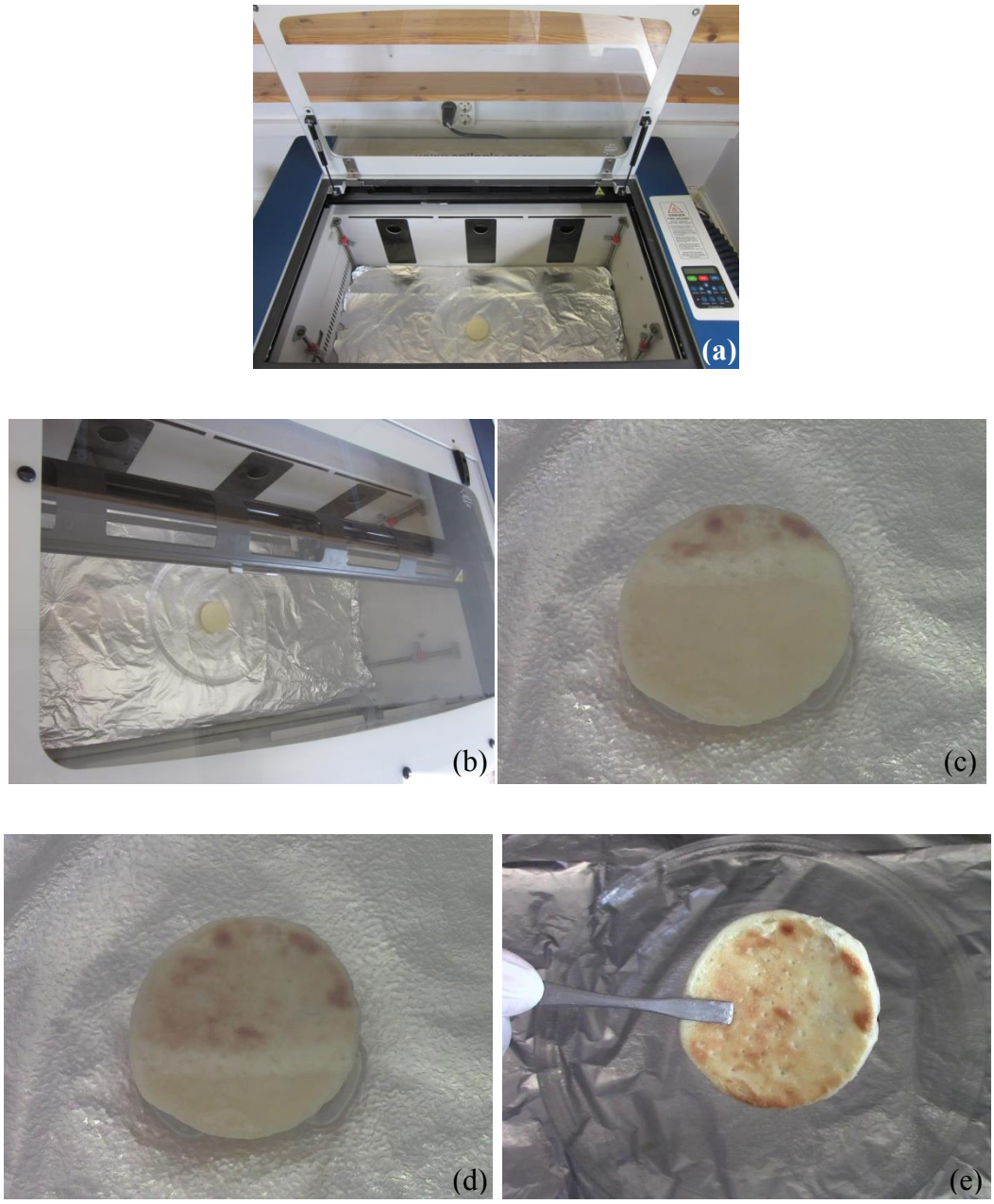

Figure 3.3. (a) General view of the Epilog Laser Equipment; (b) Cooking process; (c) (d) (e) Cooking stages of the pizza dough

3.2.2.1.3. Mashed potatoes

Cooking time per side was 3 min and 8 s. Samples were only cooked from the top side, where laser beam impacted. The area of cooking was a full black square of 50x50 mm. Operation conditions given by Epilog software were: Engraver mode (Raster); 500 dpi resolution; 100% power; 5000 Hz frequency; 62% speed. This cooking time condition

will be named from now as IR Laser 62. Mashed potatoes were cooked starting from upper pole to lower pole.

3.2.2.2. IR laser cooking with Foodini Equipment

An innovative IR laser cooking system, designed and developed by NM with patent number EP3200612A4 (Gracia & Sepulveda, 2014), was adapted to cook inside Foodini (2 Vegan Natural Machines, Barcelona, Spain). The system was composed of five main units (figures 3.4, 3.5, 3.6, 3.7 and 3.8):

1) CO_2 laser lamp (laser type TEMoo, QIWEI Aviation (HK) International Holding Co., Limited, Hong Kong, China)
2) Galvo-scanner head for CO_2 laser with gold coated mirrors (10 mm aperture, model MT-GN-CO_2, Mactron Technology Co., Ltd, Dongguan, China)
3) Single-board computer unit (Raspberry Pi 3 Model B+, Raspberry Pi Trading, Ltd., Cambridge, UK) with an integrated audio amplifier module (model Pi-DigiAMP+, IQaudio Limited, Cricklade, UK)
4) Long-wave infrared (LWIR) thermal camera module (LWIR sensor wavelength 8 to 14 µm, model Lepton®, FLIR Systems, Inc., Wilsonville,Oregon, USA)
5) Software to control the movement of galvo-scanner motors (developed by Natural Machines)

Control software was based on Lissajous curves which allowed complex harmonic motion of scan mirrors. Lissajous curves movement was transmitted by audio signal from amplifier stereo output to drivers that controlled the movement of galvo-motors (galvanometers) of the mirrors.

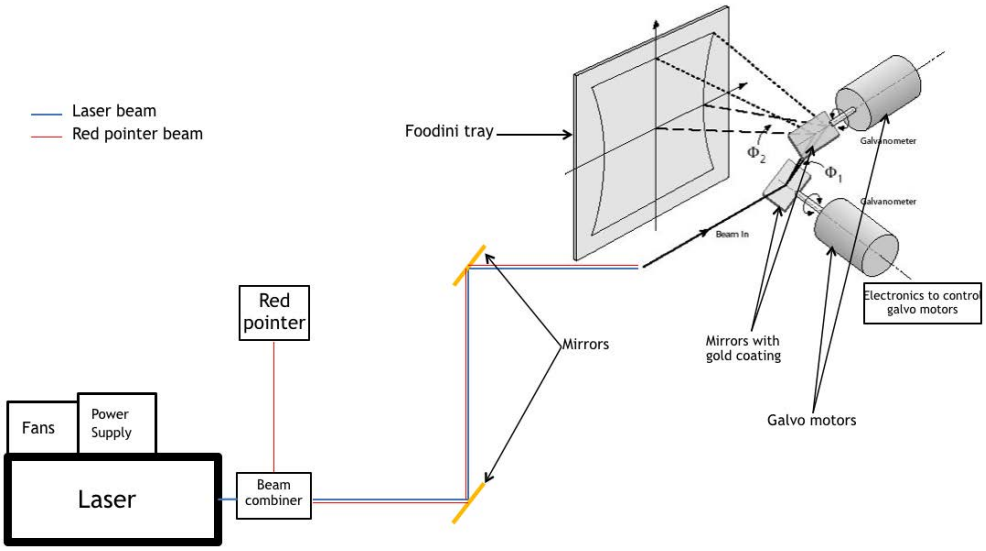

Figure 3.4. Diagram of the CO_2 IR laser Foodini

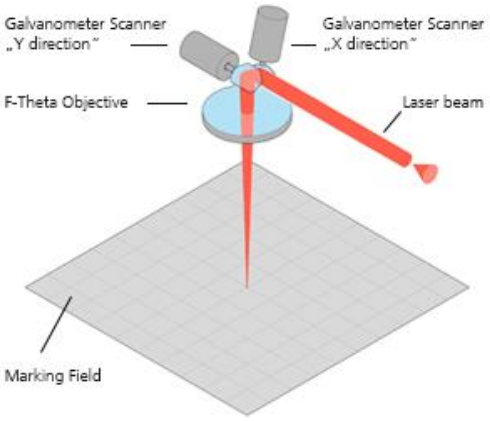

Figure 3.5. Area of laser impact given by galvanometers movement

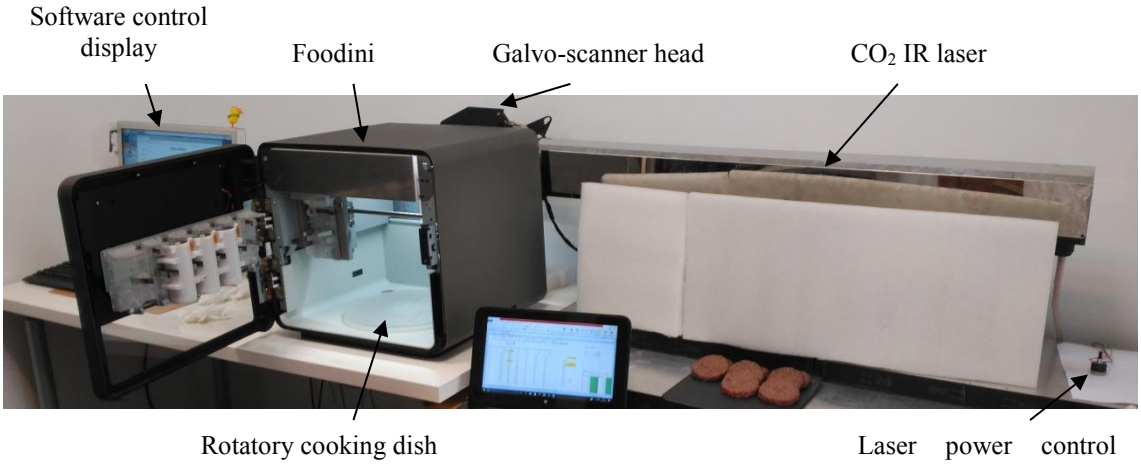

Figure 3.6. CO_2 IR Laser Foodini Equipment (global view)

Single-board computer

Foodini screen UI/UX

Figure 3.7. Foodini (frontal view)

Galvo-scanner head

Thermal camera position

Gold coated mirrors and galvanometers

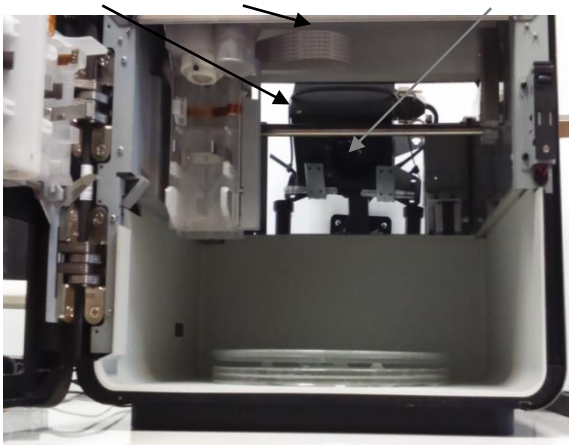

Figure 3.8. Laser cooking zone inside Foodini

The operation of the laser cooking system is described as follows. IR laser beam, generated from CO_2 laser lamp, impacted on both scan mirrors. From scan mirrors, laser beam was applied over food samples placed over the crystal dish inside Foodini. Rapid motion of scan mirrors allowed homogeneous heating of a specified area. Cooking area was determined by control software. The thermal camera allowed an overview of the cooking area. Foodini crystal dish was constantly in motion (2 rpm) to allow homogeneous distribution of heat radiation. Laser beam impacted over food sample to cook top side and lateral side at the same time. To cook bottom side, food samples were turned once top side was cooked.

The control software operated with the thermal camera vision and determined the heating area and the curve motion frequency. Heating area and curve motion frequency were given by the frequency and size length of X and Y axes, which generated a specified Lissajous motion curve. A Lissajous curve is a graphic given by a system of parametric equations:

$$\mathbf{x = A \sin(at+\delta),\ y = B \sin(bt).}$$

In our case, parametric values of the equations corresponded to: A = (size length X axis/2); a = frequency of X axis; t = time; $\delta = (\pi/2)$; B = (size length Y axis/2); b = frequency of Y axis. Software parameters are described in the table 3.3.

Table 3.3. Software parameters for Lissajous curves which drive laser beam motion

Software parameters	Definition	Lissajous curves parameter
Freq X	Frequency X axis	a
Freq Y	Frequency Y axis	b
Size X	Theoretical length (cm)*	A = (Length X axis/2)
Size Y	Theoretical length (cm)*	B = (Length Y axis/2)

*Real size length is increased due to the distance from the mirror to dish.

The way of the application of laser radiation over the sample, defined by Lissajous motion curves, determined the cooking strategy for each type of food, since physical conditions were already fixed by the prototype equipment inside Foodini.

Beef burgers, vegetarian patties and pizza dough were cooked with CO_2 IR laser Foodini equipment. Specific cooking conditions applied for each food matrix are described as follows:

3.2.2.2.1. Beef burgers and vegetarian patties

Beef burgers and vegetarian patties were cooked using the same conditions. Samples were placed on the center of the cooking dish. Cooking time applied was 9 min per side. Burger sides were cooked consecutively. Control software conditions are described in table 3.4. This cooking treatment will be named from now as IR Laser.

Table 3.4. Software parameters for laser cooking of beef burgers and vegetarian patties

Software Parameters	**Values**
Frequency X	1
Frequency Y	350
Size X	9
Size Y	3

The Lissajous system of parametric equations which determined mirrors motion and laser beam cooking area was:

$$\mathbf{x = (9/2)\ \sin((1t)+(\pi\ /2)),\quad y = (3/2)\ \sin(350t)}$$

The graphic representation of the above Lissajous curve (figure 3.9) was plotted with Matplotlib version 3.0.2. (Hunter *et al*, 2007).

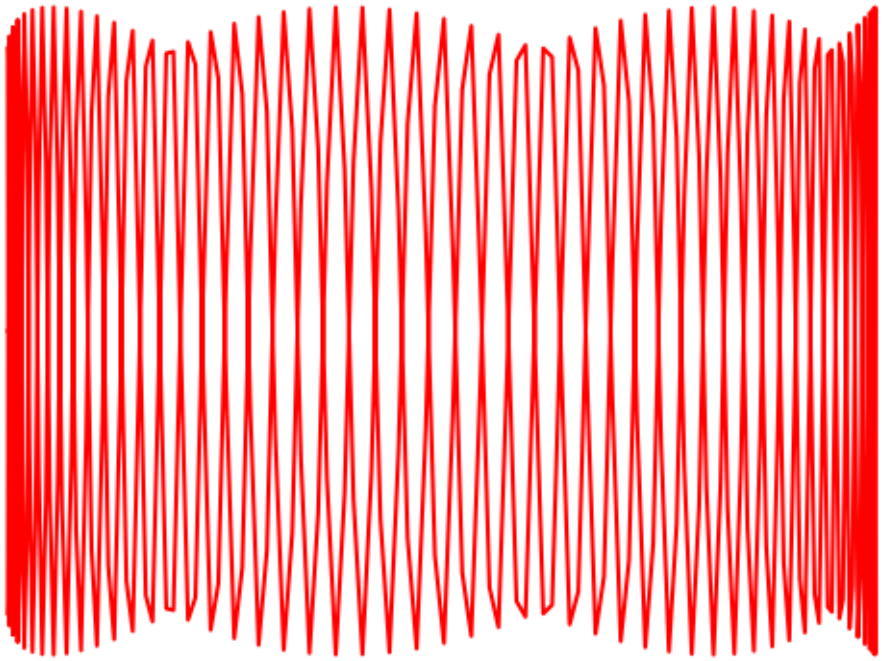

Fig 3.9. Lissajous curve motion used for laser cooking of beef burger and vegetarian patties

Control software fixed the parameter of frequency X = 1 equivalent to 1 s. Then, the time to cover the cooking area was 0.5 s from left to right.

The cooking area covered by the curve, corresponding to the area of laser impact, was theoretically 90x30 mm. Due to the distance from the mirror to the sample, and the inner physical characteristics of galvo-scanner system, the real area of impact measured on the dish was (79±1 mm) x (40±1mm). This area covered the whole surface of the sample because of dish rotation (figures 3.10 and 3.11). Moreover, galvanometers were closed to their working capacity limit, since it was not possible to increase the size of both axis or the frequency of Y axis due to overheating of galvo-scanner system.

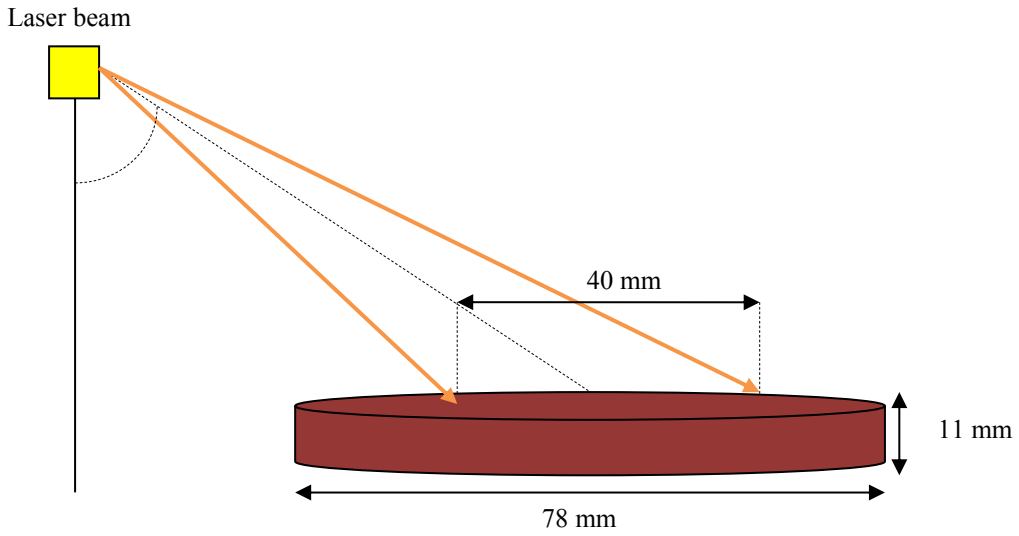

Fig 3.10. Side view of the cooking area for beef burgers and vegetarian patties

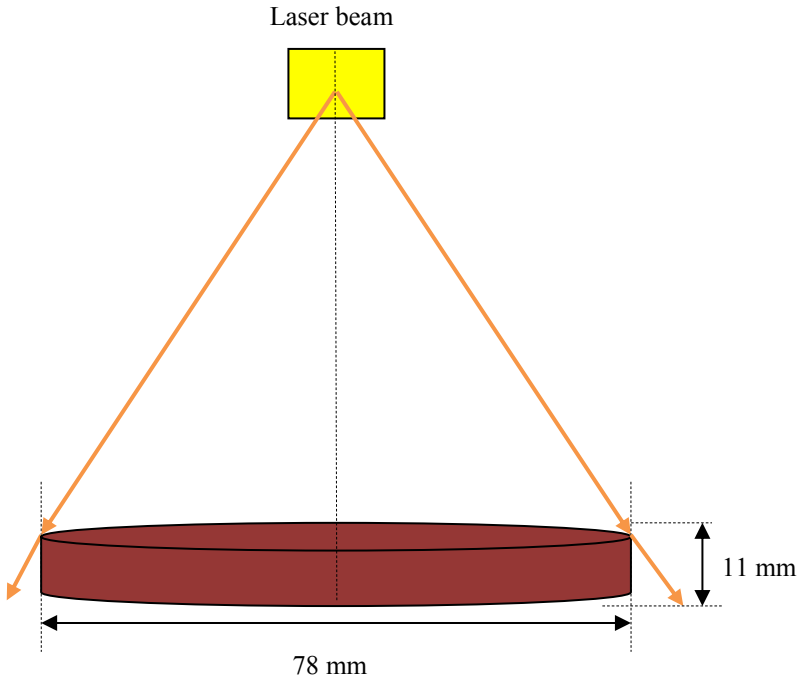

Fig 3.11. Frontal view of the cooking area for beef burgers and vegetarian patties.

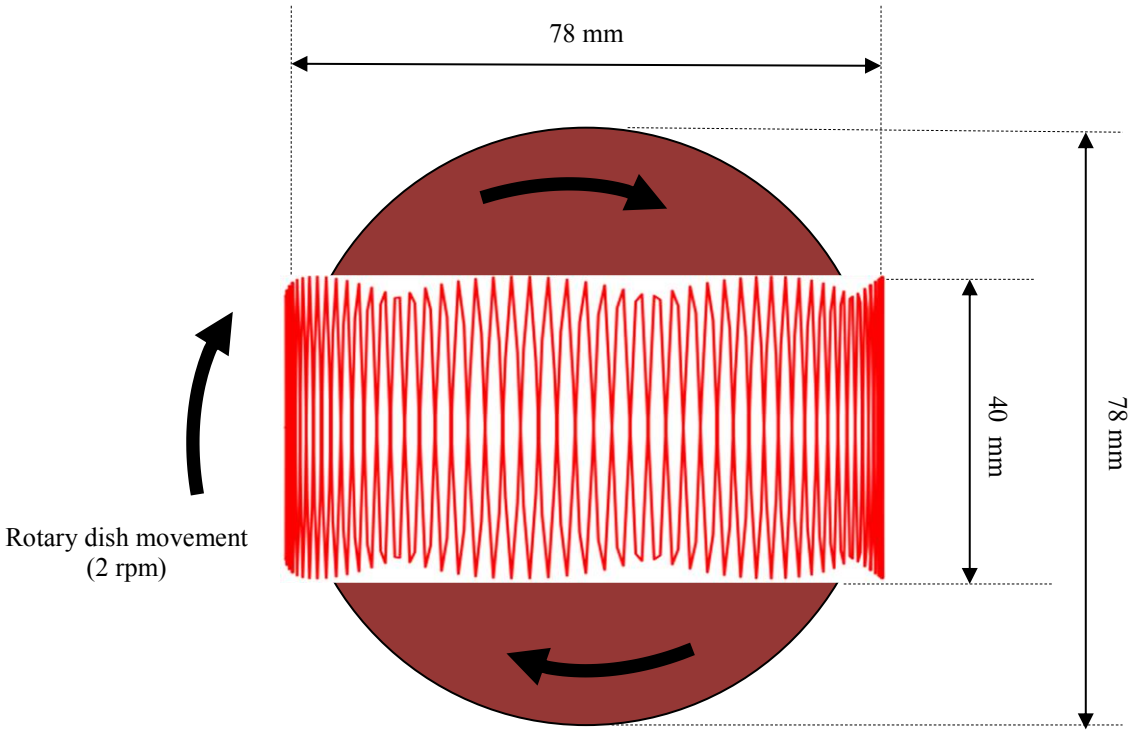

Fig 3.12. Top view of the cooking area for beef burgers and vegetarian patties.

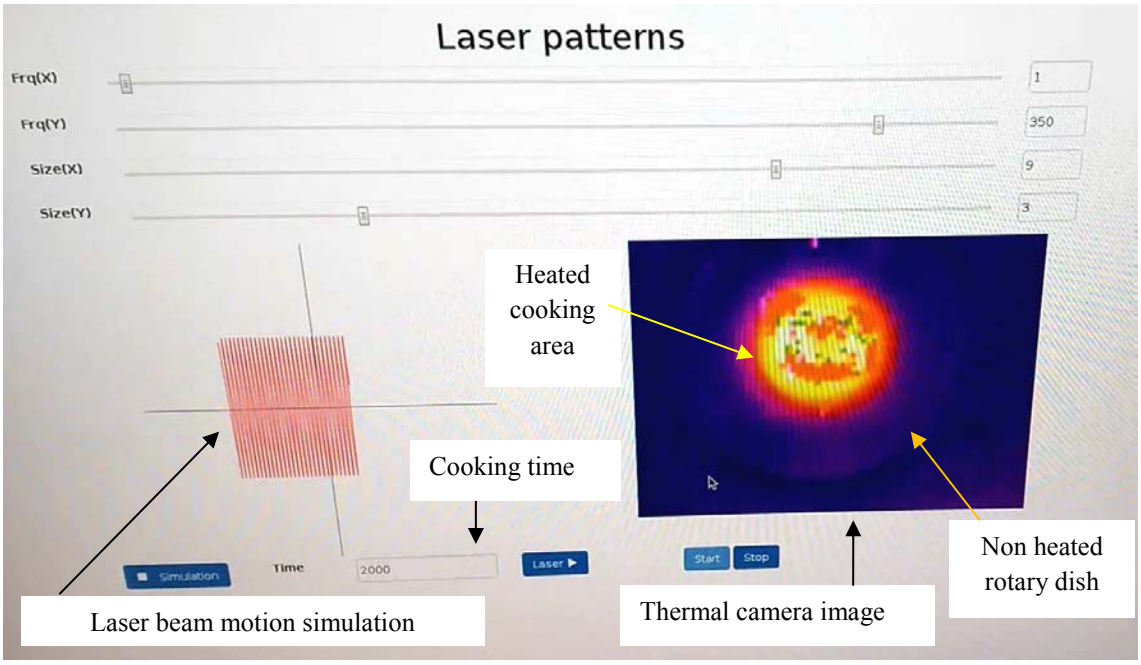

Fig 3.13. Control software display of the CO_2 IR laser Foodini Equipment

Since the dish was continuously rotating, the cooking area became a circle which covered the entire sample surface: top side and lateral side (figures 3.11 and 3.12). Thermal

camera (figure 3.13) showed that radiation heat was only applied in the cooking area where laser beam was directed. The non-heated areas of the dish, where laser beam did not impact, remained at room temperature.

3.2.2.2.2. Pizza dough

Pizza dough samples were placed on the geometrical center of the cooking dish. Cooking time applied was 16 min for the first side and 11.5 min for the second side. Pizza sides were cooked consecutively. Software parameters and their time of application varied during cooking process. Cooking conditions for each pizza dough side are described in table 3.5. This cooking treatment will be named from now as IR Laser.

Table 3.5. Software conditions for laser cooking of pizza dough

			Software Parameters			
Side	Lissajous equation	Time (min)	Frequency X	Frequency Y	Size X	Size Y
Top[a]	1	10	1	250	11	4
Top	2	3.5	1	250	12	3
Top	3	1.5	1	250	12	2
Top	4	1	1	250	12	1
Bottom[b]	1	7	1	250	11	4
Bottom	2	2.5	1	250	12	3
Bottom	3	1.5	1	250	12	2
Bottom	4	0.5	1	250	12	1

[a]first side; [b]second side

The Lissajous system of parametric equations for each software condition was:

Lissajous equation 1: $\mathbf{x = (11/2)\ \sin((1t)+(\pi/2)),\quad y = (4/2)\ \sin(250t)}$

Lissajous equation 2: $\mathbf{x = (12/2)\ \sin((1t)+(\pi/2)),\quad y = (3/2)\ \sin(250t)}$

Lissajous equation 3: $\mathbf{x = (12/2)\ \sin((1t)+(\pi/2)),\quad y = (2/2)\ \sin(250t)}$

Lissajous equation 4: $\mathbf{x = (12/2)\ \sin((1t)+(\pi/2)),\quad y = (1/2)\ \sin(250t)}$

An example of the graphic representation of Lissajous equations plotted with Matplotlib version 3.0.2. (Hunter *et al*, 2007) can be observed in figure 3.14.

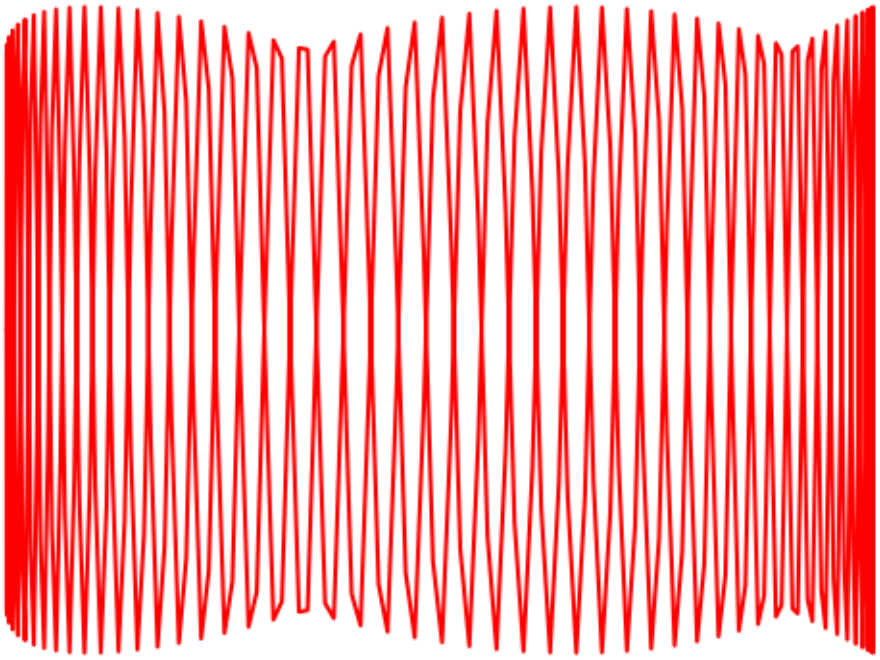

Fig 3.14. Lissajous curve (equation 1) applied for laser cooking of pizza

The cooking area covered by the curve, corresponding to the area of laser impact, changed depending on software conditions. Theoretical areas and the corresponding real measured areas for each software condition are shown in table 3.6. Figures 3.15, 3.16, 3.17 and 3.18 show the laser impact on the surface of pizza dough for each Lissajous curve (using real scale).

Table 3.6. Theoretical and measured cooking areas of Pizza dough for each software conditions and Lissajous equation.

	Theoretical area		Measured area	
Lissajous equation	Size X (mm)	Size Y (mm)	Size X (mm)	Size Y (mm)
1	11	4	9.9±3	5.5±2
2	12	3	10.7±3	4.0±1
3	12	2	10.7±2	2.7±1
4	12	1	10.7±1	1.5±1

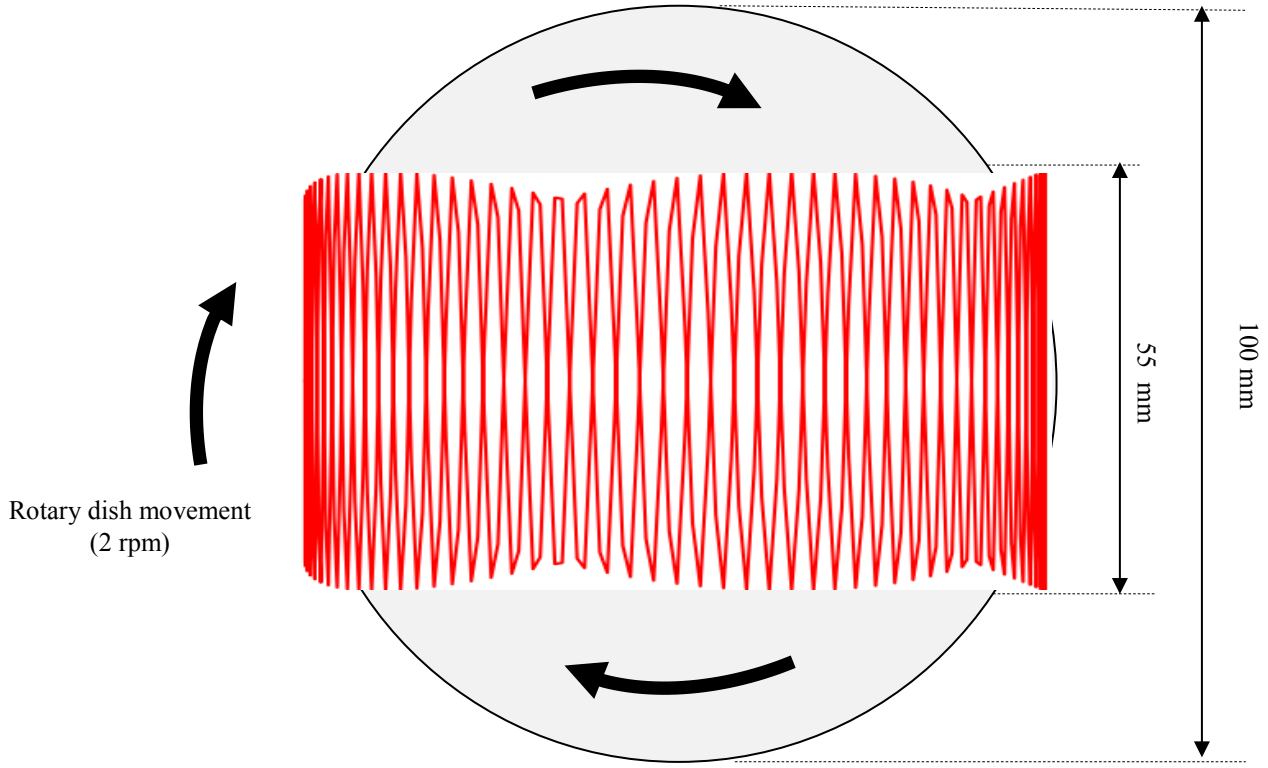

Fig 3.15. Top view of pizza cooking area for the first software condition (equation 1). .

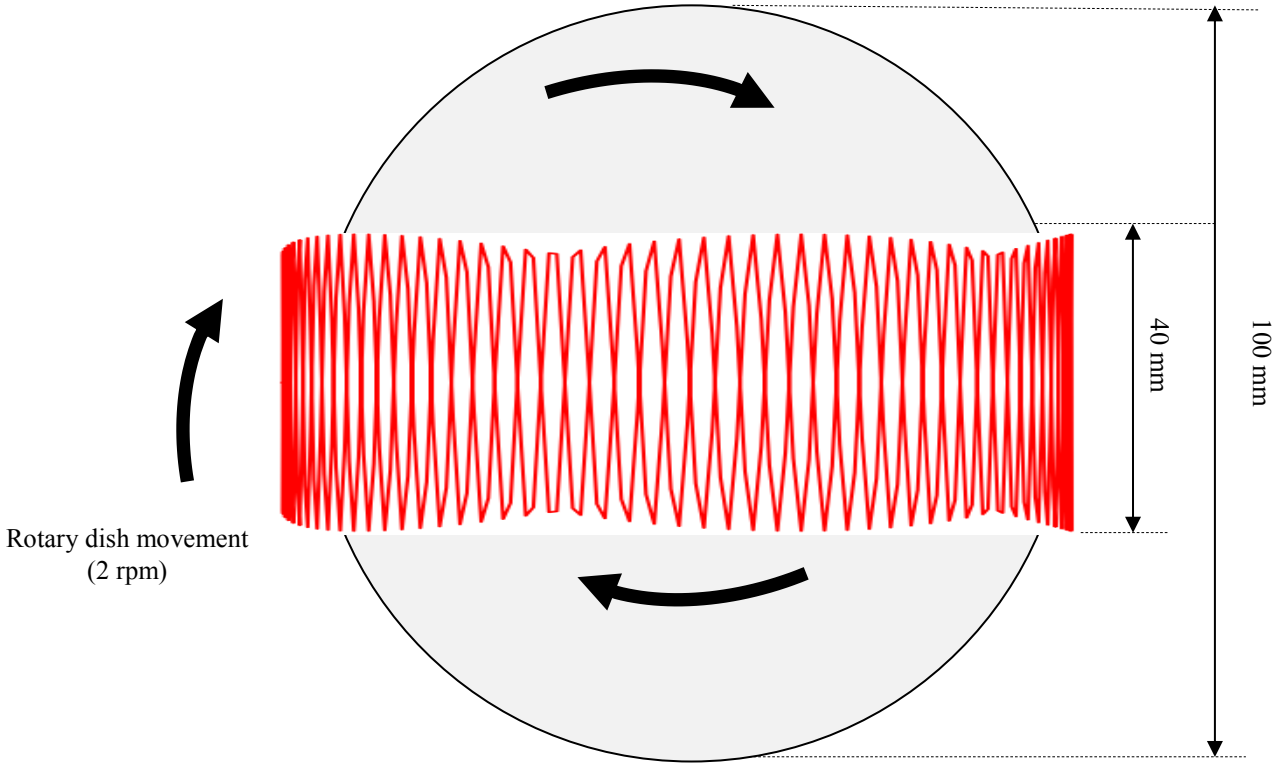

Fig 3.16. Top view of pizza cooking area for the second software condition (equation 2).

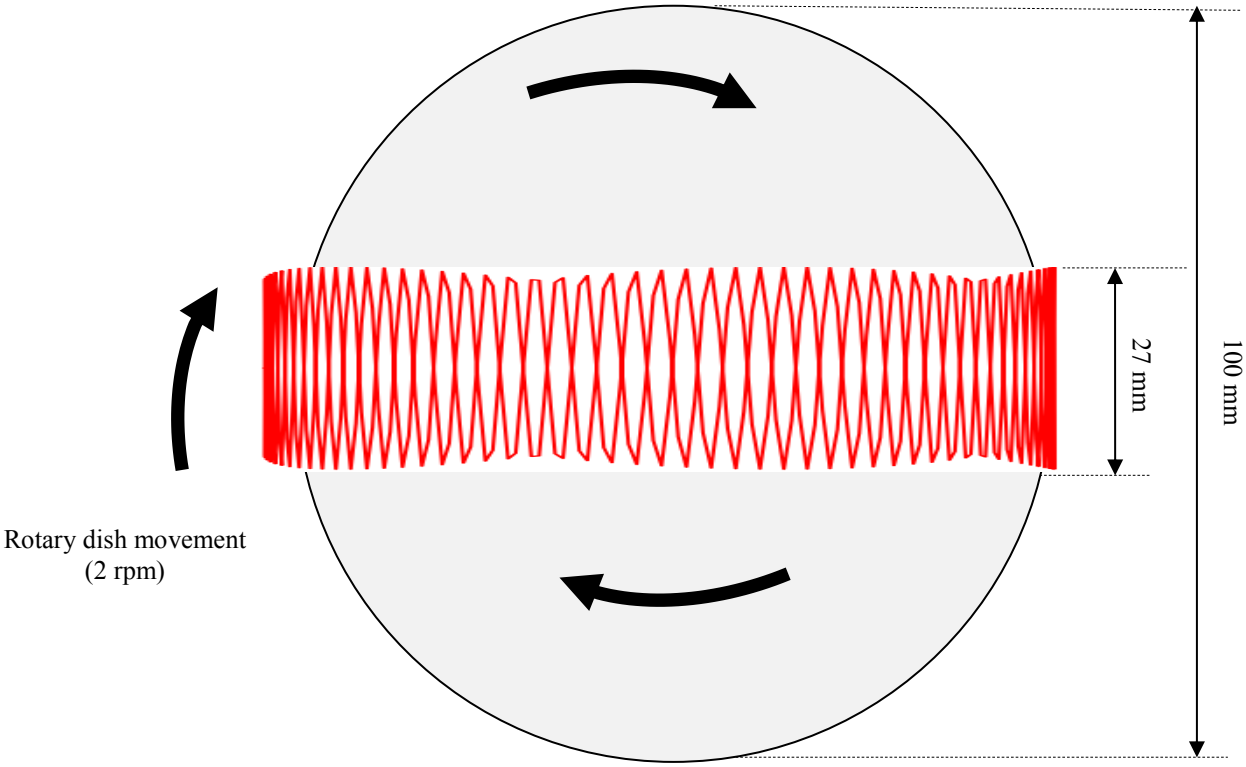

Fig 3.17. Top view of pizza cooking area for the third software condition (equation 3).

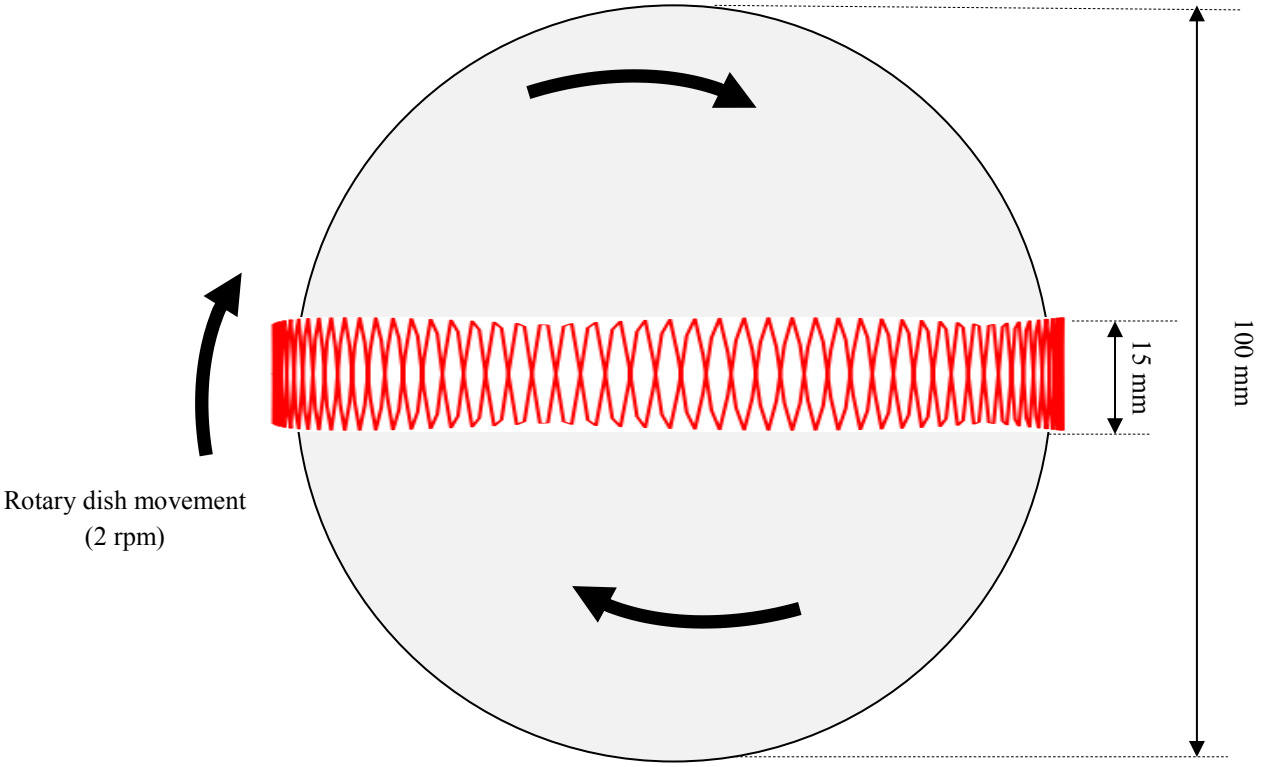

Fig 3.18. Top view of pizza cooking area for the fourth software condition (equation 4).

3.2.3. IR oven cooking

Beef burgers, vegetarian patties, pizza dough and mashed potatoes were cooked with an IR oven (medium wavelength 2.2 – 3.2 μm) (B25.001, 1300 W, BEEM GmbH, Hesse, Germany). Samples were cooked using convector mode and placed in the middle stage of cooking chamber. Time and temperature conditions are described in table 3.7. This cooking treatment will be named from now as IR Oven.

Table 3.7. Temperature and time applied in infrared oven for each food matrix

Food matrix	Temperature	Time
Beef burger	175°C	15 min 30 s
Vegetarian patty	175°C	16 min 30 s
Pizza dough (Finissima)	220°C	3 min 30 s
Pizza dough (Tradizionale)	220°C	6 min
Mashed potatoes bites	180°C	5 min 30 s

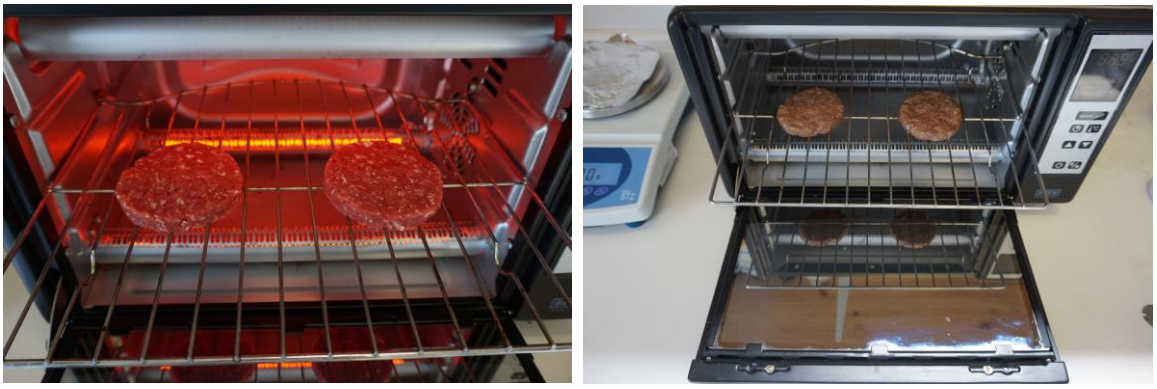

Fig 3.19. Beef burgers cooking process with Infrared oven treatment

3.2.4. Electric barbeque grill

Beef burgers were cooked with an electric barbeque grill (PG 2791, 2500 W, SEVERIN Elektrogeräte GmbH, Sundern, Germany). Burgers were cooked during 5 min and 25 s per side, at maximum power, with grill surface at 125ºC. This cooking treatment will be named from now as BBQ Grill

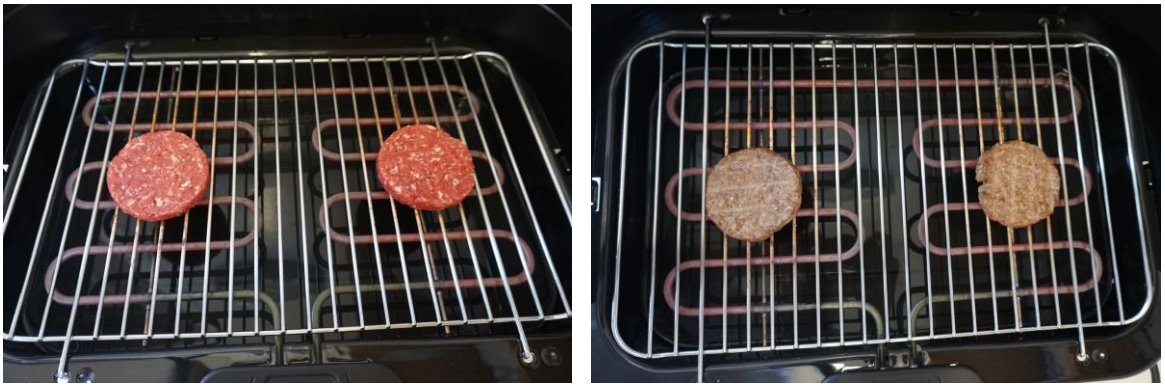

Fig 3.20. Beef burgers cooking process with electric barbecue grill treatment

3.2.5. Electric flat grill

Beef burgers and vegetarian patties were cooked with an electric flat grill (Table Grill Pro 102300, 2000 W, Smartwares Group, PRINCESS®, Tilburg, Germany). Burgers and patties were cooked during 2 min and 30 s per side at 180 °C. This cooking treatment will be named from now as Flat Grill.

Fig 3.21. Beef burgers cooking process with electric flat grill treatment.

3.2.6. Deck oven

Finissima pizza dough was cooked with a deck oven (Model DC-21, 14.4 kW, Sveba Dahlen AB, Fristad, Sweeden). Samples were cooked at 220°C during 5 min. This cooking treatment will be named from now as Deck Oven.

3.2.7. Convection oven

Tradizionale pizza dough was cooked with a convection oven (Model TY350BCL, 1500 W, MyWave, Pasapair S.L., Madrid, Spain). Samples were cooked at 220°C during 7 min 40 s. This cooking treatment will be named from now as Convection Oven.

3.2.8. Traditional method

To prepare mashed potatoes bites, liquid ingredients were heated up to 100ºC and mixed with dry ingredients. This cooking treatment will be named from now as Traditional Method.

3.3. Parameters measured

3.3.1. Cooking loss (%)

The weight of beef burgers, vegetarian patties, pizza dough and mashed potatoes bites was measured at 20±2°C before and after cooking to calculate cooking loss using the formula: Cooking Loss (%) = (weight before cooking- weight after cooking) x 100 / weight before cooking.

3.3.2. Moisture and proximate analyses

Moisture and proximate analyses of protein, fat and ash content were performed for beef burgers, vegetarian patties, pizza dough and mashed potatoes bites following the official methodology described by the Association of Official Analytical Chemists (AOAC International, 2005).

3.3.3. Water activity

Water activity of beef burgers, vegetarian patties, pizza dough and mashed potatoes bites were measured with a dew point hygrometer (Aqualab® model S3/TE, Decagon Devices, Inc., Washington, USA) at 25°C.

3.3.4. Texture analysis

Texture analyses were carried out using a TA-TX2 texture analyzer (Stable Micro Systems, Surrey, UK) equipped with a 30-kg load cell.

3.3.4.1. Beef burgers

Texture profile analysis and cutting force analysis were performed on three samples taken from a single burger, prepared specifically for each type of analysis. Uniform circular samples of 25 mm diameter and 10 mm thickness were obtained with a cutter mold.

Texture profile analysis was carried out using a 50 mm diameter aluminum cylindrical probe, and probe speed was set to 5 mm/s to compress the center of the burger to a 50% of its original height. Time between compressions was 5 s. Parameters measured were hardness (= peak force of the first compression) and springiness (= height of sample after second compression/height of sample after first compression).

Cutting force analysis was performed using a Warner–Bratzler blade with a guillotine aluminum probe. Probe speed was set to 2 mm/s. The center of the burger was cut completely and the maximum cutting force was recorded.

3.3.4.2. Vegetarian patties

Cutting force analysis was performed on three samples taken from a single burger. Uniform circular samples of 25 mm diameter and 10 mm thickness were obtained with a cutter mold. Measures were performed using a Warner–Bratzler blade with guillotine aluminum probe. Probe speed was set to 2 mm/s. The center of the patty was cut completely and the maximum cutting force was recorded.

3.3.4.3. Pizza dough

Penetration analysis was performed on three different points of each single pizza dough sample. Measures were performed using a cylindrical penetration stainless steel probe with 3 mm diameter and 50 mm length. Probe speed was set to 0.5 mm/s. Pizza dough sample was pierced completely and the maximum penetration force was recorded.

3.3.4.4. Mashed potatoes bites

Compression analysis was individually performed for each mashed potatoes bite sample. Measures were performed using a 100 mm diameter aluminum cylindrical probe, and probe speed was set to 1 mm/s to compress the sample for 2.5 mm distance. The maximum force of compression was recorded.

3.3.5. Differential scanning calorimetry

Thermograms were obtained by differential scanning calorimetry (DSC) using a Mettler–Toledo calorimeter (model 821, Massachusetts, EUA). Samples of 10–15 mg were weighed to an accuracy of 0.1 mg on a 40 µL aluminium pan. Beef burgers were scanned at a heating rate of 1°C/min from 25 to 95°C and pizza dough samples were scanned at a heating rate of 5°C/min from -50 to 150°C. The reference pan contained 30 mg of aluminium oxide (Al_2O_3) (Aldrich-Chemical Co, Gillinham-Dorset, UK) to approximate the heat capacity of the sample. From the curve obtained, the onset temperature (To) and conclusion temperature (Tc) were used to calculate peak areas ΔH (J/g) using the software provided by the manufacturer.

3.3.6. Color analysis

External and internal color of beef burgers, vegetarian patties, pizza dough and mashed potatoes bites were measured with a Hunter Lab colorimeter miniScan XTE (Hunter Associates Laboratory INC, Reston, Virginia, USA). First, external color of food samples was measured and, then, each burger was horizontally cut by half to analyze internal color. Three measures were taken on different zones of both external and internal surfaces of two burgers. CIE L^*, a^* and b^* values were measured with an illuminant of D65 and a standard observer of 10°. L^* represents the lightness, with values from 0 (black) to 100 (white), which indicates a perfect reflecting difuser. Chromatic components are represented by a^* and b^* axes. Positive values of a^* are red and negatives values are green, where positive values of b^* are yellow and negative values are blue. ΔE^* (total color difference) was calculated using the formula $\Delta E^* = \sqrt{((\Delta L^*)^2 + (\Delta a^*)^2 + (\Delta b^*)^2)}$.

3.3.7. Polycyclic aromatic hydrocarbons (PAHs) analysis

Polycyclic aromatic hydrocarbons (PAHs) analyses were carried out for beef burgers and Tradizionale pizza dough samples in the second experimental study. PAHs analyses were performed by the Laboratory of Public Health Agency of Barcelona (ASPB). Raw and cooked samples were grinded and homogenized, and extraction procedure was achieved with methylene dichloride (DCM) using an accelerated solvent extraction equipment (ASE) at 85°C and 1500 psi. Extract was purified by a preparative liquid chromatography system (GPC) using a gel filtration column, which allowed a molecular weight separation,

and a collector of different fractions. Fraction containing PAHs was evaporated and dried, and residual components were solved in acetonitrile. PAHs determination was assessed by high performance liquid chromatography method (HPLC) using gradient elution with purified water type 1 and acetonitrile. Chromatographic column was a C18-type specially designed for PAHs, and a fluorescence detector (FLD) for liquid chromatography was used by adapting optimal excitation and emission wavelength for each group of components. Quantification was calculated by external standard method, considering as a correction factor the recovery value of the method for each analyte.

Table 3.8. List of PAHs measured with the minimum detection limit and the recovery values applied for each PAH.

PAH compounds	Detection limit	Recovery values
Cyclopenta[c,d]pyrene	< 10,0 µg/kg	91.3%
Benzo[a]anthracene	< 0,50 µg/kg	89.4%
Chrysene	< 0,50 µg/kg	90.7%
5-Methylchrysene	< 0,50 µg/kg	86.8%
Benzo[j]fluoranthene	< 10,0 µg/kg	89.3%
Benzo[b]fluoranthene	< 0,50 µg/kg	90.4%
Benzo[k]fluoranthene	< 0,50 µg/kg	86.3%
Benzo[a]pyrene	< 0,50 µg/kg	84.9%
Dibenzo[a,l]pyrene	< 0,50 µg/kg	80.8%
Dibenzo[a,h]anthracene	< 0,50 µg/kg	88.0%
Benzo[g,h,i]perylene	< 0,50 µg/kg	88.5%
Indeno[1,2,3,c,d]pyrene	< 0,50 µg/kg	88.6%
Dibenzo[a,e]pyrene	< 0,50 µg/kg	85.8%
Dibenzo[a,i]pyrene	< 1,00 µg/kg	80.0%
Dibenzo[a,h]pyrene	< 2,00 µg/kg	80.8%
Total amount of benzo[a]pyrene, benzo[a]anthracene, benzo[b]fluoranthene and chrysene.	< 2,00 µg/kg	

3.3.8. Sensory evaluation

Consumer tests were carried out for beef burgers, vegetarian patties, pizza dough and mashed potatoes bites. In the first experimental study, two consumer tests were performed for beef burgers with 54 and 52 people, respectively; one consumer test for Finissima

pizza dough with 51 people; and one consumer test for mashed potatoes bites with 50 people. In the second experimental study, one consumer test was carried out with each kind of food: beef burgers, vegetarian patties and Tradizionale pizza dough, with 50 people each. People who participated in sensory tests were regular consumers of the food products evaluated.

Immediately after cooking beef burgers, vegetarian patties and pizza dough Tradizionale, samples were cut by half and placed in codified dishes using three digits randomly. Finissima pizza dough and mashed potatoes bites were placed entirely and individually in codified dishes. One whole sample of each food type from each cooking method was shown to testers to evaluate the general appearance. Consumers evaluated different sample attributes, described in the working plan, using intensity and acceptability scales of seven points. A preference test between samples was also performed following the method described by Kramer et al. (1974). Consumers were asked to rank the samples in order of preference. To obtain the ranking of each sample, each rank position was multiplied by the number of consumers that had selected it, and the sum of the rankings of each sample was calculated. Low values in rank sum of samples indicated that the sample had mainly been ranked in first order of preference.

3.3.9. Microbiological analysis

3.3.9.1. Analysis of non-inoculated samples

Aerobic mesophilic bacteria and lactose-positive *Enterobacteriaceae* (coliforms) were analized in beef burgers and vegetarian patties.

Aerobic mesophilic bacteria were counted on Tryptone Soya agar (TSA) (Oxoid Ltd., Basingstoke, UK). Lactose-positive *Enterobacteriaceae* were counted on Violet Red Bile agar (VRBA) (Oxoid), and on Brilliant Green Bile Lactose broth (BGBL) (Oxoid) by the three-tube most probable number (MPN) method. Raw and cooked samples (25 g) were immediately transferred to a sterile plastic stomacher bag with lateral filter (bbag-03 blender bag, Corning® Gosselin™, Corning, New York, USA) with 225 mL of buffered peptone water (BPW) (Oxoid) and homogenized in a Stomacher® 400 Circulator (Seward Ltd., Worthing, UK) for 1 min. Serial decimal dilutions were prepared and 0.1 mL of each dilution was spread in TSA using a spiral plater instrument (Eddy Jet; IUL Instruments,

Barcelona) (samples with detection limit < 2 log CFU/g) or 1 mL was pour plated on TSA and VRBA (samples with detection limit < 1 log CFU/g). TSA plates were incubated for 48 h at 31°C, and VRBA plates were incubated for 24 h at 31°C.

To enumerate total coliforms by MPN method, 1ml from 1:10, 1:100 and 1:1000 dilutions was inoculated into three sets of tubes containing 10 ml of BGBL broth and inverted Durham tubes. The tubes were incubated for 48 h at 31°C. BGBL broth tubes were examined for gas production or effervescence when tubes were gently agitated. MPN of coliforms was calculated from the proportion of tubes with gas production.

3.3.9.2 Inoculated samples

As described in the Working Plan, in the first and second experimental studies, beef burgers and vegetarian patties were inoculated with *Salmonella* Typhimurium and *Salmonella* Senftenberg at ~7 log CFU/g and ~3 log CFU/g. In the second study, beef burgers were also inoculated with *Escherichia coli* O157:H7 at both concentration levels.

3.3.9.2.1. Bacterial strains and preparation of bacterial cultures

Salmonella Typhimurium (*Salmonella enterica* subsp. *enterica* serovar Typhimurium, CECT 4594, Valencia, Spain), *Salmonella* Senftenberg (*Salmonella enterica* subsp. *enterica* serovar Senftenberg, CECT 4565), and *Escherichia coli* serotype O157:H7 non-verotoxin-producing (CECT 5947) were used in this study. Bacterial strains were grown overnight at 37°C in 25 mL of tryptone soya broth (TSB) (Oxoid) to obtain a suspension of optical density (OD_{600}) 1. The OD 1 bacterial suspension contained ~9 log CFU/mL.

3.3.9.2.2. Inoculation

Inoculated beef burgers and vegetarian patties were prepared with two contamination levels (~3 log CFU/g and ~7 log CFU/g) for each bacterial strain. Ten mL of ~9 log CFU/mL bacterial suspension were added to 500 g of raw sample preparation and thoroughly mixed to obtain ~7 log CFU/g. Bacterial suspension was diluted to obtain a ~5 log CFU/mL suspension that was added to 500 g of raw sample preparation and

thoroughly mixed to obtain ~3 log CFU/g. Inoculated beef burgers and vegetarian patties (50 g) were prepared and stored at 4°C. All inoculated samples were cooked and analyzed the same day of preparation.

Previous to inoculation, non-inoculated raw beef burgers and vegetarian patties were prepared to verify the absence of endogenous *Salmonella* spp., or *E. coli* 0157 in meat.

3.3.9.2.3. Microbiological analysis of Salmonella Typhimurium*, Salmonella* Senftenberg *and E. coli* 0157:H7.

Samples (10 g of beef burger; 25 g of vegetarian patty) were transferred to a sterile stomacher bag with 90 mL of BPW and homogenized in a stomacher (Seward) for 1 min. Serial decimal dilutions were prepared and spread in Xylose Lysine Deoxycholate agar (XLD) (Oxoid) plates for *Salmonella*, or in Cefixime Tellurite-Sorbitol MacConkey agar (CT-SMAC) (Oxoid) plates for *E. coli* 0157:H7, using an spiral plater instrument. After incubation for 24 h at 37 °C, *Salmonella* or *E. coli* O157:H7 colonies were counted. At least five colonies were picked from XLD or CT-SMAC plates and checked using immuno-agglutination latex tests (Salmonella Test Kit and E. coli O157 Latex Test; Oxoid).

3.3.9.2.4. Survival of Salmonella Typhimurium*, Salmonella* Senftenberg *and E. coli* 0157:H7 *following cooking treatment.*

Samples without presence of *Salmonella* colonies in XLD plates were pre-enriched adding 90 ml of BPW and incubated for 24 h at 37°C. Pre-enriched samples were inoculated in two selective enrichment media: 1 mL into 10 mL of Müller-Kauffmann Tetrathionate Novobiocine broth (MKTTn) (bioMérieux®, Marcy l'Etoile, France) and 0.1 mL into 10 ml of Rappaport-Vassiliadis Soya broth (RVS-T) (bioMérieux®). Inoculated MKTTn broth was incubated for 24 h at 37°C, and inoculated RVS-T broth was incubated for 24 h at 41.5°C. Both inoculated broths of each sample were spread in XLD agar and in chromogenic medium for selective isolation and identification of *Salmonella* (CHROMID® Salmonella ELITE, bioMérieux®), using a spiral plater instrument. After incubation for 24 h at 37 °C, at least five colonies from both XLD and chromogenic medium plates were checked using the i±uno-agglutination latex test Salmonella Test Kit (Oxoid).

Samples without presence of *E. coli* O157:H7 colonies in CT-SMAC plates were enriched with 90 mL of BPW, and incubated for 24 h at 37°C. Samples were spread in CT-SMAC agar and in chromogenic medium for selective isolation and identification of *E. coli* O157:H7 (CHROMID® E.coli O157:H7, bioMérieux®) using a spiral plater instrument. After incubation for 24 h at 37 °C, at least five colonies were picked from the CT-SMAC and chromogenic medium plates and checked using the immuno-agglutination latex test *E. coli* O157 Latex Test (Oxoid).

3.3.10. Experimental design and statistical analysis

For each food matrix, three independent experiments were conducted to evaluate the effect of cooking methods on microbiological characteristics and three more independent experiments to evaluate the cooking effect on physico-chemical characteristics.

For microbiological analyses, in each experiment, two food units of each product for each cooking method were prepared and analyzed (n=6).

For physico-chemical analyses, a variable number of food units, depending on the type of product, were prepared in order to have enough sample amount to carry out the different analyses: burgers, 6 units; patties, 4 units; pizzas, 4 units; bites, 8 units.

For cooking loss, water activity, moisture and proximate composition analyses, two units per experiment were used, and one sample per unit was analyzed (n=6). For differential scanning calorimetry, two units per experiment were used, and two samples per unit were analyzed (n=12). For TPA, cutting and penetration texture analyses, two units per experiment were used, and three samples per unit were analyzed (n=18). For compression analysis, six units per experiment were used, and one sample per unit was analyzed (n=18).

For color analyses, number of measures varied depending on the type of product. For internal color of burgers and patties, two units per experiment were used, and six samples per unit were analyzed (n=36). The same number of measures were taken for external color (n=36). For external color of pizzas, each cooking side was analyzed separately, two units per experiment were used, and three samples per unit and per side were analyzed (n=18). For external color of bites, six units per experiment were used, and one sample per unit was analyzed (n=18).

For PAHs analyses, three units from a single experiment were analyzed (n=3).

For consumer tests, specific experiments to elaborate enough samples for sensory analyses were performed (n≥50).

Results were analyzed by analysis of variance (ANOVA) using Statgraphics® (model Centurion™ XVII.II, Statpoint Technologies, Inc., Warrenton, Virginia, USA). Tukey test was used for comparison of sample means. Evaluations were based on a significance level of $p<0.05$.

3.4. Numerical Model

In this section, the features of the computational fluid dynamics (CFD) model employed to simulate the cooking process of beef burgers and vegetal patties by means of the ray tracing method are explained in detail. First, the experimental measure of the internal temperatures and cooking loss in food samples employed to validate the numerical model is explained. Then, the physical equations that regulate the heat transfer procedure are introduced. The boundary conditions are also detailed, defining the energy input from the laser beam and the dispersive conditions. Finally, some details on the discretization process needed to carry out finite-volume heat transfer simulations are given.

3.4.1. Evolution of the internal temperature and cooking loss in food samples cooked with the CO2 IR Laser Foodini system

Evolution of cooking loss and internal temperatures were measured in beef burgers and vegetarian patties. Two internal temperatures were measured using a penetration probe-type thermocouple (0900 0530, Instrumentos Testo S.A.): temperature at the geometrical centre of sample (defined as *Central Temperature*), and temperature at 6±1 mm of penetration depth from central lateral side (defined as *Lateral Temperature*). Evolution of cooking loss and temperatures was measured each minute during 18 min (9 min per side). One new raw sample was prepared and cooked to measure the temperature at each time point.

Three independent experiments were conducted. Two units per experiment and time point were used, and one sample per unit was analyzed (n=6).

3.4.2. Governing equation for food cooking processes

The numerical simulation of the meat cooking process was approached in this work by resolving the heat conduction equation in a domain that represents the burger shape. The following equation was solved:

$$\rho c_p \frac{\partial T}{\partial t} = \nabla \cdot (k \nabla T) \qquad [1]$$

where the left side term is the accumulated heat, while the right hand term represents the conductive term. The various magnitudes are listed here:

- t time [s]
- T temperature [K]
- ρ density [kg/m^3]
- c_p specific heat [J/kgK]
- k thermal conductivity [W/mK]

This equation models the heat transfer flux for non-boundary volumes. The physical properties were calculated taking into account food components: water, protein, fat, carbohydrates and ashes. In the case of beef meat, only water, protein, fat and ashes were

used for calculations, since it was considered that carbohydrates content was negligible. In our model, the various thermo-physical coefficients assumed variable values along the simulation as function of the temperature, and cooking losses in terms of water were taken into account. Time dependence for each component was expressed in polynomial form, using the correlation proposed in ASHRAE, 2006 (tables 3.9, 3. 10 and 3.11).

Thermal conductivity (W/m·K): parallel model consists of the sum of the thermal conductivities of the food constituents multiplied by their volume fractions (y_i):

$$k = \sum_{i}^{n} y_i k_i \qquad [2]$$

Table 3.9. Thermal conductivity model for food components (-40 ≤ t ≤150°C) and for water (0 ≤ t ≤150°C).

Food component	Thermal conductivity model
Protein	$k = 1.7781 \times 10^{-1} + 1.1958 \times 10^{-3}t - 2.7178 \times 10^{-6}t^2$
Fat	$k = 1.8071 \times 10^{-1} - 2.7604 \times 10^{-4}t - 1.7749 \times 10^{-7}t^2$
Carbohydrate	$k = 2.0141 \times 10^{-1} + 1.3874 \times 10^{-3}t - 4.3312 \times 10^{-6}t^2$
Ash	$k = 3.2962 \times 10^{-1} + 1.4011 \times 10^{-3}t - 2.9069 \times 10^{-6}t^2$
Water	$k = 5.7109 \times 10^{-1} + 1.7625 \times 10^{-3}t - 6.7036 \times 10^{-6}t^2$

Specific heat (kJ/kg·K): specific heat of an unfrozen food is determined as function of the mass fraction (x_i) of the i element:

$$c_p = \sum_{i}^{n} x_i c_{p,i} \qquad [3]$$

Table 3.10. Thermal specific heat model for food components (-40 ≤ t ≤150°C) and for water (0 ≤ t ≤150°C).

Food component	Specific heat model
Protein	$C_p = 2.0082 + 1.2089 \times 10^{-3}t - 1.3129 \times 10^{-6}t^2$
Fat	$C_p = 1.9842 + 1.4733 \times 10^{-3}t - 4.8008 \times 10^{-6}t^2$
Carbohydrate	$C_p = 1.5488 + 1.9625 \times 10^{-3}t - 5.9399 \times 10^{-6}t^2$
Ash	$C_p = 1.0926 + 1.8896 \times 10^{-3}t - 3.6817 \times 10^{-6}t^2$
Water	$C_w = 4.1289 - 9.0864 \times 10^{-5}t + 5.4731 \times 10^{-6}t^2$

Density (kg/m^3): similarly, the density was calculated as

$$\rho = \sum_{i}^{n} x_i \rho_i \qquad [4]$$

Table 3.11. Thermal density model for food components (-40 ≤ t ≤150°C) and for water (0 ≤ t ≤150°C).

Food component	Density model
Protein	$\rho = 1.3299 \times 10^3 - 5.1840 \times 10^{-1} t$
Fat	$\rho = 9.2559 \times 10^2 - 4.1757 \times 10^{-1} t$
Carbohydrate	$\rho = 1.5991 \times 10^3 - 3.1046 \times 10^{-1} t$
Ash	$\rho = 2.4238 \times 10^3 - 2.8063 \times 10^{-1} t$
Water	$\rho = 9.9718 \times 10^2 + 3.1439 \times 10^{-3} t - 3.7574 \times 10^{-3} t^2$

Based on the results obtained by Sargolzaei *et al*. (2011), CFD analysis was applied in our numerical study with the additional feature of taking into account the time and space variable thermal properties of beef burger and vegetarian patty.

3.4.3. Boundary conditions

3.4.3.1. Top boundary condition

In the top part of the burger (or patty) a moving superficial heat source was set, mimicking the heating process applied with the laser beam (ray tracing method). The laser center position was described by the following sinusoidal functions:

$$x_f = \frac{9}{2} sin\left(t + \frac{\pi}{2}\right) \qquad [5]$$

$$y_f = \frac{3}{2} sin(350t) \qquad [6]$$

The actual position of the laser beam was then computed taking in to account the rotation of the burger inside the oven at a constant rotation velocity ω = 0.2094 rad/s (2rpm):

$$x'_f = x_f \cos(\omega t) - y_f \sin(\omega t)$$

$$y'_f = x_f \sin(\omega t) + y_f \cos(\omega t) \qquad [7]$$

[8]

The laser power $Q_{n,laser}$ was multiplied by a dispersive coefficient, C_{losses}. This dispersive coefficient C_{losses} had a given value of 90% during the cooking process of the first sample side, and a value of 80% during the second one. In the points in which the laser was not acting, a dispersive flux, Q_{losses}, was set. The later includes convective, radiative and evaporative effects. This flux was estimated by carrying out a rough balance of the heating process of the burger:

$$\rho c_p \frac{\Delta T}{\Delta t} V = Q_{n,laser} C_{losses} - Q_{losses} \quad [9]$$

where V is the burger volume, ρ and c_p are the average meat properties, and $\Delta T / \Delta t$ is a general temperature gradient extracted from experimental data. Hence, in numerical simulation, a time and space varying Neumann boundary condition was set.

3.4.3.2. Lateral boundary condition

In the lateral boundaries, a Newton boundary condition was applied, mimicking the convective heat transfer between the air at environment temperature and the burger surface:

$$Q_{losses,lat} = h_{lat} S_{lateral} (T_{lateral} - T_{env}) \quad [10]$$

where $S_{lateral}$ is the surface of the lateral boundary, $T_{lateral}$ is the temperature at the lateral surface, and T_{env} is the temperature of the environment (air). A standard convective heat transfer coefficient, h_{lat}, was set.

3.4.3.3. Bottom boundary condition

The bottom boundary condition (sample/glass contact surface) presented a variable temperature during the cooking process. This boundary could not be considered a fixed flux boundary condition nor a fixed temperature one. A specific 0-D numerical model designed for the cooking conditions of the CO_2 IR Laser Foodini system has been implemented, in order to estimate the temperature evolution at the bottom boundary.

The 0-D model considers the presence of the glass dish below the burger, which changes its temperature along the heating process by absorbing part of the heat released by the burger. The system, shown in Figure 3.22, consists of 2 sub-domains. S1 is the burger subdomain, whose dynamic behavior depends on the energy input, $\mathbf{q_{laser}}$; the heat losses

to the lower plate, $\mathbf{q_{plate,1}}$; and the heat losses to the environment, $\mathbf{q_{losses,1}}$. The latter depends on a global loss coefficient, h_b, which includes convective, radiative and evaporative losses. The governing discrete equation for the subdomain S1 reads as:

$$\rho_b c_{p,b} \frac{T_b^{i+1} - T_b^i}{\Delta t} V_b = q_{laser} S_{laser} - h_b S_{burger \to air} \left(T_b^i - T_{env}\right) - q_{plate,1} S_{burger \to plate} \quad [11]$$

In the equation, a formulation for $\mathbf{q_{plate,1}}$ is missing. In our model, it was considered as a conductive heat flux trough a thin sector of the burger (thickness, *H1*) in contact with the plate of temperature T_s, thus reading as:

$$q_{plate,1} = k_b \frac{T_b^i - T_s}{H1} \quad [12]$$

On the other side, S2 is the glass plate subdomain, whose behavior depends on the energy input released by the bottom part of the hamburger, $\mathbf{q_{plate,2}}$, and the heat losses to the environment, $\mathbf{q_{losses,2}}$, again, depending on a global convective coefficient, h_p. The governing discrete equation reads as:

$$\rho_p c_{p,p} \frac{T_p^{i+1} - T_p^i}{\Delta t} V_p = -h_p S_{plate \to air} \left(T_p^i - T_{env}\right) + q_{plate,2} S_{burger \to plate} \quad [13]$$

In this case, $\mathbf{q_{plate,2}}$ is also considered as a conductive flux through a superficial slice of thickness H2, reading as:

$$q_{plate,2} = k_p \frac{T_p^i - T_s}{H2} \quad [14]$$

The thicknesses H1 and H2 are considered as 1/8 of the thickness of the burger and the plate, respectively. The solution process for the proposed 0-D model consists in solving the temperature, T_p and T_b for each time step, imposing the equality of the fluxes through the plate-burger contact. An iterative process is needed at each time step to identify the value of T_s that satisfies the equality of the fluxes. The complete algorithm was depicted in Figure 3.23, delivering the time evolution of temperatures T_s, T_p and T_b.

Figure 3.24 shows a typical plot for the evolution of T_p, T_b and T_s. It can be observed that the obtained profile for T_b followed closely the experimental results. Experimental results of the *Central Temperature* of beef burgers are shown in the figure 3.24 since they are needed for validation of the 0-D model.

Hence, in numerical simulations the time-varying profile of T_s was set as bottom boundary condition (Dirichlet function boundary condition).

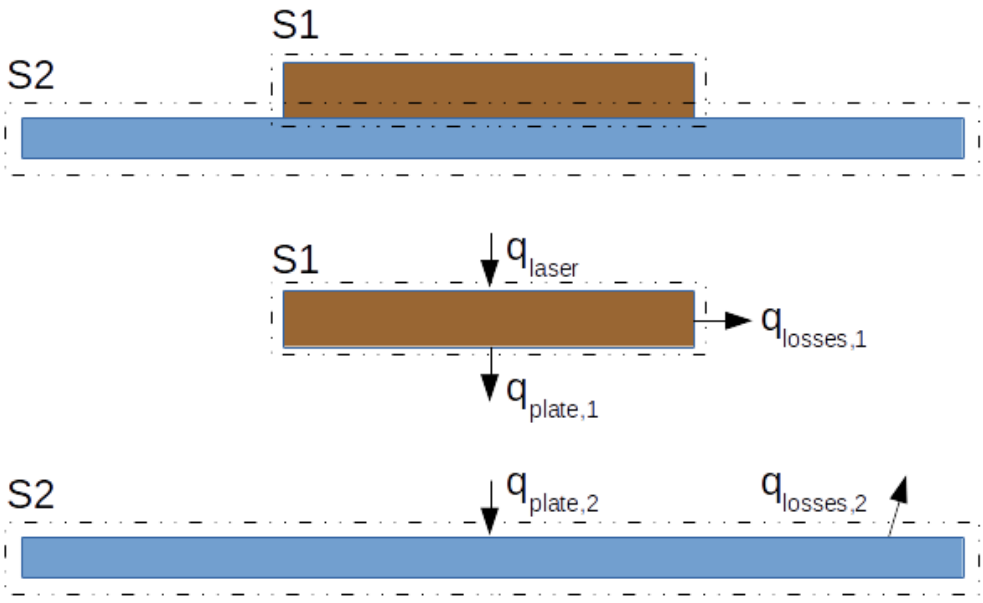

Figure 3.22. Scheme of the 0-D model for the plate-burger system.

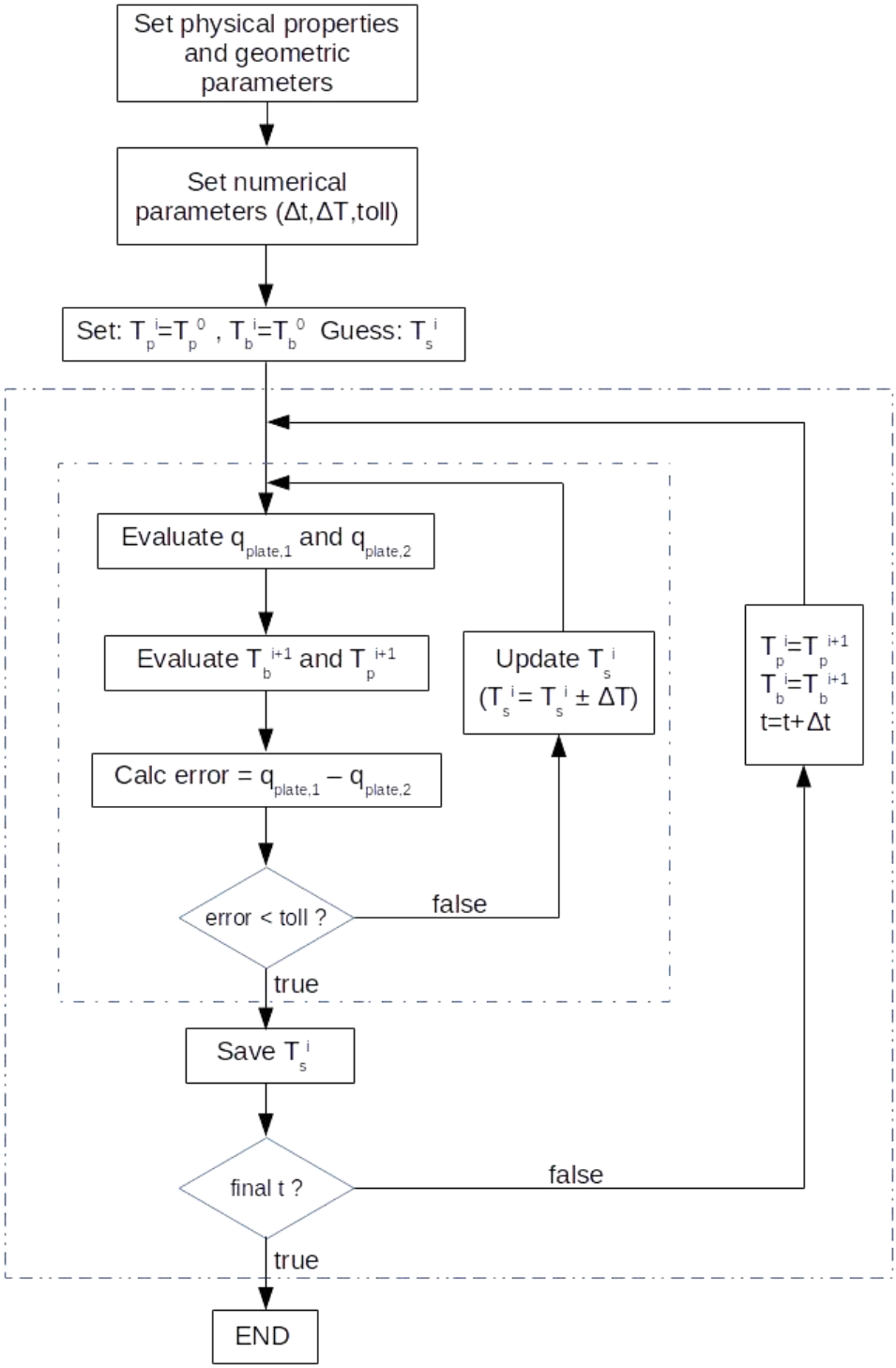

Figure 1.23. Algorithm employed for the resolution of the 0-D model. The result consists in the estimated profile of the contact temperature between plate and burger, Ts. Toll value is fixed at 0.001.

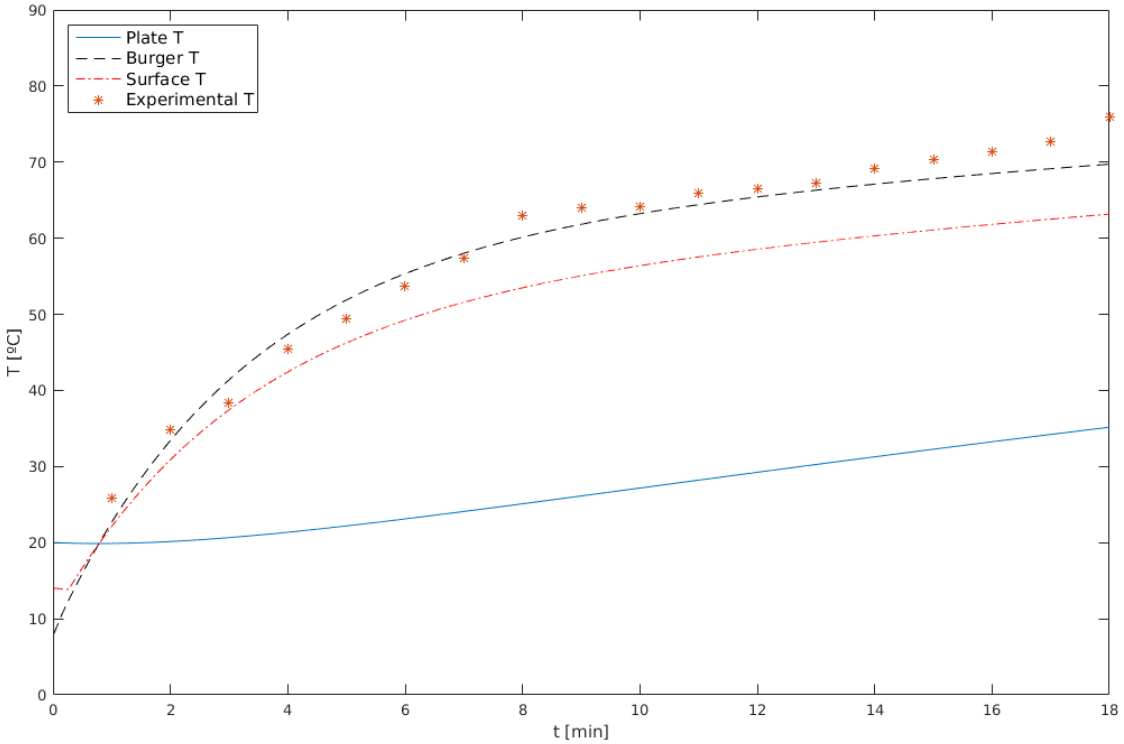

Figure 3.24. Temperature profiles obtained from the 0-D model used for the estimation of Ts (beef burger case).

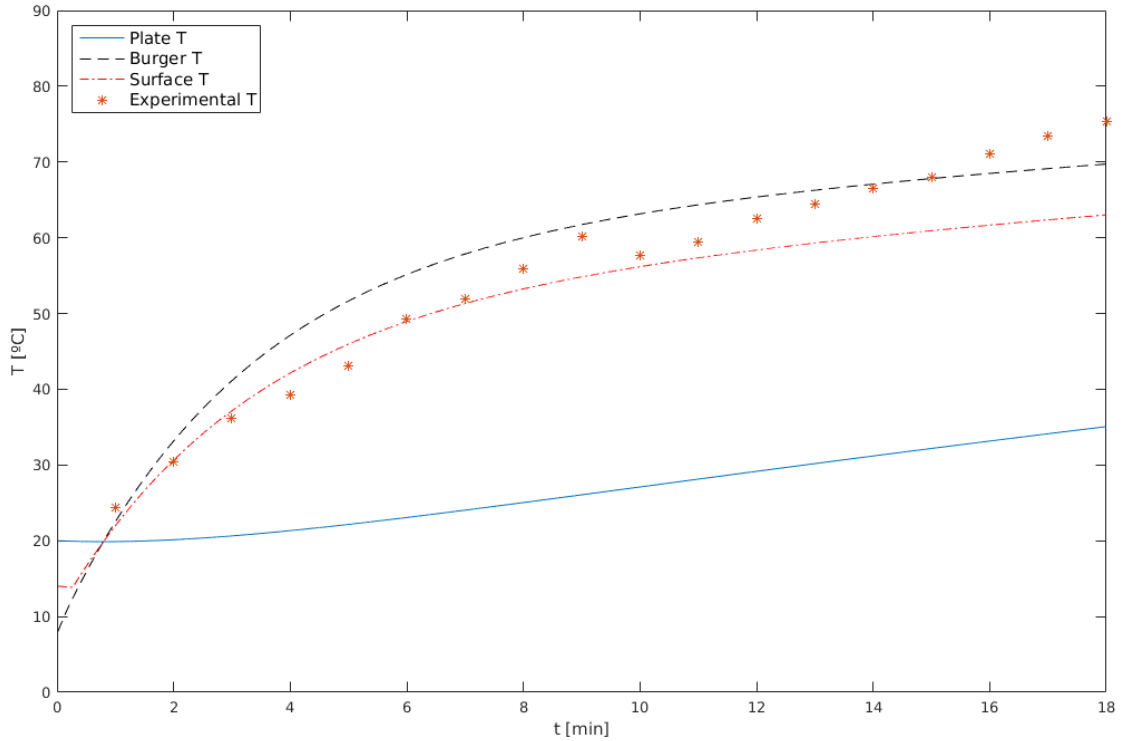

Figure 3.25. Temperature profiles obtained from the 0-D model used for the estimation of Ts (vegetarian patty case).

3.4.4. Explanation of the numerical model

3.4.4.1. Discretization

The simulations were carried out by employing a finite-volume strategy. The approach consisted in subdividing the domain into several small hexahedron cells named as *control volumes* (CV). The governing equation was then discretized and resolved within each CV. In its discrete form, on a simplified 2D basis, the equation reads as:

$$\rho c_p \frac{T_C^{i+1} - T_C^i}{\Delta t} V = k_n \frac{T_N^i - T_C^i}{d_N} \Delta x - k_s \frac{T_C^i - T_S^i}{d_S} \Delta x + k_e \frac{T_E^i - T_C^i}{d_E} \Delta y - k_s \frac{T_C^i - T_W^i}{d_W} \Delta y \qquad [15]$$

where V is the CV volume (V=ΔxΔy) and Δt is the time step. Figure 3.25 depicts the positioning of discrete quantities, as well as the other geometrical features. Thermal conductivities k_i were calculated in intermediate points, *n, s, w, e* between cell center *C*, and neighbors *N, S, W, E*. The scheme was discretized in time by following an explicit scheme, hence, the unknown at each time step was the temperature, T_c^{i+1} Patankar (1980). A Conjugate Gradient Method algorithm (Shewchuk, 1994) was employed to solve the equation at each time step.

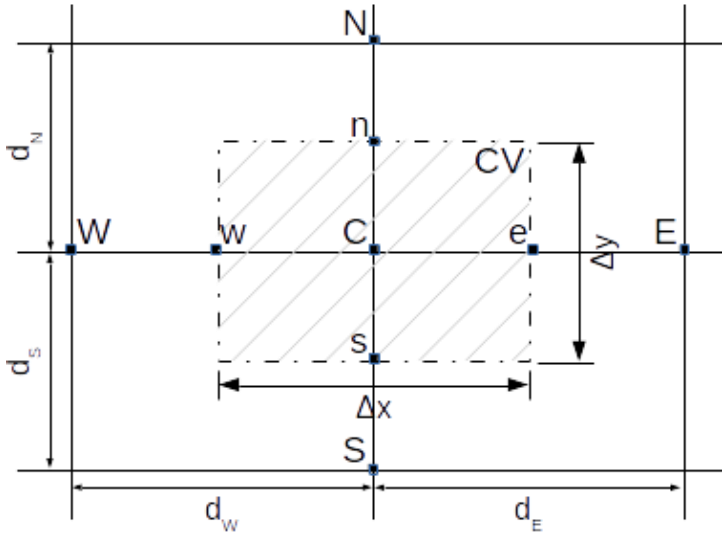

Figure 3.26. Discretization scheme around a control volume CV

3.4.4.2. Boundary conditions

Particular discretization arrangements must be taken in proximity of domain boundaries, depending on the boundary condition that has to be applied.

In the case of given heat flux (Neumann boundary condition, depicted in Figure 3.26), the equation reads as follows:

$$\rho c_p \frac{T_C^{i+1} - T_C^i}{\Delta t} V = k_n \frac{T_N^i - T_C^i}{d_N} \Delta x - k_s \frac{T_C^i - T_S^i}{d_S} \Delta x + k_e \frac{T_E^i - T_C^i}{d_E} \Delta y + q \Delta y \qquad [16]$$

This case applied to the top boundary surface, where an inlet or outlet heat flux was given, mimicking the laser source or the heat dispersion, respectively. In this case, CV was the half by respect to the discretization of an internal cell.

In the case of given air flow (Newton boundary condition), the scheme reported in Figure 3.27 applied, and the equation reads as:

$$\rho c_p \frac{T_C^{i+1} - T_C^i}{\Delta t} V = k_n \frac{T_N^i - T_C^i}{d_N} \Delta x - k_s \frac{T_C^i - T_S^i}{d_S} \Delta x + k_e \frac{T_E^i - T_C^i}{d_E} \Delta y - h_{air}(T_C^i - T_{air}) \Delta y \qquad [17]$$

where h_{air} and T_{air} are the convective heat transfer coefficient and the environment temperature, respectively. This condition applies to the lateral boundaries of the burger.

Finally, in the case of given temperature (Dirichlet boundary condition), the central temperature was directly set. This condition was applied at the bottom surface, where the temperature T_s is given by the 0-D model, following the process explained in Section 3.4.3.3 (Bottom boundary condition).

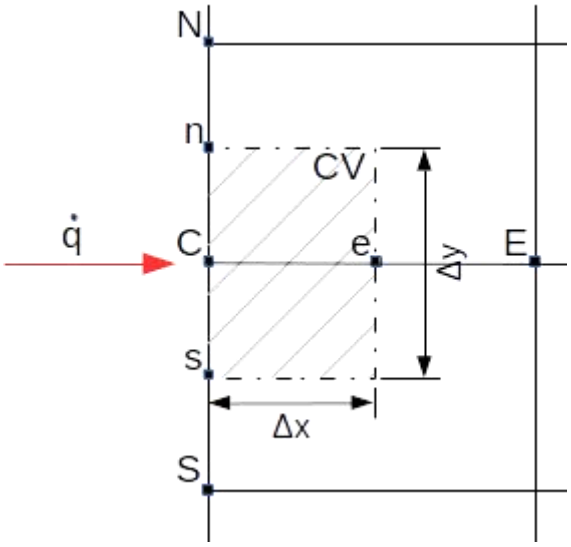

Figure 3.27. Boundary cell discretization: given flux case (Neumann boundary condition).

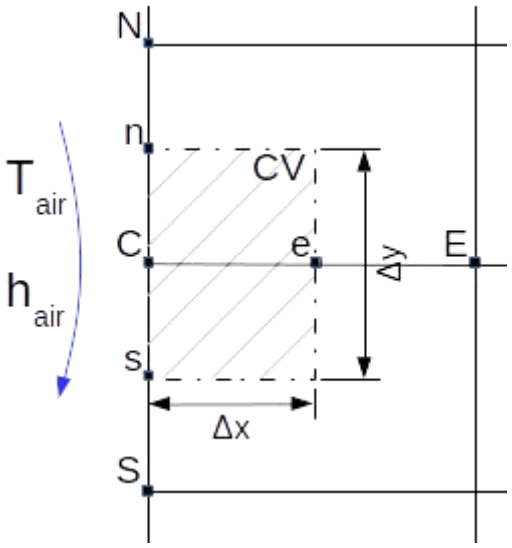

Figure 3.28. Boundary cell discretization: convective flow case (Newton boundary condition).

3.4.5. Physical parameters used for the numerical simulation.

The heat transfer coefficient used for the lateral boundary condition was: h_{lat}=10 W/m^2·K. In the 0-D model, for the modelization of the bottom boundary condition, the following values were used: h_b = 100 W/m^2·K; h_p = 2 W/m^2·K. Moreover, the values of the meat burger and the vegetarian patty were: ρ_{burger} = 1081 kg/m^3, ρ_{patty} = 1183 kg/m3, $C_{p\ burger}$ = 3502 J/kg·K, $C_{p\ patty}$ = 3243 J/kg·K, $k_{\ burger}$ = 0.534 W/m·K and $k_{\ patty}$ = 0.522 W/m·K. The density of the glass (plate) was 2600 kg/m^3 and the specific heat was 750 J/kg·K (www.engineeringtoolbox). The global convective coefficient h_b was considered the same for beef burger and vegetarian patties and it was extrapolated from the O-D model. The height of the glass plate was 8 mm. All this parameters were also used for the vegetarian patty simulation.

In both the CFD and 0-D models, the initial temperature of the beef meat and vegetarian patty dough was considered 8°C, and the initial temperature of the glass plate and the environment was 20°C.

3.4.6. Domain, mesh and time step

The numerical domain consisted in the cylinder reported in Figure 3.28, representing the burger volume (diameter = 78 mm; height = 11 mm). The cells were cubic in the center part of the domain, while they got a certain curvature on the lateral sectors to fit the domain boundaries. The size of the structured mesh was set after carrying out a specific mesh convergence study.

The simulation consisted in carrying out a cooking process with the laser source set at a fixed value on a single side of the burger for a time of around 16 min. The numerical simulation was performed on 4 meshes characterized by a decreasing characteristic length (defined as the lateral size of the cubic hexahedron in the domain center). The simulated temperature at the center of the burger (named as *Central T*) was calculated and reported in the plot of Figure 3.29. Results showed that **mesh 3** (around $4 \cdot 10^5$ elements), guaranteed a sufficient degree of convergence of the solution.

Next, a time step convergence study was carried out to choose the correct time step to be employed in simulations. As shown in Figure 3.30, a dt = 0.05 s was sufficient to reach a good degree of convergence of the solution on **mesh 3**.

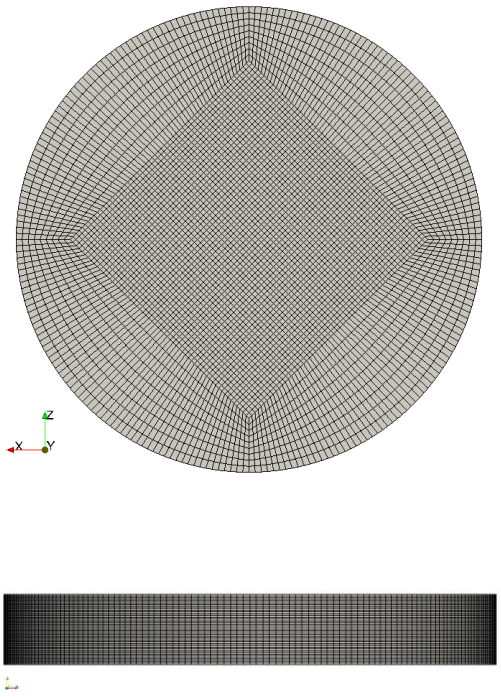

Figure 3.29. Mesh employed for simulations.

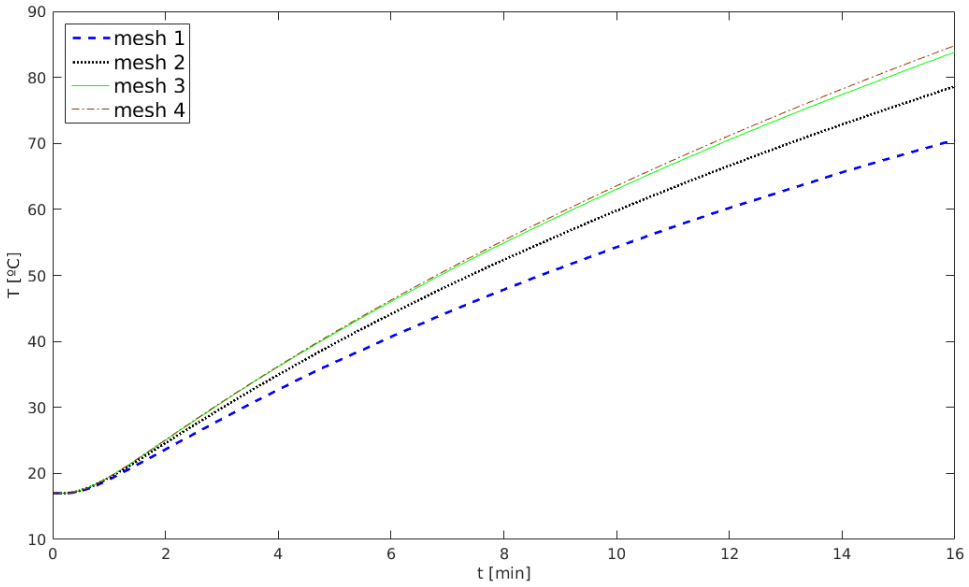

Figure 3.30. Mesh convergence analysis of *Central T*.

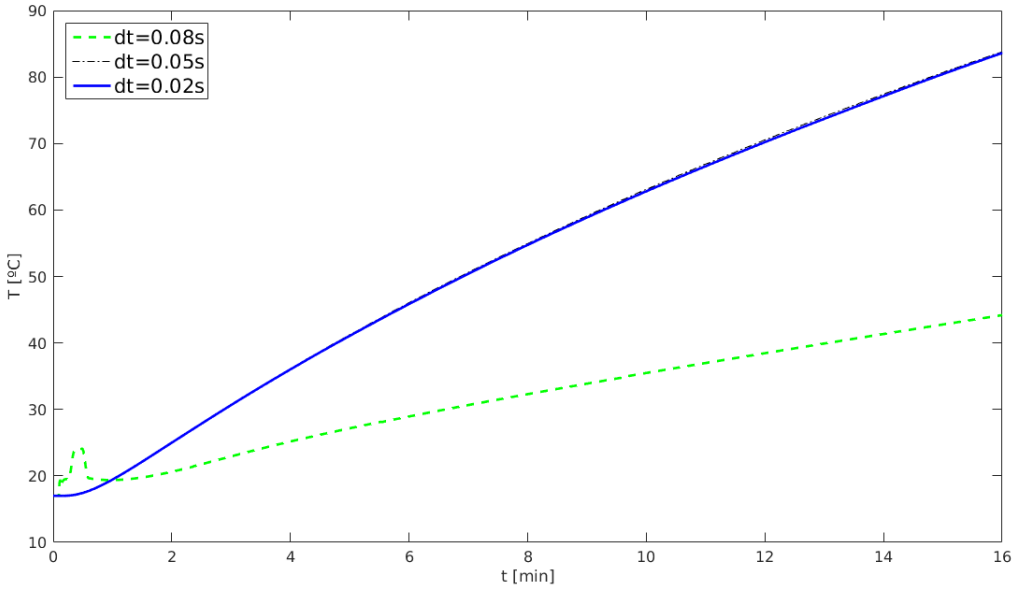

Figure 3.31. Time step convergence analysis of *Central T*.

CHAPTER 4

RESULTS

4.1. Previous Work

Considering the limitations of cooking inside 3D Food Printer Foodini and the solutions and advantages provided by IR lasers, it was decided to carry out exploratory/concept tests based and trial and error methodology with a CO_2 cutter and engraver (Epilog Laser HELIX 24, Golden, Colorado, USA) provided by the company Laser Project (L'Hospitalet de Llobregat, Spain). The tests were carried out in the headquarters of Laser Project. Different food matrices and several operations conditions were tested. After several trials, results were promising since products like meat burgers, meat and fish fillets, egg, and pizza dough were cooked using this IR laser equipment. Products as cookies, crackers or tortilla dough were not homogenously cooked, since parts of the dough remained stuck at the bottom side or the shape was lost when turned. Anyway, the good results obtained with meat products assured the continuity with the next step of the study.

Fig 4.1. Laser cutter and engraver Epilog Laser HELIX 24 75W

At the same time, lasers for medical applications were used to study the effect in different foodstuff. Tests were carried out in the LaserMèdic Clinical Center (Clínica Tres Torres, Barcelona). The equipment used combined Er:Yag (2.94 μm) laser and CO_2 laser (Lumenis Derma K®, Yokneam, Israel). These tests were interesting since the Er:Yag lasers are near the maximum absorption of electromagnetic radiation of water, located at 3000 nm. The results were not satisfactory since we only get a surface dehydration or burning of the different food matrices: the surface became overcooked while the product remained raw inside. The manual control of the equipment made difficult to distribute the heat over the food sample and the power was limited due to its medical applications.

Also, tests with Nd:Yag 1064 nm diode laser equipment engraver and cutter (Laser Writer Open, Castelnuovo del Garda, Verona, Italy) were done in the company Hispanatec (Tecnología Hispana S.L., Barcelona). This equipment is mainly used as a marker of metals, especially, in jewelry applications. One of the limitations of this equipment was the diameter of laser spot (around 25 μm), which concentrated too much energy in each point area of the surface. This caused product dehydration and an overcooked surface while the inner part remained undercooked or raw. In comparison with the diameter of Nd:Yag laser spot, CO_2 laser allowed to choose a bigger spot diameter that helped to distribute the energy in the surface, thus facilitating the heat transmission from the surface to the centre and allowing to cook uniformly the product without overheating the external side.

At this stage of the project, and with that commercially available equipment and test conditions applied, the results obtained with CO_2 laser Epilog equipment were the only considered successful to cook food (data not shown).

Exploratory tests continued by hiring a CO_2 equipment (Epilog Laser MINI 24) to proceed with tests in the UAB laboratory facilities (Department of Animal and Food Science). These tests were carried out with different products such as beef burgers, crackers dough, Maria style cookies, butter cookies, chocolate cookies or pizza dough. Technical problems with the equipment regarding the loss of laser power retarded the systematic execution of experiments. Finally, this equipment was replaced by another Epilog Laser (Zing model). This was the CO_2 laser equipment used to carry out the first experimental study.

4.2. Results of the first experimental study with CO_2 IR Laser Epilog Equipment

Beef burgers, pizza dough and mashed potatoes bites were cooked using CO_2 IR Laser Epilog Equipment and other standard methods.

4.2.1. Beef burgers

4.2.1.1. Internal cooking temperature

Internal cooking temperatures of all cooking treatments were above 72ºC (FSAI, 2018; AMSA, 2016; www.fda.gov) and no significant differences ($p<0.05$) were found between them.

Table 4.1. Internal cooking temperature (°C) of beef burgers for each cooking method applied.

Treatments	Internal cooking temperature* (°C)
IR Laser 29	75.36 ± 2.39
IR Laser 25	74.66 ± 2.03
IR Oven	73.16 ± 0.52
BBQ Grill	75.08 ± 1.99
Flat Grill	74.86 ± 1.90

*Mean values ± standard deviations (n=6).

4.2.1.2. Cooking loss, moisture, proximate analysis and water activity.

Cooking losses between IR laser treatments and other cooking methods did not show significant differences (table 4.2). Moisture, protein and ashes contents were significantly different between raw and cooked burgers, but there were no differences between cooking treatments. Moisture content decreased in cooked burgers, whereas protein and ashes content increased. Fat content on wet basis did not change but results of fat expressed on dry basis (Raw burger: 23.35 ± 0.70; IR Laser 29: 22.31 ± 1.47; IR Laser 25: 21.86 ± 1.16; IR Oven: 21.89 ± 1.95; BBQ Grill: 20.92 ± 1.43; Flat Grill: 18.16 ± 1.15) show that some fat was lost during cooking, particularly when samples were cooked with BBQ Grill and Flat Grill ($p<0.05$).

There were not significant differences between water activity values of raw beef and cooked meat, neither between the different cooking treatments. Water activity of raw beef burger was 0.976 ± 0.003, and the values of cooked burgers ranged between 0.969 ± 0.005 (IR Oven) and 0.972 ± 0.002 (Flat Grill).

Table 4.2. Cooking loss, moisture and proximate analysis results of raw and cooked beef burgers.

Treatments	Cooking loss (%)	Moisture content (%)	Protein content (%)	Fat content (%)	Ashes content (%)
Raw		70.75 ± 0.95^{a}	18.95 ± 0.60^{b}	6.30 ± 1.34	2.47 ± 0.10^{b}
IR Laser 29	20.98 ± 1.13	64.75 ± 1.13^{b}	23.85 ± 0.77^{a}	7.43 ± 1.23	3.01 ± 0.11^{a}
IR Laser 25	21.38 ± 1.15	64.11 ± 1.17^{b}	24.80 ± 0.72^{a}	7.45 ± 1.09	3.06 ± 0.11^{a}
IR Oven	21.83 ± 1.91	64.39 ± 1.07^{b}	24.87 ± 0.70^{a}	7.33 ± 1.18	2.93 ± 0.09^{a}
BBQ Grill	21.64 ± 2.83	64.69 ± 1.55^{b}	23.74 ± 2.30^{a}	7.09 ± 1.02	2.91 ± 0.15^{a}
Flat Grill	23.23 ± 3.10	65.15 ± 1.59^{b}	25.11 ± 0.66^{a}	6.05 ± 0.94	2.84 ± 0.09^{a}

$^{(a-b)}$ Mean values ± standard deviations (n=6). Values labeled with a different letter in the same column are significantly different ($p<0.05$).

4.2.1.3. Texture analysis

Table 4.3 shows the results of compression and penetration analyses. Cooking with IR oven, IR Laser 25 and BBQ Grill yielded the hardest burgers, whereas Flat Grill and IR Laser 29 produced the burgers with the lowest hardness values, although there were no significant differences with BBQ Grill. Results of cutting force show a similar trend: IR Oven and BBQ Grill cooking methods gave burgers with the highest cutting force, followed by IR Laser 25 and Flat Grill and, finally, IR Laser 29 treatment, which rendered the burgers with the lower cutting force ($p<0.05$). For springiness values, significant differences were found between raw beef and cooked burgers, but not between cooking treatments.

Table 4.3. Hardness, Springiness and Cutting Force of raw and cooked beef burgers.

Treatments	Hardness (N)	Springiness	Cutting Force (N)
Raw	14.01 ± 1.45^{d}	0.65 ± 0.05^{b}	1.40 ± 0.11^{d}
IR Laser 29	79.14 ± 2.33^{c}	0.85 ± 0.03^{a}	10.90 ± 0.66^{c}
IR Laser 25	$88.50 \pm 3.30^{a,b}$	0.86 ± 0.02^{a}	13.87 ± 0.65^{b}
IR Oven	93.38 ± 3.45^{a}	0.87 ± 0.02^{a}	16.93 ± 0.93^{a}
BBQ Grill	$82.36 \pm 9.98^{a,b,c}$	0.87 ± 0.02^{a}	$15.95 \pm 1.70^{a,b}$
Flat Grill	74.21 ± 5.39^{c}	0.85 ± 0.02^{a}	13.41 ± 1.22^{b}

$^{(a-d)}$ Mean values ± standard deviations (n=18). Values labeled with a different letter in the same Column are significantly different ($p<0.05$).

4.2.1.4. Color analysis of beef burgers

Color analyses were performed on the internal and external surfaces of beef burgers (table 4.4). Regarding internal color, lightness (L*) values were significantly lower in raw burger than in cooked burgers and, between treatments, lightness of IR Laser 29 cooked burgers was significantly lower than the rest. Chromatic component a* decreased after cooking treatments and, between cooked samples, IR Laser treatments gave the burgers with the highest values of a* although there were no significant differences between IR Laser 25 and IR Oven. Chromatic component b* did not change between raw and cooked samples, neither within cooked samples. All cooked samples showed the same total color difference (ΔE*) with raw samples ($p>0,05$) regardless of the cooking treatment.

Regarding external color, burgers cooked with Flat Grill and BBQ Grill showed significantly highest values of lightness, whereas there were no significant differences between burgers cooked by IR Laser 29 and 25 and raw burgers. Chromatic component a* was significantly higher in raw than in cooked samples. Values of a* were significantly higher in burgers cooked with IR Laser 29, IR Laser 25 and IR Oven than in those cooked with BBQ Grill and Flat Grill. As observed in internal color, chromatic component b* did not change between raw and cooked samples, neither within cooked samples. Total color difference (ΔE*) between samples cooked with Flat Grill and BBQ Grill and raw samples was higher than ΔE* between samples cooked with any of IR methods and raw samples.

Table 4.4. CIE *L**, *a** and *b** values and total color difference (ΔE*) of the internal and the external side of raw and cooked beef burgers.

	Cooking methods					
	Raw	IR Laser 29	IR Laser 25	IR Oven	BBQ Grill	Flat Grill
Internal color						
L*	39.44 ± 1.95^{c}	49.91 ± 0.27^{b}	51.62 ± 0.56^{a}	51.45 ± 0.41^{a}	51.25 ± 0.50^{a}	51.28 ± 0.22^{a}
a*	15.20 ± 1.91^{a}	5.60 ± 0.17^{b}	5.32 ± 0.13^{b,c}	5.04 ± 0.23^{c,d}	4.86 ± 0.17^{d}	4.79 ± 0.06^{d}
b*	15.48 ± 0.61	15.16 ± 0.34	14.86 ± 0.20	15.04 ± 0.26	15.18 ± 0.25	15.36 ± 0.49
Internal ΔE^{*}	-	14.23 ± 1.53	15.71 ± 0.97	15.75 ± 0.69	15.74 ± 0.63	15.78 ± 0.42
External color						
L*	39.69 ± 1.05^{c}	40.35 ± 1.63^{c,b}	41.58 ± 1.19^{c,b}	42.53 ± 0.90^{b}	43.73 ± 0.63^{a,b}	45.35 ± 1.54^{a}
a*	15.07 ± 1.60^{a}	7.96 ± 0.75^{b,c}	8.47 ± 0.27^{b}	6.89 ± 0.31^{c}	5.71 ± 0.04^{d}	5.38 ± 0.48^{d}
b*	14.86 ± 0.59	16.75 ± 1.58	17.58 ± 0.20	14.64 ± 0.55	15.76 ± 0.26	15.53 ± 0.58
External ΔE^{*}	-	7.82 ± 0.82^{b}	7.30 ± 1.45^{b}	8.81 ± 0.82^{b}	10.29 ± 0.60^{a}	11.36 ± 1.59^{a}

$^{(a-d)}$ Mean values ± standard deviations (n=36). Values labeled with a different letter in the same row are significantly different (p<0.05).

4.2.1.5. Images of samples during the cooking process

Images of beef burger samples were taken before, during and after cooking treatments to illustrate changes and differences in appearance.

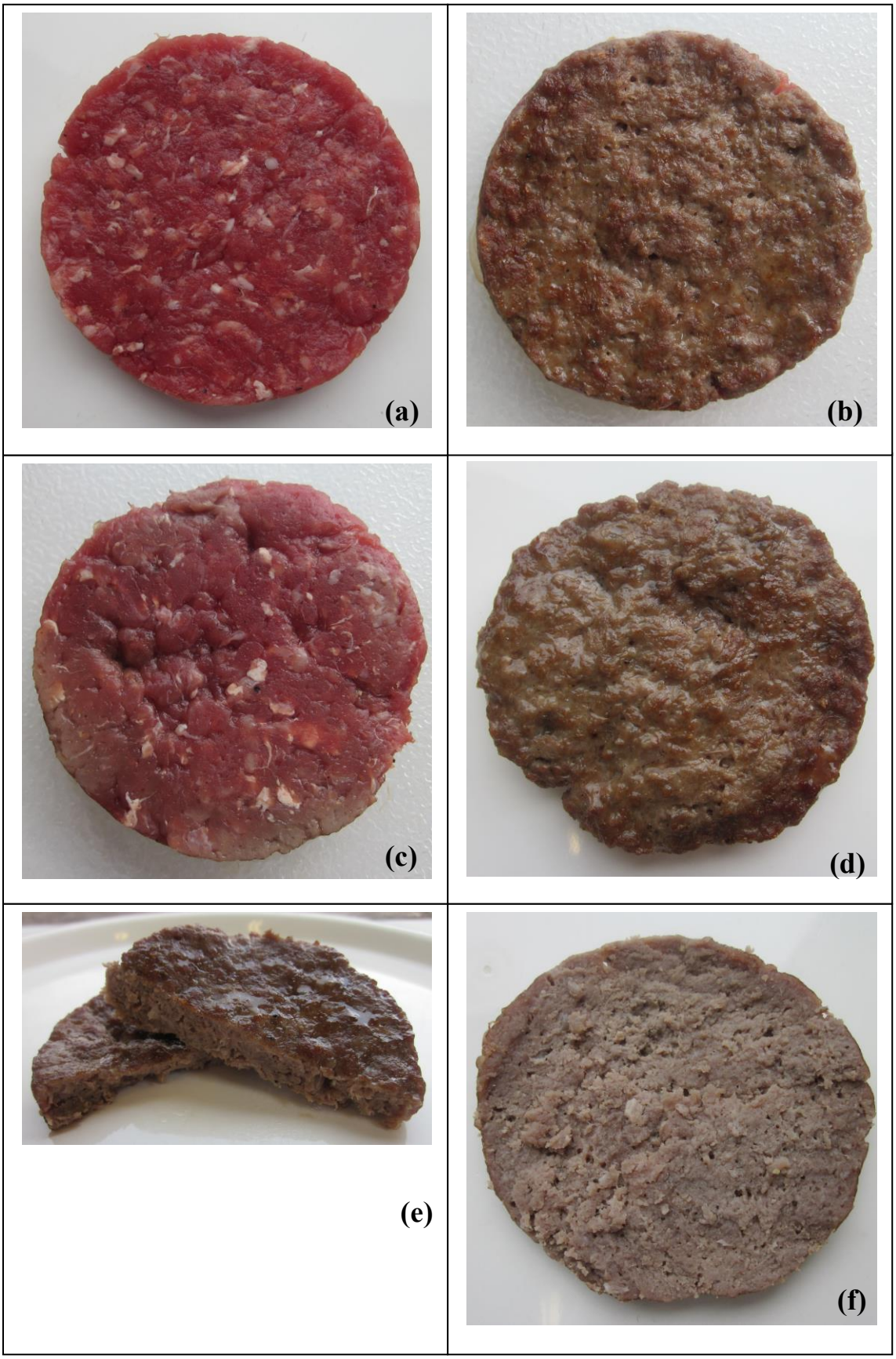

Fig 4.2. Cooking process of beef burger treated with IR Laser 29. (a) First side, raw burger; (b) End of cooking of first side; (c) Second side, after cooking of first side; (d) End of cooking of second side; (e) Cooked burger, vertical cross-section; (f) Cooked burger, horizontal cross-section.

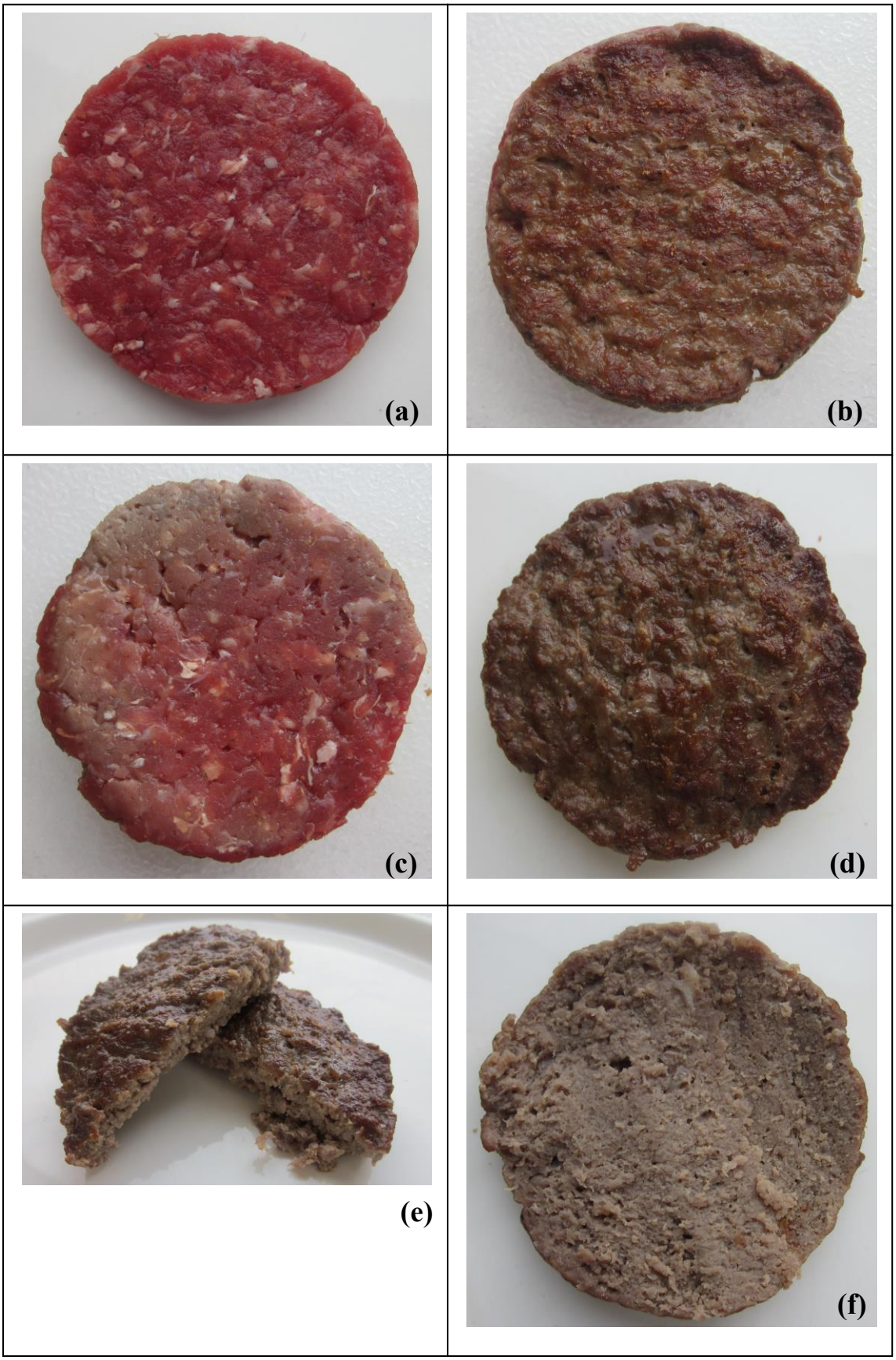

Fig 4.3. Cooking process of beef burger treated with IR Laser 25. (a) First side, raw burger; (b) End of cooking of first side; (c) Second side, after cooking of first side; (d) End of cooking of second side; (e) Cooked burger, vertical cross-section; (f) Cooked burger, horizontal cross-section.

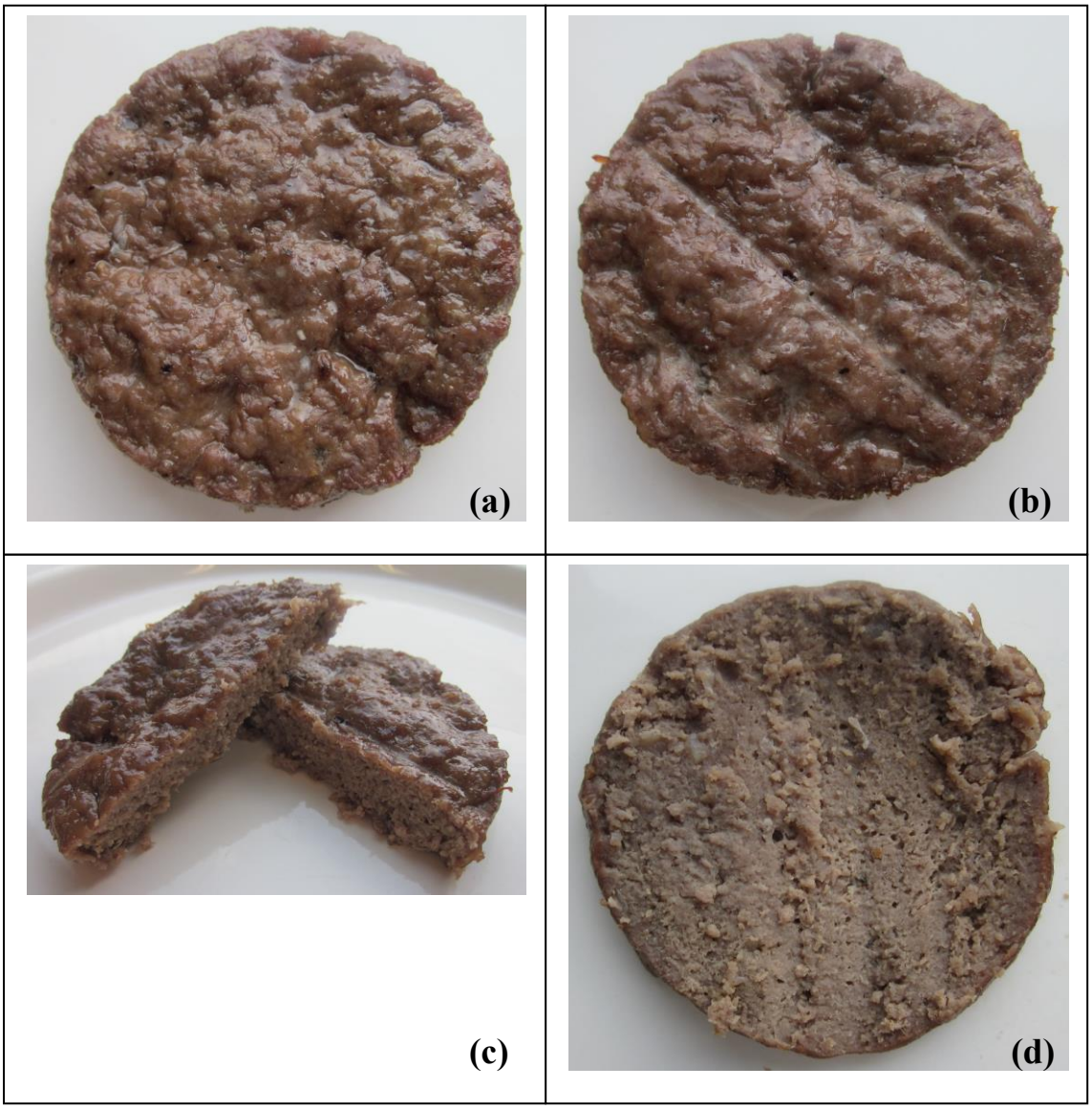

Fig 4.4. Beef burger cooked with IR Oven. (a) Top side; (b) Bottom side, in contact with the rack grill; (c) Vertical cross-section; (d) Horizontal cross-section.

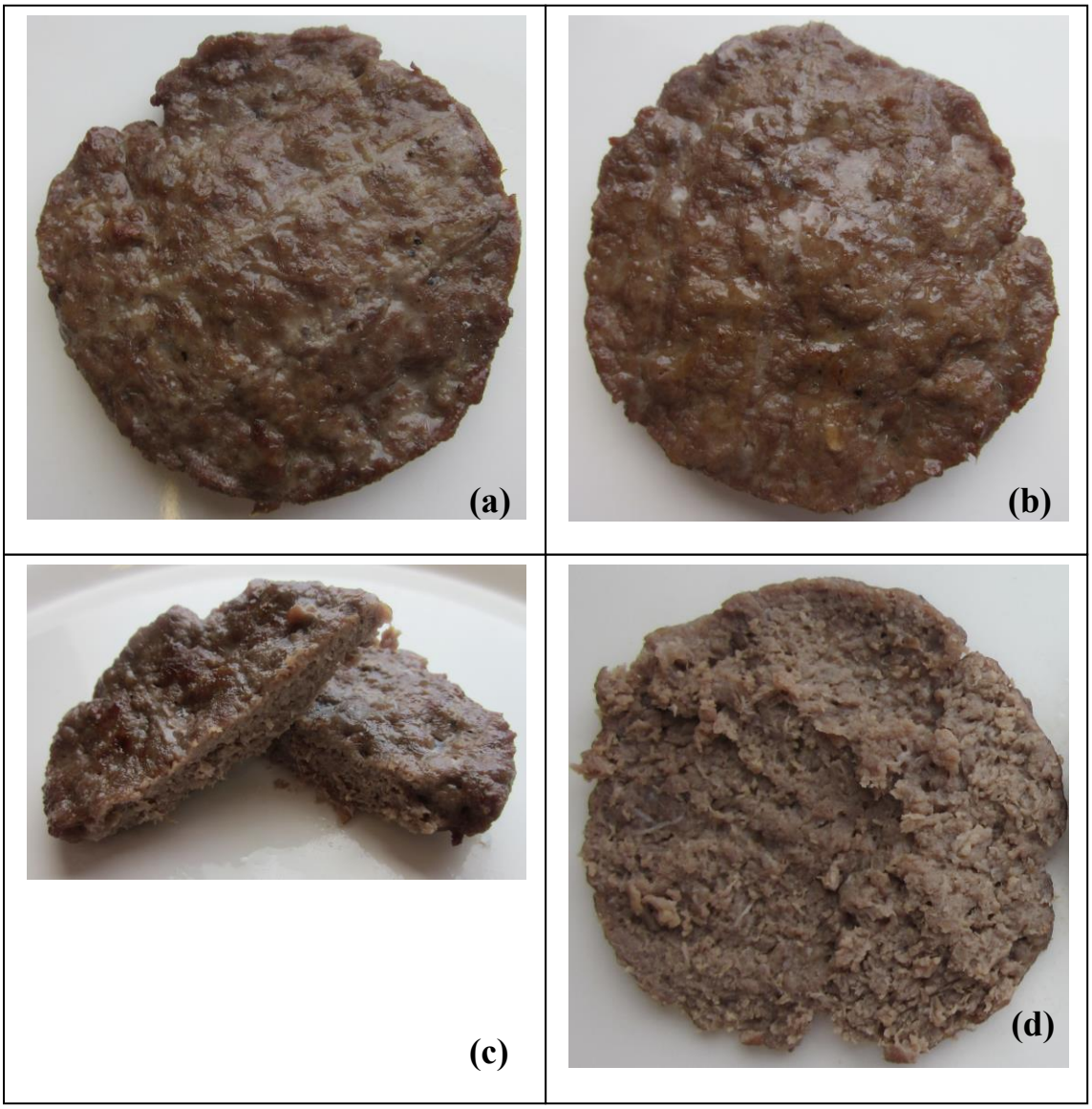

Fig 4.5. Beef burgers cooked with BBQ Grill. (a) First side in contact with the rack grill; (b) Second side in contact with the rack grill; (c) Vertical cross-section; (d) Horizontal cross-section.

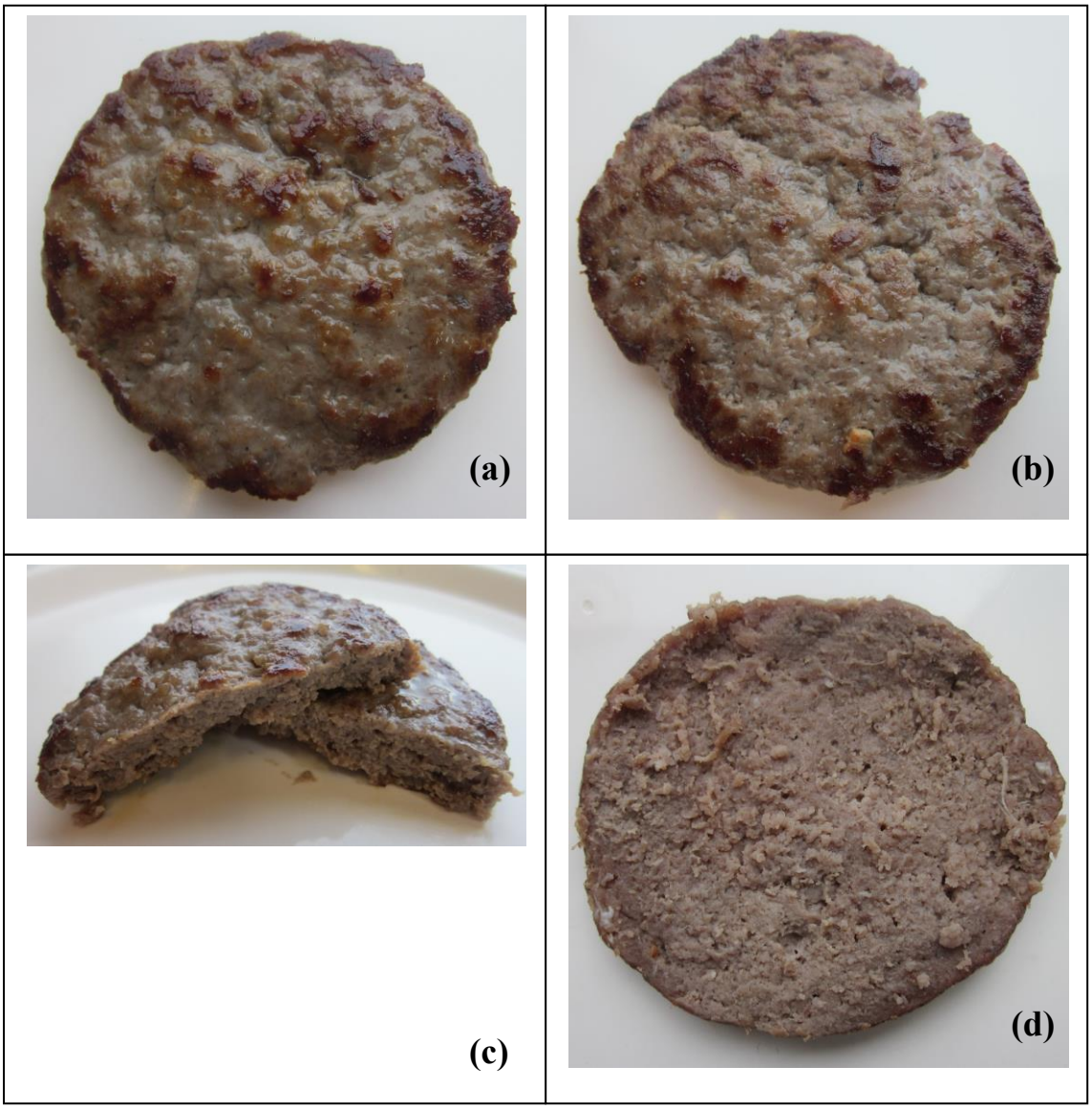

Fig 4.6. Beef burgers cooked with Flat Grill. (a) First side in contact with the flat grill surface; (b) Second side in contact with the flat grill surface; (c) Vertical cross-section; (d) Horizontal cross-section.

4.2.1.6. Sensory analysis

Consumers considered that burgers cooked with IR Laser 29, IR laser 25 and IR Oven had a significantly better general appearance than burgers cooked with Flat Grill, whereas the appearance of burgers cooked with BBQ Grill did not show significant differences with the rest (figures 4.2, 4.3, 4.4, 4.5, 4.6).

When consumers evaluated the intensity of sensory attributes, external color, internal color and taste of burgers received the same scores independently from the cooking method (table 4.5). Consumers considered that burgers cooked with Flat Grill had a significantly higher level of doneness in comparison with burgers cooked with IR Laser 29, IR Laser 25 and IR Oven, whereas the level of doneness of burgers cooked with BBQ Grill showed no differences with other treatments. Consumers evaluated burgers cooked with IR Laser 25, IR Laser 29, IR Oven and BBQ Grill as significantly juicier than burgers cooked with Flat Grill.

Regarding acceptability, internal color and taste of all burgers received similar ratings ($p>0,05$). External color and juiciness of burgers treated with IR Laser 29, IR Laser 25 and IR Oven received significantly higher scores than burgers cooked using Flat Grill, whereas the scores received by burgers cooked with BBQ Grill were not different from the rest. Doneness of burgers cooked with IR Laser 29, IR Laser 25 and IR Oven was significantly better accepted than doneness of burgers cooked with Flat Grill whereas doneness of burgers cooked with BBQ Grill received scores similar to those of burgers cooked with IR Oven and Flat Grill. Consumers considered that burgers cooked with Flat Grill were significantly less tender than burgers cooked with IR Laser 29 and IR Laser 25, whereas there were no significant differences in tenderness of burgers cooked with IR Laser 29, IR Laser 25, IR Oven and BBQ Grill.

Preference test showed that beef burgers cooked with IR Laser 29, IR Laser 25 and IR Oven were the most preferred by consumers (table 4.6). Burgers cooked with BBQ Grill were ranked between them and the least preferred, which were burgers cooked with Flat Grill ($p<0.05$).

Table 4.5. Results of the consumer test for beef burgers cooked with different cooking.

	IR Laser 29	IR Laser 25	IR Oven	BBQ Grill	Flat Grill
General appearance	4.99± 1.26[a]	5.04 ± 1.18[a]	4.97 ± 1.37[a]	4.64 ± 1.27[a,b]	4.02 ± 1.45[b]
Intensity					
External color	4.91 ± 1.26	4.80 ± 1.28	4.88 ± 1.24	4.98 ± 1.14	5.34 ± 1.36
Internal color	4.90 ± 1.09	4.80 ± 1.07	4.82 ± 1.19	5.17 ± 1.15	5.17 ± 1.36
Doneness	4.83 ± 1.07[b]	4.90 ± 0.80[b]	5.00 ± 0.91[b]	5.18 ± 1.04[a,b]	5.57 ± 1.26[a]
Tenderness	4.11 ± 1.19[a]	4.21 ± 1.13[a]	4.10 ± 1.07[a]	3.81 ± 1.01[a,b]	3.31 ± 1.32[b]
Juiciness	4.46 ± 1.31[a,b]	4.49 ± 1.20[a]	4.38 ± 1.17[a,b]	3.81 ± 1.13[b]	3.10 ± 1.26[c]
Taste	4.64 ± 1.62	4.73 ± 1.49	4.44 ± 1.39	4.06 ± 1.38	3.55 ± 1.51
Acceptability					
External color	4.94 ± 1.19[a]	5.12 ± 1.18[a]	4.77 ± 1.29[a]	4.59 ± 1.20[a,b]	3.96 ± 1.77[b]
Internal color	4.91 ± 1.26	4.80 ± 1.28	4.88 ± 1.24	4.98 ± 1.14	5.34 ± 1.36
Doneness	4.93 ± 1.45[a]	4.98 ± 1.24[a]	4.54 ± 1.22[a,b]	4.13 ± 1.30[b,c]	3.76 ± 1.65[c]
Tenderness	4.61 ± 1.54[a]	4.90 ± 1.41[a]	4.38 ± 1.52[a,b]	4.18 ± 1.35[a,b]	3.63 ± 1.58[b]
Juiciness	4.64 ± 1.62[a]	4.73 ± 1.49[a]	4.44 ± 1.39[a]	4.06 ± 1.38[a,b]	3.55 ± 1.51[b]
Taste	5.06 ± 1.27	4.98 ± 1.31	4.59 ± 1.46	4.39 ± 1.17	4.07 ± 1.37

[(a-c)] Mean values ± standard deviations (n=51). Values labeled with a different letter in the same row are significantly different (p<0.05)

Table 4.6. Results of preference test for beef burgers cooked with different methods.

	Number of answers for each order of preference (1-5) and multiplied by its order of preference					
	*1	*2	*3	*4	*5	Sum
IR Laser 29	15	28	27	32	20	122[a]
IR Laser 25	19	24	30	28	10	111[a]
IR Oven	11	20	48	32	25	136[a,b]
BBQ Grill	3	22	33	76	30	164[b]
Flat Grill	2	6	12	32	165	217[c]

[(a-c)] Values labeled with a different letter in the same column are significantly different (p<0.05)

4.2.1.7. Microbiological results

4.2.1.7.1. Microbiological analysis of non-inoculated samples

Counts of aerobic mesophilic bacteria were significantly reduced after cooking treatments except in burgers cooked with IR Laser 29, whose TSA counts did not differ from those of raw burgers ($p>0.05$) (table 4.7). Cooking with IR Laser 25 caused a significant reduction of ~ 1,5 log CFU/g of initial TSA counts. Flat Grill and IR Oven cooking methods caused the highest aerobic mesophilic bacteria reductions (~ 3,5 and 4 log CFU/g, respectively), followed by BBQ Grill.

Naturally present coliform counts in raw burger were reduced below the detection limit in burgers cooked with IR Laser 25, IR Oven and BBQ Grill. In burgers cooked with IR Laser 29, coliforms were detected in 4 out of 6 samples analyzed by MPN method, and in 3 out of 6samples analyzed by VRBA plating. In burgers cooked with Flat Grill, coliforms were detected in 1 out of 6 samples both in MPN and VRBA counts.

Table 4.7. Counts of aerobic mesophilic bacteria (TSA) and coliforms (MPN in BGBL; VRBA) in non-inoculated raw and cooked beef burgers.

Treatments	TSA Count*	BGBL Count**	VRBA Count***
Raw	4.35 ± 0.20^{a}	1.88 ± 0.86	2.59 ± 1.61^{a}
IR Laser 29	$3.74 \pm 1.39^{a,b}$	n.d.(1) / 0.68 ± 0.25	0.51 ± 0.38^{b}
IR Laser 25	2.85 ± 0.37^{b}	n.d.	n.d.
IR Oven	0.33 ± 0.58^{c}	n.d.	n.d.
BBQ Grill	$1.43 \pm 1.84^{b,c}$	n.d.	n.d.
Flat Grill	0.79 ± 0.60^{c}	n.d.(2)/1.63	0.43 ± 0.74^{b}

(a-c) Mean (log CFU/g) ± s.d. (n=6). Values labeled with a different letter in the same column are significantly different ($p<0.05$). n.d.: not detected. *Detection limit: <2 log CFU/g. **Detection limit: <0.48 log CFU/g. ***Detection limit: <1 log CFU/g. (1) <0.48 log CFU/g in 2 out of 6 samples. (2)<0.48 log CFU/g in 5 out of 6 samples.

Due to the low reductions in TSA and coliforms counts in burgers cooked with IR Laser 29, this method was not applied in the experiments with inoculated samples.

Raw samples that were analyzed to investigate the presence of *Salmonella* in meat before inoculation gave negative results.

4.2.1.7.2. Microbiological analysis of inoculated samples.

Survival of *Salmonella* Typhimurium and *Salmonella* Senftenberg after cooking was similar in samples inoculated at ~7 log CFU/g (table 4.8). IR Oven cooking caused the highest reduction in plate counts, followed by Flat Grill. BBQ Grill caused a reduction around ~ 4 log CFU/g in both types of *Salmonella* whereas reduction caused by IR Laser 25 was only ~ 2 log CFU/g. *Salmonella* was detected after enrichment of cooked samples regardless of the cooking method applied.

Table 4.8. Survival of *Salmonella* Typhimurium and *Salmonella* Senftenberg inoculated at ~7 log CFU/g in raw beef burgers after cooking with different methods.

	Salmonella Tyhphimurium		*Salmonella* Senftenberg	
Treatment	Count	Detection[1]	Count	Detection
Raw	7.43 ± 0.21^{a}		7.61 ± 0.27^{a}	
IR Laser 25	5.54 ± 0.19^{b}	6/6	5.40 ± 0.57^{b}	6/6
IR Oven	n.d.	6/6	n.d.	2/6
BBQ Grill	$3.59 \pm 3.11^{b,c}$	3/6	3.04 ± 0.67^{c}	4/6
Flat Grill	0.57 ± 0.98^{c}	6/6	0.98 ± 1.71^{c}	6/6

[(a-c)] Mean (log CFU/g) ± s.d. (n=6). Values labeled with a different letter in the same column are significantly different (p<0.05). n.d.: not detected; limit of detection: <2 log CFU/g.
[1] +/6: positive samples after enrichment and growth in selective medium.

In samples inoculated at ~ 3 log CFU/g (Table 4.9), cooking with IR Laser 25 gave samples with positive counts after plating in selective media and in all plates after sample enrichment. Reduction achieved with this method was ~ 2 and 2.5 log CFU/g in *S.* Typhimurium and *S.* Senftenberg, respectively. The rest of cooking methods caused higher reductions than IR Laser 25 but none of them caused the complete inactivation of *Salmonella*.

Table 4.9. Survival of *Salmonella* Typhimurium and *Salmonella* Senftenberg inoculated at ~3 log CFU/g in raw beef burgers after cooking with different methods.

	Salmonella Tyhphimurium		*Salmonella* Senftenberg	
Treatment	Count	Detection[1]	Count	Detection[1]
Raw	3.19 ± 0.12[a]		3.58 ± 0.24[a]	
IR Laser 25	0.70 ± 0.70[b]	6/6	1.52 ± 0.07[b]	6/6
IR Oven	n.d.	1/6	n.d.	0/6
BBQ Grill	n.d.	3/6	0.23 ± 0.40[c]	5/6
Flat Grill	n.d.	1/6	n.d.	3/6

[(a-c)] Mean (log CFU/g) ± s.d. (n=6). Values labeled with a different letter in the same column are significantly different ($p<0.05$). n.d.: not detected; limit of detection: <2 log CFU/g.
[1] +/6: positive samples after enrichment and growth in selective medium.

4.2.1.8. Differential scanning calorimetry

Peak areas of all cooked samples were significantly lower than those of raw burgers (table 4.10). There were not significant differences between peak areas of different cooking treatments. Fig. 4.7 depicts an example of a typical DSC curve for each sample.

Cooking caused a decrease in peak temperatures. Although there were not significant differences between peak temperatures of cooked samples, peak temperatures of burgers cooked with both IR laser methods were not significantly different from those of raw burgers.

Table 4.10. Peak areas and peak temperatures from DSC analysis of raw and cooked burgers.

Treatments	Area (J/g)	Peak Temperature (°C)
Raw	992.88 ± 93.23[a]	79.15 ± 2.27[a]
IR Laser 29	742.13 ± 41.37[b]	76.20 ± 2.16[a,b]
IR Laser 25	761.54 ± 66.44[b]	76.24 ± 0.57[a,b]
IR Oven	718.11 ± 81.50[b]	74.13 ± 1.80[b]
BBQ Grill	714.21 ± 29.09[b]	74.87 ± 1.84[b]
Flat Grill	717.76 ± 20.96[b]	74.67 ± 2.21[b]

[(a-b)] Mean values ± standard deviations (n=12). Values labeled with a different letter in the same column are significantly different ($p<0.05$).

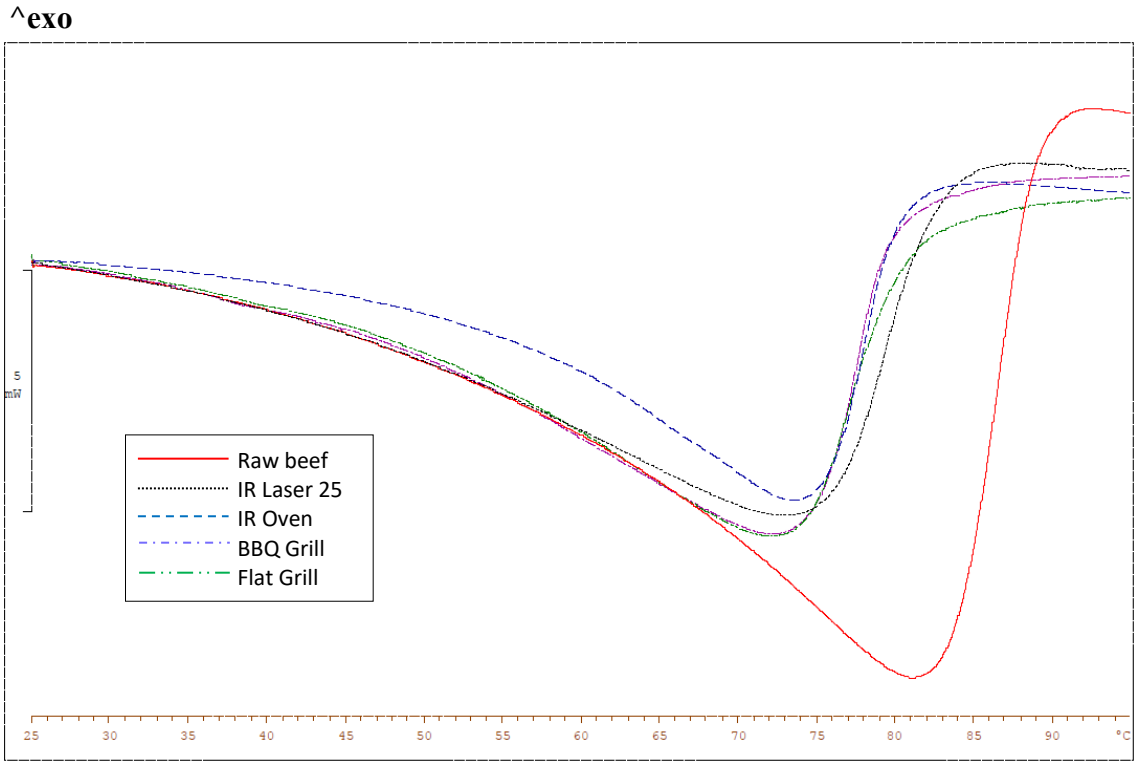

Fig 4.7. DSC thermograms of raw and cooked burgers.

4.2.2. Pizza dough

4.2.2.1. Cooking loss, moisture, proximate analysis and water activity.

Cooking loss was significantly different between all treatments (table 4.11). Doughs cooked with Deck Oven rendered the pizzas with the highest cooking loss, followed by the ones cooked in IR Oven. IR Laser 20 cooking caused the lowest losses. Moisture content results changed accordingly to weight losses. Hence, pizza doughs cooked with Deck Oven had the lowest water content, followed by samples cooked with IR Oven. Pizzas cooked with IR Laser 20 kept a significantly higher percentage of moisture ($p<0.05$).

Fat content of cooked pizzas was significantly higher than fat content of raw doughs, but there were no differences between cooking treatments. Results of fat percentage expressed on dry basis did not change ($p>0.05$) between raw and cooked pizzas neither between cooking methods (Raw: 9.74 ± 0.78; IR Laser 20: 10.52 ± 0.06; IR Oven: 10.61 ± 0.11; Deck Oven: 10.28 ± 0.65).

Protein and ashes content were also significantly higher in cooked pizzas than in doughs. Pizza cooked with the IR Oven had the highest amount of protein, followed by pizza cooked with Deck Oven whereas pizza cooked with IR Laser 20 had the lowest protein content. Ashes content of cooked pizzas followed a similar trend, although no significant differences were observed between pizza samples cooked with IR Oven and IR Laser 20.

Table 4.11. Cooking loss, moisture and proximate analysis results of raw and cooked Finissima pizza dough.

Treatments	Cooking loss (%)	Moisture content (%)	Fat content (%)	Protein content (%)	Ashes content (%)
Raw		35.24 ± 0.09^{a}	6.31 ± 0.50^{b}	6.90 ± 0.02^{d}	1.93 ± 0.03^{c}
IR Laser 20	15.87 ± 1.26^{c}	21.21 ± 1.40^{b}	8.29 ± 0.19^{a}	7.18 ± 0.11^{c}	2.38 ± 0.07^{b}
IR Oven	20.14 ± 0.81^{b}	17.28 ± 0.39^{c}	8.78 ± 0.10^{a}	8.86 ± 0.05^{a}	2.46 ± 0.06^{b}
Deck Oven	25.92 ± 1.40^{a}	11.87 ± 0.92^{d}	9.10 ± 0.54^{a}	8.17 ± 0.08^{b}	2.69 ± 0.07^{a}

[(a-d)] Mean values ± standard deviations (n=6). Values labeled with a different letter in the same column are significantly different ($p<0.05$).

Significant differences between all treatments reflect that water activity was affected by the cooking methods applied (table 4.12).

Table 4.12. Water activity of raw and cooked Finissima pizza dough.

Treatments	Water Activity
Raw	0.966 ± 0.003^{a}
IR Laser 20	0.858 ± 0.007^{b}
IR Oven	0.799 ± 0.016^{c}
Deck Oven	0.685 ± 0.040^{d}

(a-c) Mean values ± standard deviations (n=6). Values labeled with a different letter in the same column are significantly different ($p<0.05$).

4.2.2.2. Texture analysis

Penetration force values from pizzas cooked with Deck Oven were significantly higher than values from pizzas cooked with IR Laser 20 and IR Oven, which did not show significant differences between them (table 4.13).

Table 4.13. Penetration force of Finissima pizza dough cooked with different methods.

Treatments	Penetration force (N)
IR Laser 20	2.02 ± 0.19^{b}
IR Oven	2.96 ± 0.48^{b}
Deck Oven	8.61 ± 0.76^{a}

(a-b) Mean values ± standard deviations (n=18). Values labeled with a different letter in the same column are significantly different ($p<0.05$).

4.2.2.3. Color analysis

Color of first cooking side was analyzed separately from color of second cooking side because there were significant differences between sides in the case of IR Laser 20 and Deck Oven methods (table 4.14).

Regarding color of first cooking side, it could be observed that lightness (L*) and chromatic component a* did not show significant differences between raw doughs and

pizzas cooked with IR Oven and Deck Oven treatments. On the contrary, lightness of pizzas cooked with IR Laser 20 was significantly lower and a*, the reddish component, increased significantly. Chromatic component b* values of raw doughs were significantly lower than those of cooked pizzas, being IR Laser 20 cooked pizzas the samples that presented the highest increase in the yellowish component. Hence, total color difference (ΔE*) of IR Laser 20 samples was significantly higher than ΔE* calculated from the other cooking treatments, which did not show significant differences between them.

To analyze the color of second cooking side, cooking treatments were compared only between them, as raw pizza had been previously compared with the first cooking side, and second side was already partially cooked at the end of first side cooking in the case of IR Laser 20 treatment. There were not significant differences between IR Laser 20 and Deck Oven in any of the color parameters measured, whereas there were always significant differences between those two treatments and IR Oven: lightness was significantly lower in pizzas cooked with IR Laser 20 and Deck Oven whereas chromatic components a* and b* were higher. These results led to higher values of External ΔE^* for IR Laser 20 and Deck Oven treatments. Color of samples can be observed in figures 4.8, 4.9 and 4.10, which show that pizzas cooked with IR Laser 20 and Deck Oven developed more browning.

Table 4.14. CIE *L**, *a** and *b** values and total color difference (ΔE*) of first cooking side and second cooking side in Finissima pizza dough samples treated with different cooking methods.

		Cooking methods		
	Raw	IR Laser 20	IR Oven	Deck Oven
Color of first cooking side				
L*	86.88 ± 0.77[a]	66.70 ± 0.25[b]	84.19 ± 1.85[a]	81.69 ± 3.27[a]
a*	0.76 ± 0.15[b]	11.73 ± 1.33[a]	0.28 ± 0.81[b]	0.65 ± 0.16[b]
b*	14.99 ± 0.17[c]	35.60 ± 1.01[a]	20.21 ± 2.66[b]	18.45 ± 0.76[b]
Internal Δ*E**	-	31.54 ± 4.22[a]	6.51 ± 2.56[b]	6.82 ± 2.50[b]
Color of second cooking side				
L*	-	74.28 ± 2.67[b]	83.69 ± 1.90[a]	78.85 ± 1.45[b]
a*	-	5.46 ± 1.76[a]	0.29 ± 0.66[b]	3.87 ± 1.27[a]
b*	-	29.12 ± 3.84[a]	18.75 ± 1.34[b]	24.61 ± 2.34[a]
External Δ*E**	-	20.16 ± 5.97[a]	5.52 ± 1.69[b]	13.32 ± 4.11[a]

[(a-d)] Mean values ± standard deviations (n=18). Values labeled with a different letter in the same row are significantly different ($p<0.05$).

4.2.2.4. Images of samples during the cooking process

Images of pizza dough samples were taken before, during and after cooking treatments to illustrate changes and differences in appearance.

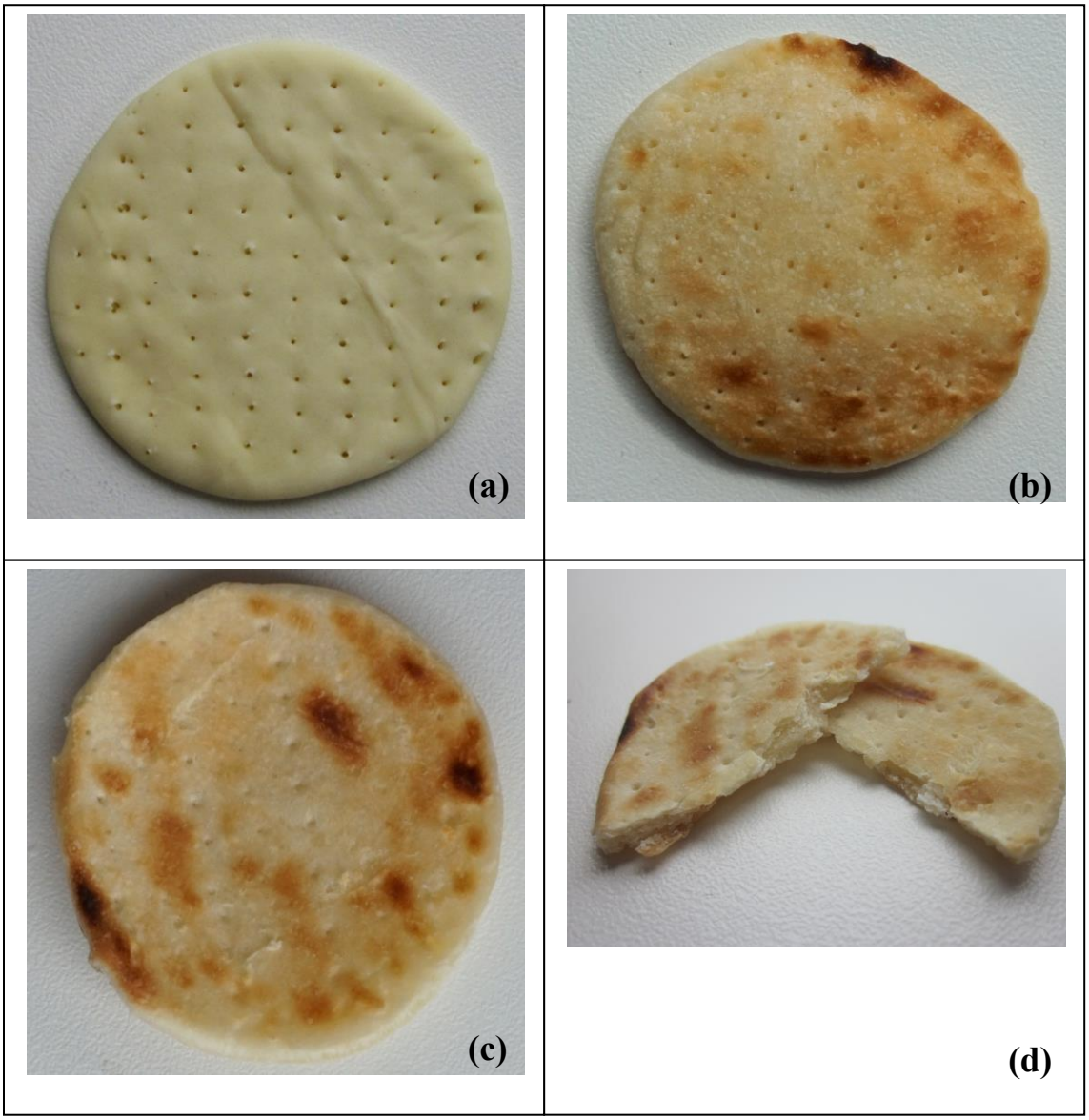

Fig 4.8. Finissima pizza dough cooked with IR Laser 20. (a) Raw pizza; (b) First side after laser impact; (c) Second side after laser impact; (d) Vertical cross-section of cooked pizza.

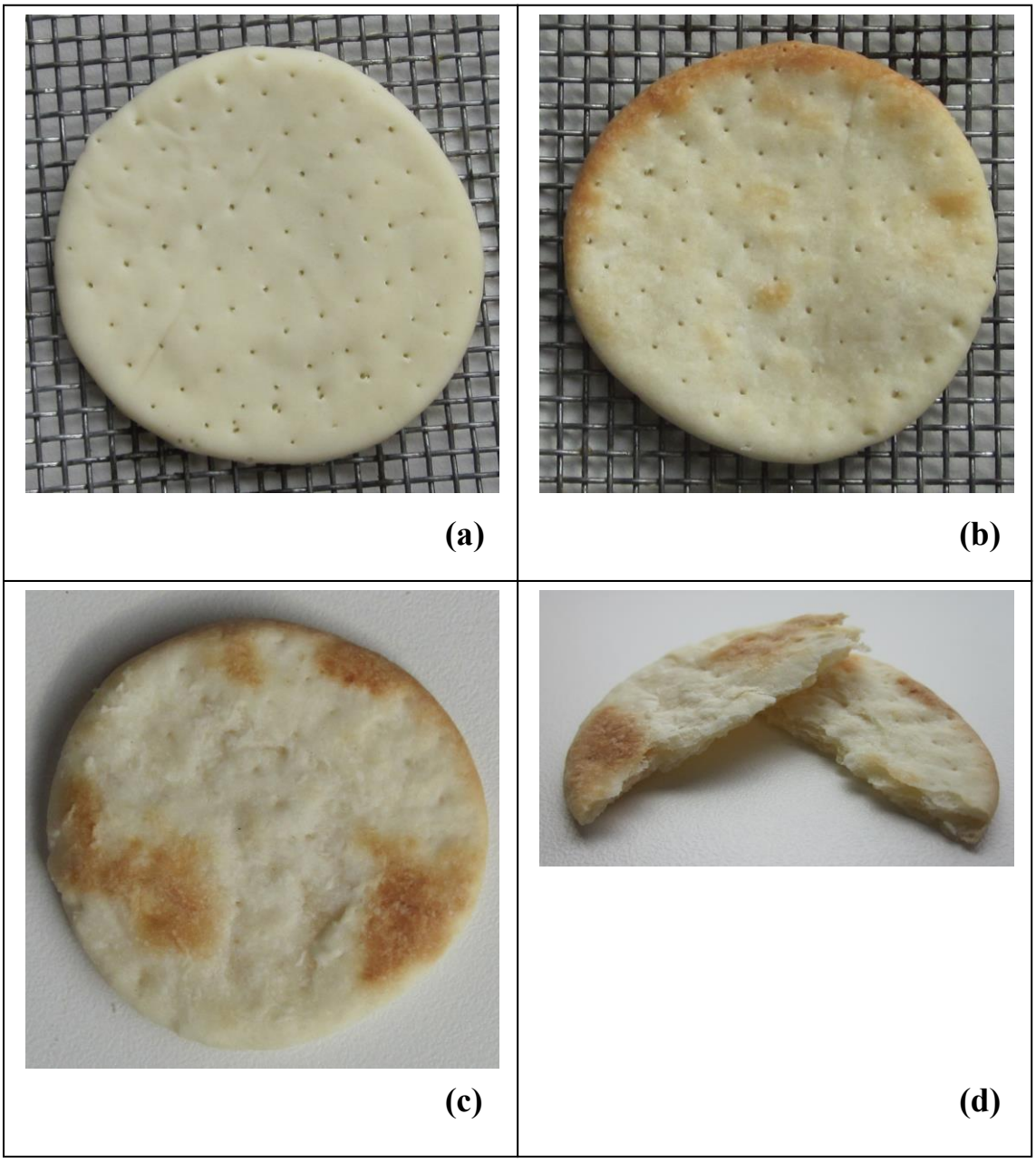

Fig 4.9. Finissima pizza dough cooked with IR Oven. (a) Raw pizza; (b) Top cooking side; (c) Bottom cooking side in contact with the rack grill; (d) Cooked pizza, vertical cross-section.

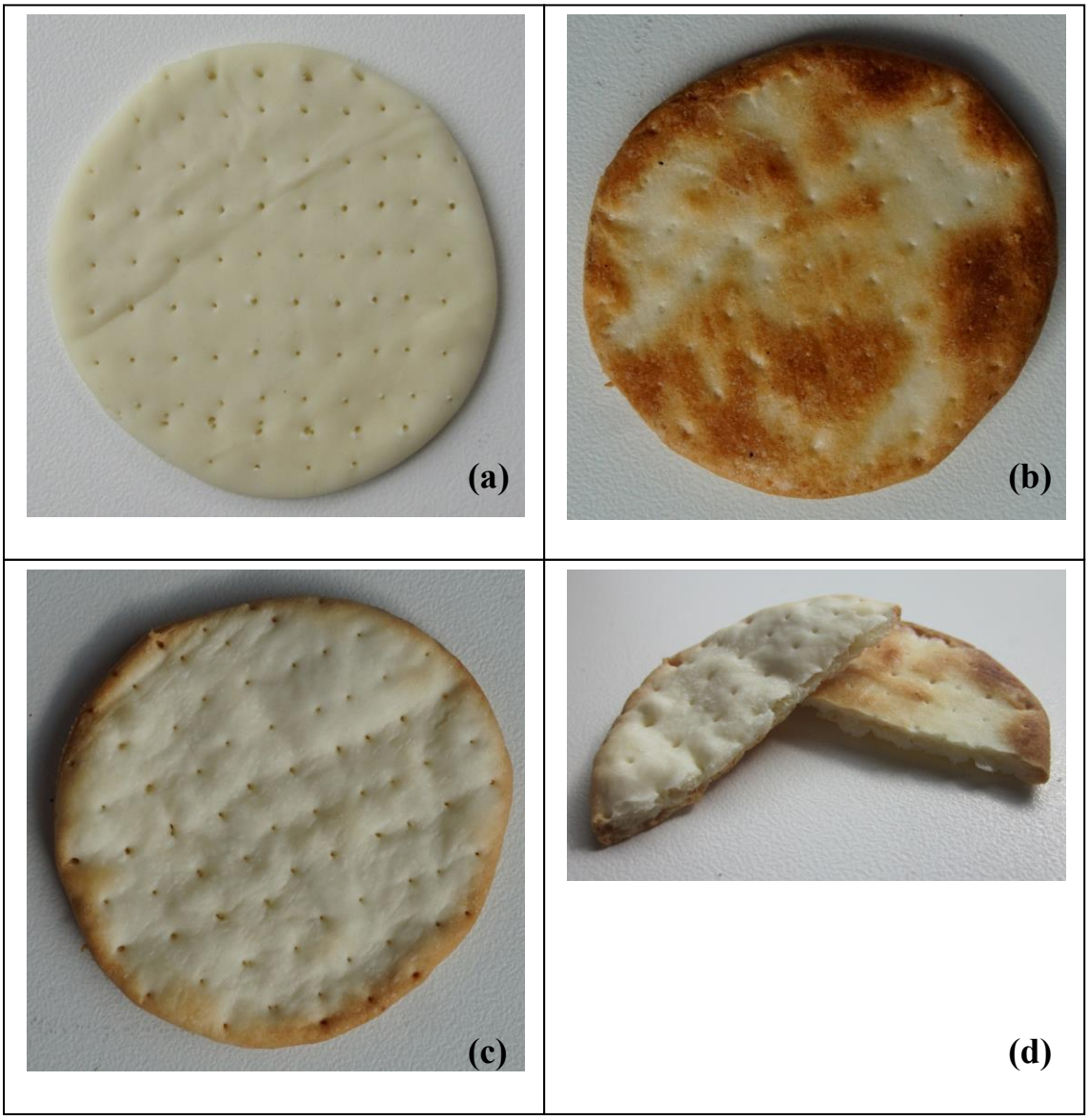

Fig 4.10. Finissima pizza dough cooked with Deck Oven. (a) Raw pizza; (b) Top cooking side; (c) Bottom cooking side in contact with the deck oven surface; (d) Cooked pizza, vertical cross-section.

4.2.2.5. Sensory analysis

Consumers evaluated the general appearance of pizzas cooked with IR Laser 20 and Deck Oven with better scores than the general appearance of samples cooked with IR Oven, which received a significantly lower rating (table 4.15 and figures, 4.8, 4.9, 4.10).

When the intensity of different attributes was evaluated, the external color of pizza cooked with IR Laser 20 was scored as the brownest, followed by Deck Oven and IR Oven, which had a significantly lighter color. The level of doneness was similar for IR Laser 20 and Deck Oven, whereas doneness was significantly lower for pizza cooked with IR Oven. Pizzas cooked with Deck Oven were the crunchiest, whereas pizzas cooked with IR based treatments were significantly softer. Taste intensity was significantly higher in pizzas cooked with IR Laser 20 and Deck Oven than in pizzas cooked with IR Oven. Three different levels of flavor intensity could be identified: the highest, which corresponded to pizzas cooked with IR Laser 20; the intermediate, for pizzas cooked with Deck Oven; and the lowest, for pizzas cooked with IR Oven ($p<0.05$).

Regarding acceptability, external color, level of doneness, taste and flavor of pizzas cooked with IR Laser 20 and Deck Oven received the highest ratings, whereas these four attributes were significantly less accepted in samples cooked with IR Oven. Crunchiness of pizzas was better accepted in samples cooked with the Deck Oven, whereas softer pizzas, obtained with IR Laser 20 and IR Oven, were less accepted.

Preference test showed that consumers preferred pizzas cooked with Deck Oven and IR Laser 20. Pizzas cooked with IR Oven were ranked in the last place (table 4.16).

Table 4.15. Results of the consumer test for Finissima pizza dough cooked with different methods.

	IR Laser 20	IR Oven	Deck Oven
General appearance	4.92 ± 1.43[a]	3.52 ± 1.60[b]	4.64 ± 1.67[a]
Intensity			
External Color	5.79 ± 0.69[a]	2.28 ± 1.07[c]	3.26 ± 1.20[b]
Doneness	4.39 ± 1.52[a]	2.99 ± 1.46[b]	4.51 ± 1.43[a]
Crunchiness	2.70 ± 1.38[b]	2.89 ± 1.40[b]	5.31 ± 1.14[a]
Taste	4.35 ± 1.32[a]	2.94 ± 1.15[b]	4.60 ± 1.17[a]
Flavor	4.78 ± 1.35[a]	2.51 ± 1.25[c]	3.79 ± 1.29[b]
Acceptability			
External Color	4.74 ± 1.50[a]	3.06 ± 1.52[b]	4.23 ± 1.71[a]
Doneness	3.92 ± 1.82[a]	2.79 ± 1.52[b]	4.46 ± 1.67[a]
Crunchiness	3.51 ± 1.81[b]	2.62 ± 1.28[c]	4.90 ± 1.68[a]
Taste	4.67 ± 1.67[a]	3.46 ± 1.40[b]	5.25 ± 1.43[a]
Flavor	4.86 ± 1.28[a]	3.02 ± 1.33[b]	4.58 ± 1.31[a]

[(a-c)] Mean values ± standard deviations (n=51). Values labeled with a different letter in the same row are significantly different (p<0.05).

Table 4.16. Results of preference test for Finissima pizza dough cooked with different methods.

	Number of answers for each order of preference (1-3) and multiplied by its order of preference			
	***1**	***2**	***3**	Sum
IR Laser 20	21	46	21	88[a]
IR Oven	6	12	117	135[b]
Deck Oven	24	44	15	83[a]

[(a-b)] Values labeled with a different letter in the same column are significantly different (p<0.05).

4.2.2.6. Differential scanning calorimetry

Peak areas of all cooked samples were significantly lower than those of raw dough (table 4.17). Calculated peak areas of IR Laser 20 and IR Oven were not significantly different between them, but the peak area of Deck Oven was significantly lower than the area of IR based treatments.

Cooking treatment caused a significant decrease in peak temperatures, being the pizzas cooked with Deck Oven the ones with the lowest peak temperatures.

Table 4.17. Peak areas and peak temperatures from DSC analysis of Finissima pizza dough.

Treatments	Area (J/g)	Peak Temperature (°C)
Raw	$384.50 \pm 44{,}24^{a}$	$109.37 \pm 0{,}19^{a}$
IR Laser 20	180.72 ± 32.15^{b}	105.40 ± 0.31^{b}
IR Oven	165.07 ± 10.64^{b}	$104.23 \pm 1.30^{b,c}$
Deck Oven	92.32 ± 4.5^{c}	102.65 ± 0.68^{c}

(a-c) Mean values ± standard deviations (n=12). Values labeled with a different letter in the same column are significantly different ($p<0.05$).

4.2.3. Mashed potatoes bites

4.2.3.1. Cooking loss, moisture, proximate analysis and water activity

Cooking loss of mashed potatoes bites was significantly different between all samples. Cooking with IR Oven caused the higher cooking loss, followed by IR Laser 62, whereas cooking with traditional method caused the lowest loss (table 4.18)

Moisture content was also significantly different between cooked mashed potatoes bites. Mashed potatoes bites treated with the IR Oven had the lowest amount of moisture, followed by the samples cooked with IR Laser 62. Bites cooked with the traditional method kept the highest percentage of moisture, in accordance with cooking losses.

Mashed potatoes cooked with IR Oven and IR Laser 62 had the highest content in protein. Samples cooked with the Traditional Method had the lowest amount of protein content, although samples cooked with this treatment did not show significant differences with the bites cooked with IR Oven. Regarding fat content, no significant differences could be observed. Ash content was significantly different between all treatments. Bites cooked with IR Oven had the highest content of ashes, followed by the IR Laser 62, whereas bites cooked with the traditional method had the lowest content.

There were not significant differences on the amounts of fat, protein and ashes expressed on dry basis (results not shown).

Table 4.18. Cooking loss, moisture and proximate analysis results of mashed potatoes bites cooked with different methods.

Treatments	Cooking loss (%)	Moisture content (%)	Protein content (%)	Fat content (%)	Ashes content (%)
Traditional method	5.45 ± 0.68^{c}	82.46 ± 0.26^{a}	1.95 ± 0.03^{b}	0.66 ± 0.06	0.80 ± 0.01^{c}
IR Laser 62	8.68 ± 0.28^{b}	81.82 ± 0.01^{b}	2.05 ± 0.02^{a}	0.73 ± 0.08	0.85 ± 0.03^{b}
IR Oven	17.28 ± 0.97^{a}	80.33 ± 0.52^{c}	$2.00 \pm 0.06^{a,b}$	0.89 ± 0.35	0.92 ± 0.02^{a}

[a-c] Mean values ± standard deviations (n=6). Values labeled with a different letter in the same column are significantly different ($p<0.05$).

There were not significant differences between water activity values of bites cooked with different methods (values ranged between 0.979 ± 0.003 and 980 ± 0.002).

4.2.3.2. Texture analysis

Force of compression between cooked mashed potatoes bites was significantly different between all treatments. IR Oven showed caused the highest force of compression in bites, followed by the IR Laser 62. Finally, bites cooked with Traditional method presented the lowest force (table 4.19).

Table 4.19. Force of compression in mashed potatoes bites treated with different cooking methods.

Treatments	Force of Compression (N)
Traditional method	5.35 ± 0.45^{c}
IR Laser 62	8.48 ± 0.21^{b}
IR Oven	15.50 ± 0.40^{a}

(a-c) Mean values ± standard deviations (n=18). Values labeled with a different letter in the same column are significantly different (p<0.05).

4.2.3.3. Color analysis

External color of top side of mashed potatoes bites was analyzed (table 4.20). There were significant differences between color parameters of all samples. Traditional cooking method produced the bites with highest lightness values and lowest values of chromatic components a* and b*. Bites cooked with IR Oven presented intermediate values of lightness and b*, but the highest value of a*. IR Laser 62 produced the bites with lowest lightness and highest b*. These samples were the ones that presented some browning in their surface (figures 4.11, 4.12 and 4.13).

Table 4.20. CIE *L**, *a** and *b** values of the external surface of mashed potatoes bites cooked with different methods.

Treatments	L*	a*	b*
Traditional method	80.62 ± 0.34^{a}	3.93 ± 0.07^{c}	22.41 ± 0.21^{c}
IR Laser 62	73.48 ± 0.04^{c}	4.40 ± 0.15^{b}	25.63 ± 0.41^{a}
IR Oven	75.16 ± 0.43^{b}	4.87 ± 0.20^{a}	24.36 ± 0.39^{b}

(a-c) Mean values ± standard deviations (n=6). Values labeled with a different letter in the same column are significantly different (p<0.05).

4.2.3.4. Images of samples during the cooking process

Images of mashed potatoes bites were taken before and after cooking treatments to illustrate changes and differences in appearance.

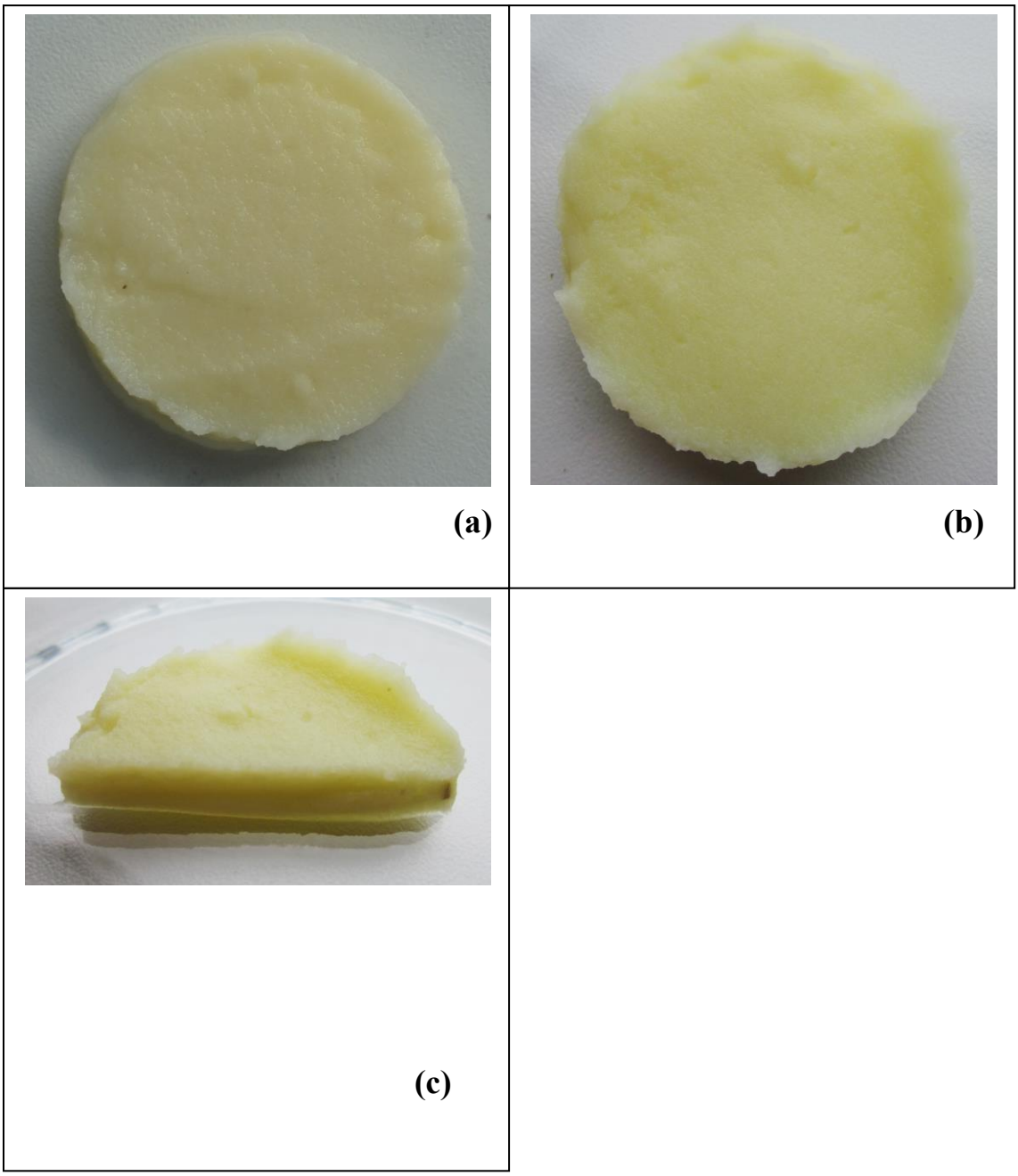

Fig 4.11. Mashed potatoes bites cooked with Traditional Method. (a) Raw; (b) Cooked, top view; (c) Cooked, vertical cross-section.

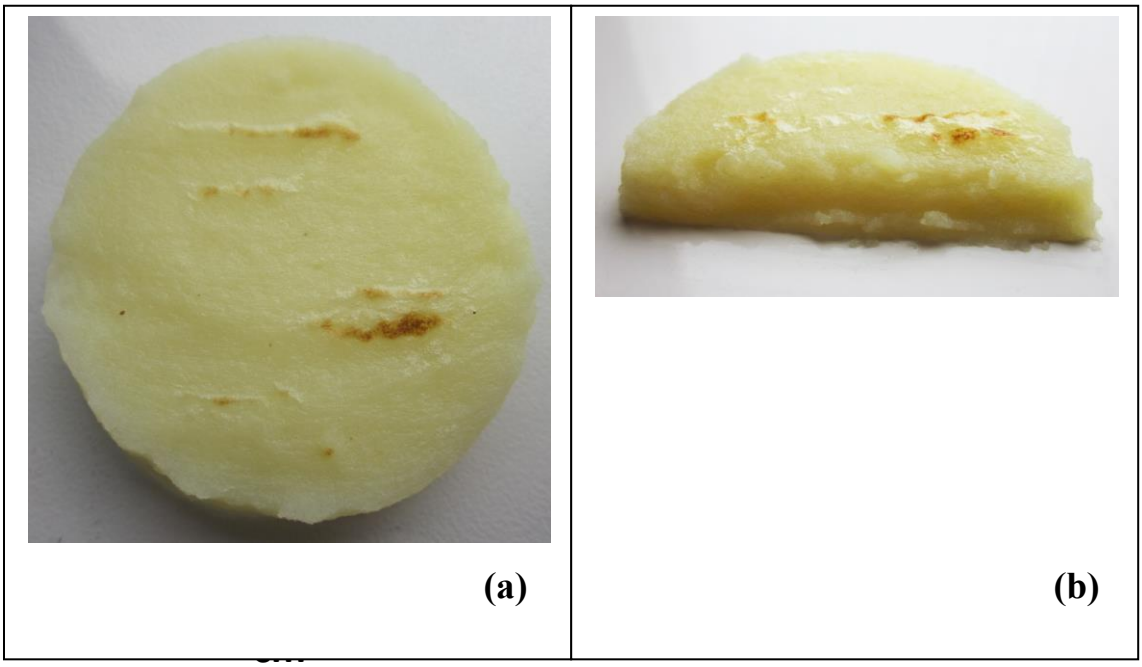

Fig 4.12. Mashed potatoes bites cooked with IR Laser 62. (a) Cooked, top view; (b) Cooked, vertical cross-section.

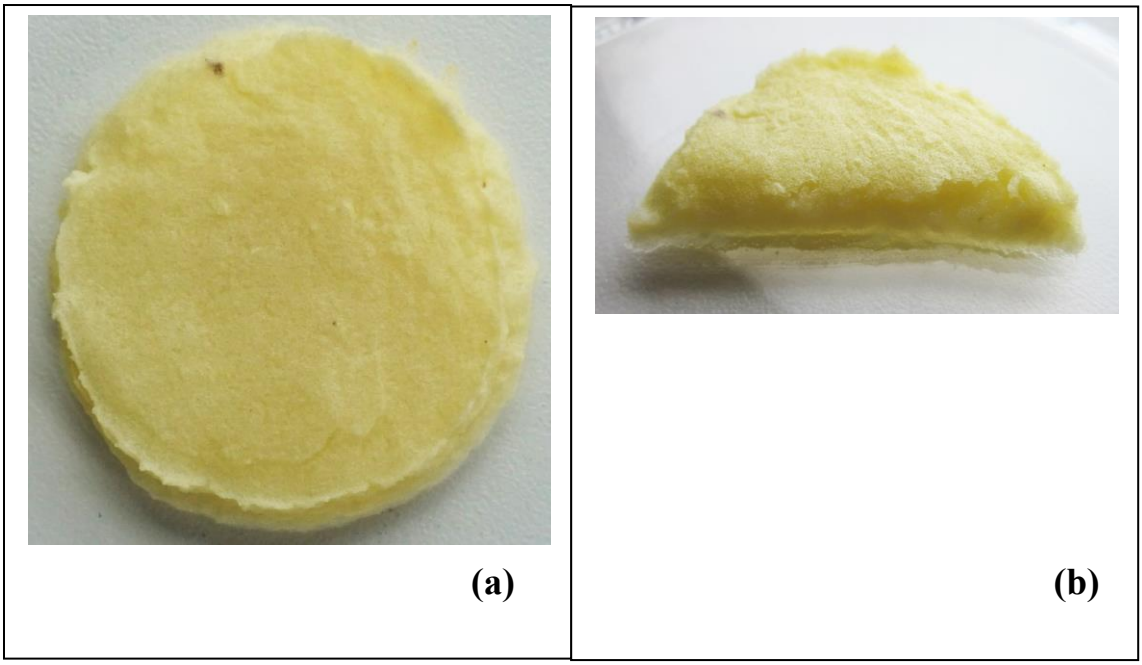

Fig 4.13. Mashed potatoes bites cooked with IR Oven. (a) Cooked, top view; (b) Cooked, vertical cross-section.

4.2.3.5. Sensory analysis

Consumers considered that there were not significant differences in the general appearance of mashed potatoes bites cooked with the different treatments (table 4.21 and figures 4.11, 4.12, 4.13).

When consumers evaluated the intensity of sensory attributes, they assessed that external color, internal color and hardness of bites cooked with IR Laser 62 and IR Oven were significantly more intense or higher than those of bites cooked with Traditional Method. Taste of samples cooked with Traditional Method was evaluated as less intense, whereas the most intense taste corresponded to samples cooked with IR Oven. Flavor of all samples was rated similarly ($p>0.05$).

Acceptability scores of external color, internal color and flavor of all samples were similar ($p>0.05$). Hardness and taste of bites cooked with IR based methods were evaluated better than those of bites cooked with Traditional Method.

Consumers preferred the mashed potatoes bites cooked using IR Laser 62 and IR Oven (Table 4.22).

Table 4.21. Results of the consumer test for mashed potatoes bites cooked with different methods.

	Traditional Method	IR Laser 62	IR Oven
General appearance	4.55 ± 1.34	4.66 ± 1.16	4.78 ± 1.31
Intensity			
External color	2.79 ± 0.88^{b}	4.36 ± 1.03^{a}	4.40 ± 1.13^{a}
Internal color	3.14 ± 1.06^{b}	4.09 ± 1.02^{a}	4.49 ± 1.20^{a}
Hardness	3.77 ± 1.21^{b}	4.79 ± 1.20^{a}	5.31 ± 0.96^{a}
Taste	3.36 ± 1.28^{a}	3.88 ± 0.97^{a,b}	4.05 ± 1.06^{b}
Flavor	3.53 ± 1.39	3.81 ± 1.01	3.97 ± 1.20
Acceptability			
External color	4.29 ± 1.45	4.59 ± 1.28	4.72 ± 1.21
Internal color	4.42 ± 1.28	4.69 ± 0.94	4.58 ± 1.23
Hardness	4.15 ± 1.44^{b}	5.06 ± 1.12^{a}	4.74 ± 1.27^{a,b}
Taste	4.26 ± 1.49^{b}	4.89 ± 1.19^{a}	4.97 ± 1.17^{a}
Flavor	4.27 ± 1.37	4.61 ± 1.17	4.73 ± 1.20

$^{(a-b)}$ Mean values ± standard deviations (n=50). Values labeled with a different letter in the same row are significantly different ($p<0.05$).

Table 4.22. Test of preference for mashed potatoes bites treated with different cooking methods.

	Number of answers for each order of preference (1-3) and multiplied by its order of preference			
	***1**	***2**	***3**	Sum
Traditional Method	11	22	81	114[b]
IR Laser 62	24	34	30	88[a]
IR Oven	15	44	39	98[a]

[(a-b)] Values labeled with a different letter in the same column are significantly different (p<0.05).

4.3. Results of the second experimental study with CO2 IR Laser Foodini system.

Beef burgers, pizza dough and mashed potatoes bites were cooked using an innovative CO_2 IR Laser Foodini system and other standard methods.

4.3.1. Beef burgers

Internal cooking temperatures of beef burgers cooked with CO_2 IR laser Foodini system are shown in section 4.4.1 (table 4.47). The internal temperatures for IR Oven, BBQ Grill and Flat Grill have been previously shown in section 4.2.1.1 (table 4.1).

4.3.1.1. Cooking loss, moisture, proximate analysis and water activity

Cooking loss was significantly higher in samples cooked with Flat Grill than in samples cooked with IR Laser and IR Oven were lower (table 4.23).

Moisture, protein, fat and ashes content were significantly different between cooked and raw burgers: moisture content decreased in cooked burgers whereas protein, fat and ashes content increased.

Between cooked samples, burgers cooked with Flat Grill were the ones with a higher moisture content whereas burgers cooked with BBQ Grill had the lowest. Burgers cooked with BBQ Grill had the highest protein content, and burgers cooked with Flat Grill the lowest. Nevertheless, looking at the results expressed on dry basis, burgers cooked with BBQ Grill and Flat Grill had the highest protein content and the lowest fat content (results not shown). Burgers cooked with Flat Grill also had the lowest percentage of fat and ashes expressed on wet basis.

Table 4.23. Cooking loss, moisture and proximate analysis results of raw and cooked beef burgers.

Treatments	Cooking loss (%)	Moisture content (%)	Protein content (%)	Fat content (%)	Ashes content (%)
Raw		70.91 ± 0.14^{a}	20.85 ± 0.26^{d}	5.38 ± 0.22^{c}	2.47 ± 0.12^{c}
IR Laser	22.01 ± 0.90^{b}	64.14 ± 0.91^{c}	26.41 ± 0.60^{a,b}	6.39 ± 0.40^{a}	3.04 ± 0.08^{a}
IR Oven	22.29 ± 0.88^{b}	65.00 ± 1.00^{b,c}	25.53 ± 1.12^{b,c}	6.48 ± 0.01^{a}	2.96 ± 0.06^{a,b}
BBQ Grill	23.34 ± 0.61^{a,b}	63.32 ± 0.80^{c}	27.07 ± 0.62^{a}	6.48 ± 0.22^{a}	3.02 ± 0.18^{a}
Flat Grill	24.24 ± 1.26^{a}	66.26 ± 0.52^{b}	25.44 ± 0.21^{c}	5.88 ± 0.09^{b}	2.82 ± 0.04^{b}

(a-d) Mean values ± standard deviations (n=6). Values labeled with a different letter in the same column are significantly different (p<0.05)

There were not significant differences between water activity values of raw beef and cooked meat, neither between the different cooking treatments. Water activity of raw beef burger was 0.986 ± 0.002, and the water activity of all cooked burgers was between 0.983 ± 0.003 (IR Laser) and 0.991 ± 0.003 (Flat Grill).

4.3.1.2. Texture analysis

Table 4.24 shows the results of compression and penetration analyses. Burgers cooked with IR Laser, IR Oven and BBQ Grill were the hardest, although not clear differences could be observed between samples cooked with BBQ Grill and Flat Grill. Cutting force values followed a similar behavior. In this case, burgers cooked with IR Oven and IR Laser presented the highest cutting force, followed by burgers cooked with BBQ and Flat Grill, although these last samples did not show significant differences with samples cooked with IR Laser. No significant differences in springiness were observed between cooking methods.

Table 4.24. Hardness, Springiness and Cutting Force of raw and cooked beef burgers.

Treatments	Hardness (N)	Springiness	Cutting Force (N)
Raw	15.04 ± 1.60^{c}	0.69 ± 0.03^{b}	1.46 ± 0.09^{c}
IR Laser	92.01 ± 5.14^{a}	0.90 ± 0.03^{a}	15.11 ± 1.38^{a,b}
IR Oven	91.33 ± 3.38^{a}	0.91 ± 0.04^{a}	16.62 ± 1.47^{a}
BBQ Grill	86.40 ± 7.84^{a,b}	0.90 ± 0.03^{a}	13.27 ± 0.36^{b}
Flat Grill	79.52 ± 5.71^{b}	0.89 ± 0.04^{a}	13.05 ± 0.83^{b}

(a-c) Mean values ± standard deviations (n=18). Values labeled with a different letter in the same column are significantly different (p<0.05).

4.3.1.3. Color analysis

Lightness (L*) values obtained during the measurement of internal color were significantly higher in cooked than in raw burgers. IR Oven and IR Laser treatments caused the highest increase, although L* values of burgers cooked with IR Laser were not significantly different from those of burgers cooked with BBQ and Flat Grill. Chromatic components a* and b* decreased significantly after cooking and there were not differences between treatments. Total color difference (ΔE*) of burgers cooked with IR Laser and IR Oven was higher than ΔE* of burgers cooked with BBQ Grill and Flat Grill, in accordance with the differences observed in L*.

Regarding external color, burgers cooked with IR Laser showed the highest lightness. L* values of burgers cooked with IR Oven were not different from raw burgers and burgers cooked with BBQ and Flat Grill ($p>0.05$). Chromatic components a* and b* decreased significantly after cooking but significant differences related to cooking methods could only be observed between a* values of burgers cooked with IR Laser and IR Oven, which showed the lowest and the highest values of a*, respectively. Burgers cooked with IR Laser showed the highest ΔE* whereas there were not significant differences between the other three systems (table 4.25).

Table 4.25. CIE *L**, *a** and *b** values and total color difference (ΔE*) of the internal and the external side of raw and cooked beef burgers.

	Cooking methods				
	Raw	IR Laser	IR Oven	BBQ Grill	Flat Grill
Internal Color					
L*	39.34 ± 0.21^{c}	$51.04 \pm 0.94^{a,b}$	51.87 ± 0.68^{a}	49.91 ± 1.04^{b}	49.43 ± 1.48^{b}
a*	18.97 ± 0.33^{a}	5.64 ± 0.12^{b}	5.78 ± 0.10^{b}	5.60 ± 0.15^{b}	5.59 ± 0.36^{b}
b*	17.10 ± 0.33^{a}	13.95 ± 0.30^{b}	13.90 ± 0.28^{b}	13.96 ± 0.52^{b}	14.53 ± 0.49^{b}
Internal ΔE^{*}	-	18.04 ± 0.82^{a}	18.49 ± 0.86^{a}	17.39 ± 0.91^{b}	17.03 ± 0.78^{b}
External Color					
L*	39.46 ± 0.09^{b}	41.60 ± 0.36^{a}	$39.83 \pm 0.17^{a,b}$	37.82 ± 1.48^{b}	39.47 ± 0.86^{b}
a*	18.84 ± 0.24^{a}	6.20 ± 0.06^{c}	7.12 ± 0.11^{b}	$6.82 \pm 0.19^{b,c}$	$6.66 \pm 0.51^{b,c}$
b*	16.69 ± 0.21^{a}	14.21 ± 0.61^{b}	13.80 ± 0.51^{b}	14.69 ± 0.44^{b}	14.75 ± 0.53^{b}
External ΔE^{*}	-	13.12 ± 0.72^{a}	12.22 ± 0.50^{b}	12.52 ± 0.53^{b}	12.49 ± 0.93^{b}

[(a-c)] Mean values ± standard deviations (n=36). Values labeled with a different letter in the same row are significantly different ($p<0.05$).

4.3.1.4. Images of samples during the cooking process

Only images of beef burgers cooked with CO_2 IR Laser Foodini system were taken during this experiment. Images from beef burgers cooked with IR Oven, BBQ Grill and Flat Grill methods were not repeated. Although, for comparison purposes, images from section 4.2. (figures 4.2, 4.3, 4.4, 4.5 and 4.6) can be used.

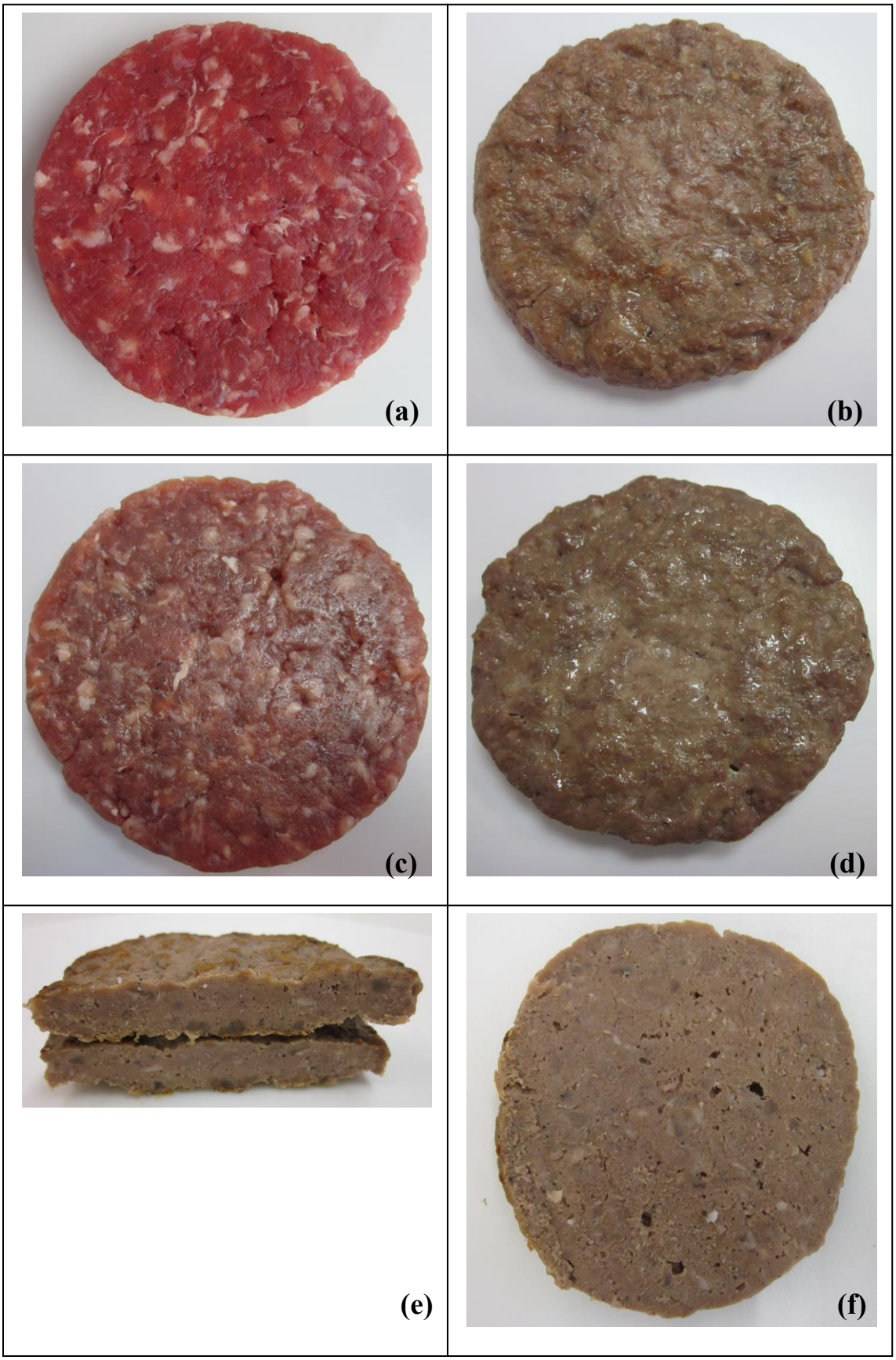

Fig 4.14. Cooking process of beef burgers treated with IR Laser. (a) First side, raw burger; (b) End of cooking of first side; (c) Second side, after cooking of first side; (d) End of cooking of second side; (e) Cooked burger, vertical cross-section; (f) Cooked burger, horizontal cross-section.

4.3.1.5. Sensory analysis

Burgers cooked with IR Laser received the highest rating in general appearance whereas burgers cooked with BBQ Grill received the lowest ($p<0.05$).

Consumers evaluated the external color of burgers cooked with BBQ Grill and Flat Grill as significantly more brownish than external color of burgers treated with IR Laser and IR Oven. Internal color of burgers cooked with BBQ Grill, Flat Grill and IR Oven was also evaluated as browner than internal color of samples cooked with IR Laser. The level of doneness was evaluated as significantly higher in samples cooked with BBQ Grill and Flat Grill than in samples cooked with IR Laser. On the contrary, samples cooked with BBQ Grill and Flat Grill were evaluated as significantly less tender than samples cooked with IR Laser, which received the highest rating in this attribute. Beef burgers cooked with IR Laser were the juiciest samples, followed by samples cooked with IR Oven and Flat Grill, which did not show significant differences in the intensity of this attribute. Samples cooked with BBQ Grill were rated as the least juicy ($p<0.05$). There were not significant differences between taste intensity of burgers treated with the different cooking methods (table 4.26).

Regarding acceptability, the attributes of external color, internal color, doneness and taste of all burgers received similar evaluations ($p>0,05$). Tenderness of burgers cooked with IR Laser and IR Oven was better rated than tenderness of burgers cooked with BBQ Grill and Flat Grill. Similarly, the juiciness of burgers cooked with IR Laser and IR Oven was significantly more accepted by consumers, followed by samples cooked with Flat Grill. Burgers cooked with BBQ Grill received the lower rating in juiciness acceptability, although it did not show significant differences with the evaluation received by samples cooked with Flat Grill method.

Preference test showed that beef burgers cooked with IR Laser were the most preferred by consumers, followed by samples cooked with IR Oven and Flat Grill (table 4.27). Burgers cooked with BBQ Grill were the least preferred ($p<0.05$).

Table 4.26. Results of the consumer test for beef burgers cooked with different methods.

	IR Laser	IR Oven	BBQ Grill	Flat Grill
General appearance	4.83 ± 1.47[a]	4.61 ± 1.34[a,b]	4.04 ± 1.54[b]	4.52 ± 1.41[a,b]
Intensity				
External Color	4.56 ± 0.98[b]	4.55 ± 1.35[b]	5.76 ± 1.05[a]	5.41 ± 1.10[a]
Internal Color	4.21 ± 1.08[b]	4.83 ± 1.14[a]	5.28 ± 1.31[a]	5.15 ± 1.04[a]
Doneness	4.62 ± 1.20[c]	5.15 ± 1.17[b,c]	5.86 ± 1.00[a]	5.47 ± 1.14[a,b]
Tenderness	4.49 ± 1.06[a]	3.93 ± 1.15[a,b]	3.07 ± 1.12[c]	3.57 ± 1.05[b,c]
Juiciness	4.58 ± 1.35[a]	3.89 ± 1.39[b]	2.72 ± 1.03[c]	3.46 ± 1.27[b]
Taste	4.36 ± 1.40	4.39 ± 1.24	4.52 ± 1.37	4.94 ± 1.09
Acceptability				
External Color	4.69 ± 1.40	4.40 ± 1.40	4.33 ± 1.60	4.64 ± 1.30
Internal Color	4.48 ± 1.51	4.45 ± 1.59	4.26 ± 1.76	4.53 ± 1.49
Doneness	4.22 ± 1.33	4.29 ± 1.50	3.67 ± 1.62	3.93 ± 1.52
Tenderness	4.55 ± 1.29[a]	4.36 ± 1.51[a]	3.28 ± 1.40[b]	3.77 ± 1.30[b]
Juiciness	4.72 ± 1.66[a]	4.05 ± 1.51[a,b]	3.23 ± 1.41[c]	3.63 ± 1.45[b,c]
Taste	4.56 ± 1.48	4.50 ± 1.29	4.33 ± 1.37	4.26 ± 1.27

[(a-c)] Mean values ± standard deviations (n=50). Values labeled with a different letter in the same row are significantly different (p<0.05).

Table 4.27. Preference test of preference for beef burgers cooked with different methods.

	Number of answers for each order of preference (1-4) and multiplied by its order of preference				
	*1	*2	*3	*4	Sum
IR Laser	26	26	12	28	92[a]
IR Oven	10	44	30	32	116[b]
BBQ Grill	3	18	42	96	159[c]
Flat Grill	11	12	66	44	133[b]

[(a-c)] Values labeled with a different letter in the same column are significantly different (p<0.05).

4.3.1.6. Microbiological results

4.3.1.6.1. Microbiological analysis of non-inoculated samples

Counts of aerobic mesophilic bacteria present in raw beef meat were significantly reduced ~ 3 log CFU/g by all cooking methods. Moreover, naturally present coliforms in meat were reduced below the minimum detection limit in all cases (table 4.28).

Table 4.28. Counts of aerobic mesophilic bacteria (TSA) and coliforms (MPN in BGBL and VRBA) in non-inoculated raw and cooked beef burgers.

Treatments	TSA Count*	BGBL Count**	VRBA Count*
Raw	5.40 ± 0.99[a]	1.52 ± 0.69	2.53 ± 0.22
IR Laser	2.30 ± 0.34[b]	n.d.	n.d.
IR Oven	2.44 ± 0.10[b]	n.d.	n.d.
BBQ Grill	2.55 ± 0.35[b]	n.d.	n.d.
Flat Grill	2.22 ± 0.22[b]	n.d.	n.d.

[(a-b)] Mean (log CFU/g) ± s.d. (n=6). Values labeled with a different letter in the same column are significantly different (p<0.05). n.d.: not detected. *Detection limit: <1 log CFU/g. **Detection limit: <0.48 log CFU/g.

Raw samples that were analyzed to investigate the presence of *Salmonella and E. coli* O157:H7 in meat before inoculation gave negative results.

4.3.1.6.2. Microbiological analysis of inoculated samples

In samples inoculated at ~ 7 log CFU/g, all cooking methods were able to reduce more than 5 log CFU/g of *S.* Typimurium, *S.* Senftenberg and *E. coli* O157:H7 (table 4.29). For *S.* Typhimurium, counts were above the detection limit (< 1 log CFU/g) and they were not significantly different between cooking methods. In the case of *S.* Senftenberg and *E. coli* O157:H7, IR Oven counts were below the detection limit of the plating method. The three inoculated microorganisms were detected in all cooked samples after enrichment and growth in selective medium.

Table 4.29. Survival of *Salmonella* Typhimurium, *Salmonella* Senftenberg and *Escherichia coli* O157:H7 inoculated in beef burgers with a contamination level of ~7 log CFU/g and cooked with different methods.

	Salmonella Typhimurium		*Salmonella* Senftenberg		*Escherichia coli* O157:H7	
Treatment	Count	Detection[1]	Count	Detection[1]	Count	Detection[1]
Raw	8.1 ± 0.06[a]		7.67 ± 0.05[a]		7.28 ± 0.09[a]	
IR Laser	1.41 ± 0.65[b]	6 / 6	2.05 ± 0.24[b]	6 / 6	1.15 ± 0.54[b]	6 / 6
IR Oven	1.29 ± 1.13[b]	6 / 6	0.23 ± 0.40[c]	6 / 6	n.d.	6 / 6
BBQ Grill	1.71 ± 1.68[b]	6 / 6	2.14 ± 0.43[b]	6 / 6	1.82 ± 0.10[b]	6 / 6
Flat Grill	2.62 ± 0.39[b]	6 / 6	1.71 ± 0.28[b]	6 / 6	1.12 ± 0.39[b]	6 / 6

[(a-c)] Mean (log CFU/g) ± s.d. (n=6). Values labeled with a different letter in the same column are significantly different ($p<0.05$). n.d.: not detected; detection limit: <1 log CFU/g. [1] +/6: positive samples after enrichment and growth in selective medium.

In samples inoculated at ~ 3 log CFU/g, all treatments caused the reduction of counts below the detection limit of the plating method (<1 log CFU/g) (table 4.30). *E. coli* O157:H7 suffered the highest level of reduction, since no colonies were detected in any of the plates used to count. For *S.* Typhimurium, the average count reduction was ≥ 3 log CFU/g in samples from all the cooking methods, whereas for *S.* Senftenberg the average count reduction was < 3 log CFU/g, except in samples cooked with IR Oven, where no colonies were detected in the plates used to count. Growth of the three inoculated microorganisms after enrichment and incubation occurred in samples from all the cooking methods, except in burgers inoculated with *S.* Typhimurium and *E. coli* O157:H7 and cooked with IR Oven.

Table 4.30. Survival of *Salmonella* Typhimurium, *Salmonella* Senftenberg and *Escherichia coli* O157:H7 inoculated in beef burgers with a contamination level of ~3 log CFU/g and cooked with different methods.

	Salmonella Typhimurium		*Salmonella* Senftenberg		*Escherichia coli* O157:H7	
Treatment	Count	Detection[1]	Count	Detection[1]	Count	Detection[1]
Raw	3.57 ± 0.23[a]		3.60 ± 0.11[a]		3.54 ± 0.05[a]	
IR Laser	n.d.	1 / 6	0.63 ± 0.59[b]	6 / 6	n.d.	3 / 6
IR Oven	n.d.	0 / 6	n.d.	1 / 6	n.d.	0 / 6
BBQ Grill	0.49 ± 0.85[b]	5 / 6	0.93 ± 0.40[b]	6 / 6	n.d.	4 / 6
Flat Grill	0.23 ± 0.40[b]	6 / 6	0.73 ± 0.63[b]	6 / 6	n.d.	2 / 6

[(a-b)] Mean (log CFU/g) ± s.d. (n=6). Values labeled with a different letter in the same column are significantly different ($p<0.05$). n.d.: not detected; detection limit: <1 log CFU/g. [1] +/6: positive samples after enrichment and growth in selective medium.

.

4.3.3.7. Polycyclic aromatic hydrocarbons analysis

Concentration of PAHs for all samples and all treatments were below the minimum detection limit of the chromatographic technique.

4.3.3.8. Differential scanning calorimetry

Peak areas of all cooked burgers were significantly lower than areas of raw burgers (table 4.31). There were not significant differences between peak areas of burgers cooked with different methods. Regarding the peak temperatures, no significant differences were observed between values of raw and cooked samples and neither within cooked samples. Figure 4.15. depicts an example of a typical DSC curve for each sample where the difference between the areas of raw and cooked burgers can be observed.

Table 4.31. Peak areas and peak temperatures from DSC analysis of raw and cooked burgers.

Treatments	Area (J/g)	Peak Temperature (°C)
Raw	1033.04 ± 22.80[a]	78.25 ± 1.54
IR Laser	778.07 ± 18.92[b]	77.00 ± 2.80
IR Oven	789.89 ± 22.06[b]	76.86 ± 1.49
BBQ Grill	775.03 ± 17.24[b]	77.19 ± 1.94
Flat Grill	795.76 ± 6.82[b]	77.06 ± 2.63

[(a-b)] Mean values ± standard deviations (n=12). Values labeled with a different letter in the same column are significantly different ($p<0.05$).

^exo

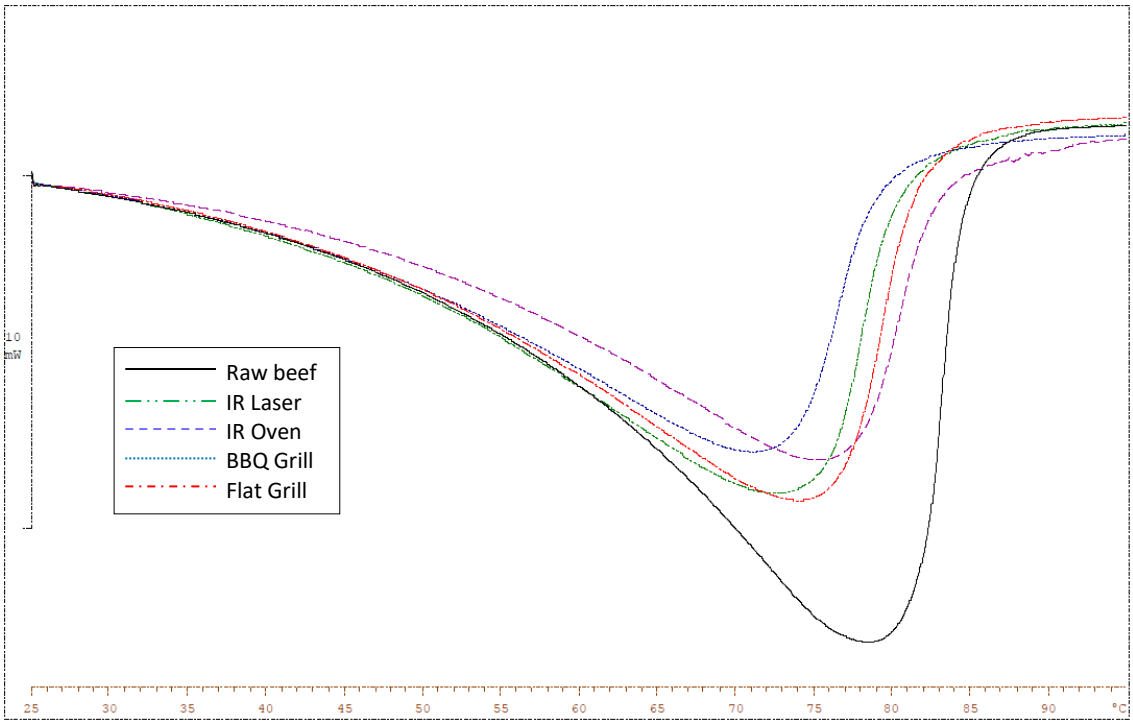

Fig 4.15. DSC thermograms of raw and cooked burgers.

4.3.2. Vegetarian patties

4.3.2.1. Internal cooking temperature

The average internal temperatures of vegetarian patties at the end of the different cooking processes were: IR Laser 75.34 ± 1.81°C; IR Oven,74.96 ± 1.52°C; Flat Grill, 75.33 ± 2.15°C.

4.3.2.2. Cooking loss, moisture, proximate analysis and water activity

Cooking loss values of cooked vegetarian patties were significantly different between treatments. Patties cooked with IR Oven had significantly higher losses, followed by the samples cooked with IR Laser. Losses of samples cooked with Flat Grill were significantly lower, around half the losses of patties cooked with IR Oven (table 4.32).

Moisture content was higher in cooked than in raw patties and, within patties, it changed according to cooking losses: patties cooked with the IR Oven had the lowest amount of moisture whereas patties cooked with IR Laser and Flat Grill kept a higher percentage ($p<0.05$).

Protein, fat and ashes content was significantly higher in cooked than in raw patties. Patties cooked with IR Oven had the highest contents of the three components although there were no significant differences in protein content between patties cooked with the different treatments. In general, no differences in protein, fat and ashes expressed on dry basis were observed (results not shown).

Table 4.32. Cooking loss, moisture and proximate analysis results of raw and cooked vegetarian patties.

Treatments	Cooking loss (%)	Moisture content (%)	Protein content (%)	Fat content (%)	Ashes content (%)
Raw		63.24 ± 0.13^{a}	5.39 ± 0.04^{b}	4.24 ± 0.09^{c}	2.36 ± 0.01^{c}
IR Laser	15.88 ± 0.24^{b}	57.88 ± 0.57^{b}	5.97 ± 0.20^{a}	5.37 ± 0.03^{b}	2.67 ± 0.05^{b}
IR Oven	20.96 ± 1.63^{a}	54.28 ± 1.30^{c}	6.28 ± 0.27^{a}	5.70 ± 0.18^{a}	2.96 ± 0.04^{a}
Flat Grill	10.50 ± 0.10^{c}	59.39 ± 1.14^{b}	6.09 ± 0.21^{a}	5.21 ± 0.03^{b}	2.65 ± 0.04^{b}

[a-c] Mean values ± standard deviations (n=6). Values labeled with a different letter in the same column are significantly different ($p<0.05$).

Water activity was not affected by cooking. Water activity of raw vegetarian patty was 0.982 ± 0.003, and the values of cooked patties ranged between 0.978 ± 0.001 (IR Oven) and 0.983 ± 0.001 (Flat Grill) (table 4.32).

4.3.2.3. Texture analysis

Cutting force was significantly higher in cooked than in raw patties and no differences between cooked patties could be observed (table 4.33).

Table 4.33. Cutting Force of raw and cooked vegetarian patties.

Treatments	Cutting Force (N)
Raw	1.24 ± 0.13^{b}
IR Laser	4.42 ± 0.20^{a}
IR Oven	4.48 ± 0.40^{a}
Flat Grill	4.96 ± 0.10^{a}

$^{(a-b)}$ Mean values ± standard deviations (n=18). Values labeled with a different letter in the same column are significantly different ($p<0.05$).

4.3.2.4. Color analysis

Internal and external color changes can be observed in table 4.34 and figures 4.16, 4.17 and 4.18. (Lightness and chromatic component b* values corresponding to measurements of internal color were significantly lower in cooked than in raw patties, and there were not significant differences between cooked patties. Chromatic component a* did not change between raw and cooked samples. Moreover, no differences were observed in total internal color difference (ΔE*) between cooking treatments p>0.05).

Regarding external color, lightness was lower in cooked than in raw samples. Within cooked samples, patties cooked with Flat Grill showed the lowest values of lightness (p<0.05). Values of chromatic component a* were significantly different between all samples: they were lower in patties cooked with IR Laser than in raw patties, whereas patties cooked with the Flat Grill showed the highest value of a*, followed by patties cooked with IR Oven. This cooking method rendered the patties with the highest b* values, followed by Flat Grill. Patties cooked with IR Laser and raw samples showed the

same values of b* ($p>0.05$). Finally, ΔE* of samples cooked with Flat Grill was significantly higher than the rest.

Table 4.34. CIE *L**, *a** and *b** values and total color difference (ΔE*) of the internal and the external side of raw and cooked vegetarian patties.

		Cooking methods		
	Raw	IR Laser	IR Oven	Flat Grill
Internal Color				
L*	59.03 ± 0.44[a]	50.48 ± 0.34[b]	50.05 ± 1.40[b]	50.72 ± 0.65[b]
a*	8.42 ± 0.24	8.27 ± 0.64	8.71 ± 0.90	8.09 ± 0.32
b*	27.59 ± 0.68[a]	22.03 ± 0.57[b]	23.03 ± 0.31[b]	22.48 ± 0.49[b]
Internal ΔE^*	-	10.25 ± 1.01	10.15 ± 1.08	9.81 ± 1.77
External Color				
L*	59.12 ± 0.22[a]	52.35 ± 0.29[b]	52.55 ± 0.78[b]	50.76 ± 0.42[c]
a*	8.36 ± 0.27[c]	7.79 ± 0.09[d]	9.45 ± 0.23[b]	10.81 ± 0.17[a]
b*	27.52 ± 0.19[c]	27.77 ± 0.21[c]	31.00 ± 0.71[a]	29.38 ± 0.27[b]
External ΔE^*	-	7.06 ± 1.49[b]	8.00 ± 1.49[b]	9.10 ± 2.04[a]

[(a-d)] Mean values ± standard deviations (n=36). Values labeled with a different letter in the same row are significantly different ($p<0.05$).

4.3.2.5. Images of samples during the cooking process

Images of vegetarian patty samples were taken before, during and after cooking treatments to illustrate changes and differences in appearance (figures 4.16, 4.17 and 4.18).

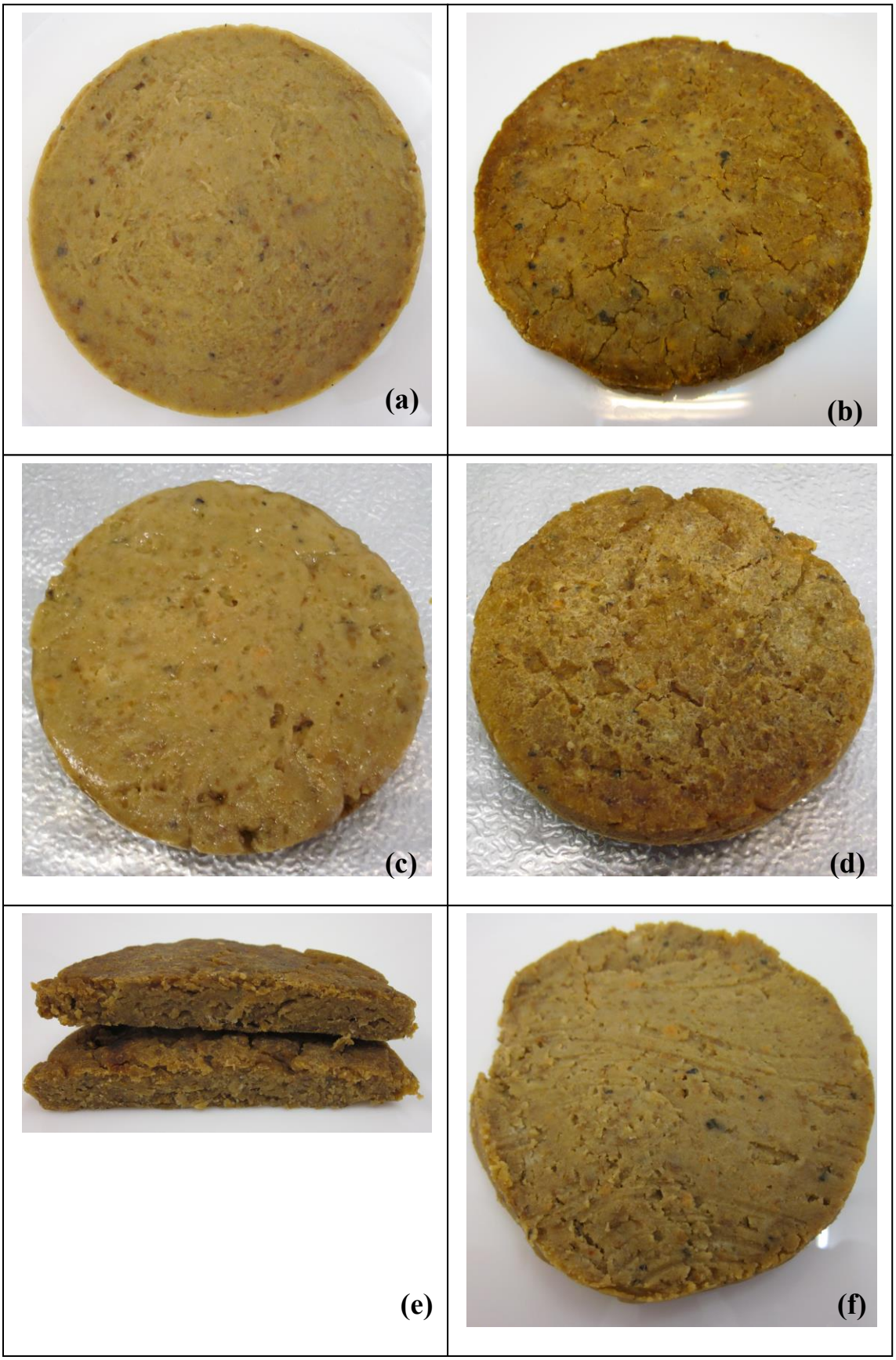

Fig 4.16. Cooking process of vegetarian patties treated with IR Laser. (a) First side, raw patty; (b) End of cooking of first side; (c) Second side, after cooking of first side; (d) End of cooking of second side; (e) Cooked patty, vertical cross-section; (f) Cooked patty, horizontal cross-section.

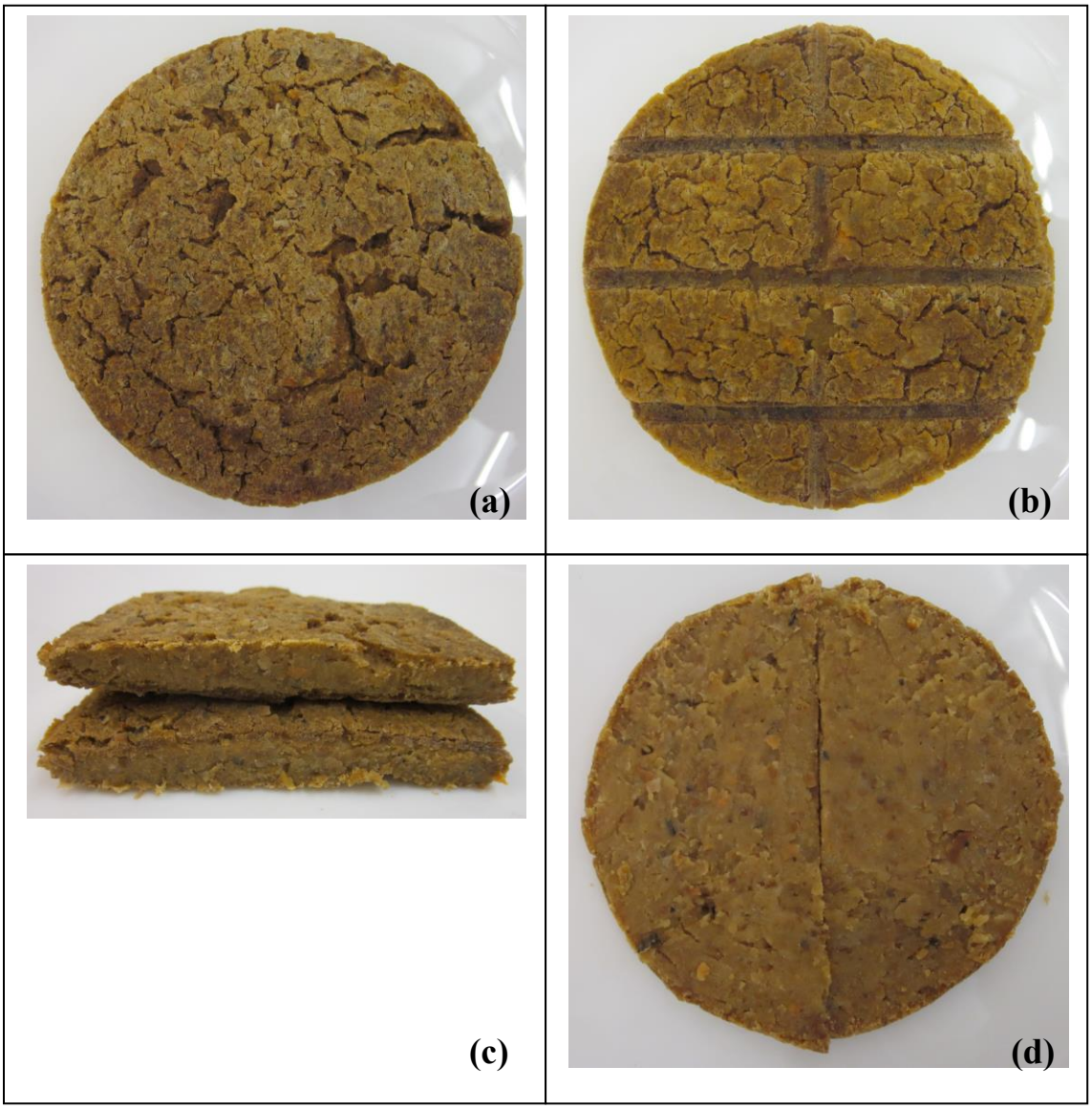

Fig 4.17. Vegetarian patty cooked with IR Oven. (a) Top side; (b) Bottom side, in contact with the rack grill; (c) Vertical cross-section; (d) Horizontal cross-section.

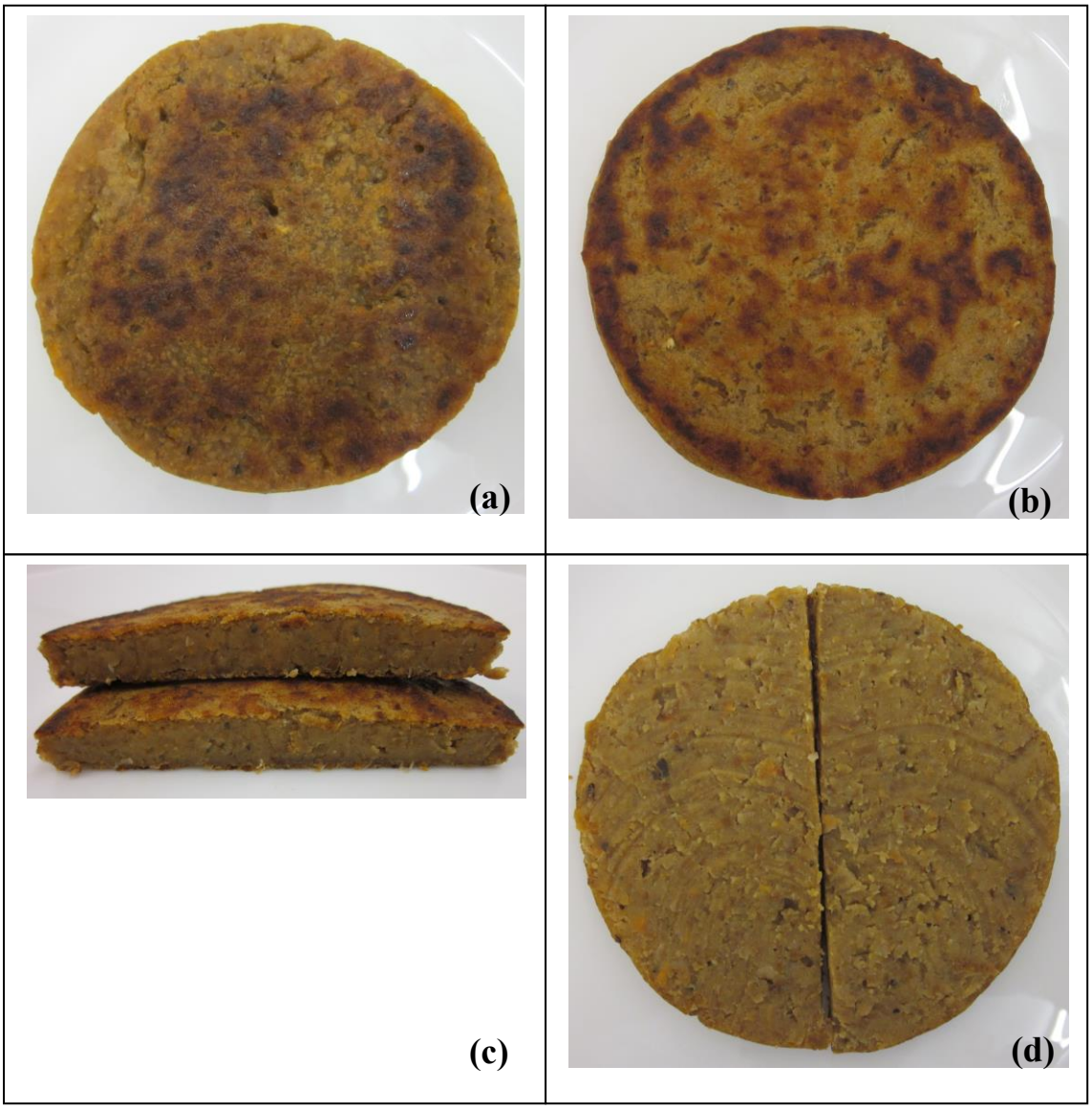

Fig 4.18. Vegetarian patty cooked with Flat Grill. (a) First side in contact with the flat grill surface; (b) Second side in contact with the flat grill surface; (c) Vertical cross-section; (d) Horizontal cross-section.

4.3.2.6. Sensory analysis

Vegetarian patties cooked with IR Laser and Flat Grill received the highest ratings in general appearance in comparison with burgers treated with IR Oven ($p<0.05$) (table 4.35).

Consumers evaluated the external color of patties cooked with Flat Grill as significantly browner than the color of patties treated with IR Oven and IR Laser. All cooking methods produced patties with comparable intensity of the attributes internal color, doneness, crunchiness and taste ($p>0.05$) but Flat Grill rendered patties that were assessed as significantly juicier than the rest.

Regarding acceptability, external color of patties cooked with Flat Grill and IR Laser received the best evaluation. As happened with the evaluation of intensity, all cooking methods produced patties with comparable acceptability of the attributes internal color, doneness, crunchiness and taste ($p>0.05$) but juiciness of patties cooked with Flat Grill received a better evaluation than the rest.

Results of preference test showed that consumers significantly preferred the patties cooked with Flat Grill and IR Laser treatments, followed by samples cooked with IR Oven (table 4.36).

Table 4.35. Results of the consumer test for vegetarian patties cooked with different methods.

	IR Laser	IR Oven	Flat Grill
General appearance	4.67 ± 1.38[a]	3,81 ± 1.23[b]	4.89 ± 1.45[a]
Intensity			
External Color	4.10 ± 1.12[b]	3.79 ± 1.38[b]	4.92 ± 1.29[a]
Internal Color	3.96 ± 0.99	3.98 ± 1.17	3.97 ± 0.99
Doneness	4.41 ± 1.09	4.18 ± 1.37	4.34 ± 0.97
Crunchiness	4.20 ± 1.11	3.80 ± 1.40	3.76 ± 1.27
Juiciness	3.14 ± 1.19[b]	3.28 ± 1.37[b]	4.10 ± 1.39[a]
Taste	4.39 ± 1.44	4.56 ± 1.21	4.12 ± 1.25
Acceptability			
External Color	4.54 ± 1.37[a]	3.76 ± 1.40[b]	5.15 ± 1.34[a]
Internal Color	4.58 ± 1.10	4.44 ± 1.76	4.71 ± 1.12
Doneness	4.52 ± 1.29	4.37 ± 1.54	4.80 ± 1.37
Crunchiness	4.37 ± 1.41	4.09 ± 1.58	4.75 ± 1.44
Juiciness	3.87 ± 1.38[b]	3.88 ± 1.67[b]	4.68 ± 1.30[a]
Taste	4.62 ± 1.52	4.36 ± 1.37	4.47 ± 1.36

[(a-b)] Mean values ± standard deviations (n=50). Values labeled with a different letter in the same row are significantly different (p<0.05).

Table 4.36. Preference test for vegetarian patties cooked with different methods.

	Number of answers for each order of preference (1-3) and multiplied by its order of preference			
	*1	*2	*3	Sum
IR Laser	16	44	36	96[a]
IR Oven	13	20	81	114[b]
Flat Grill	21	36	33	90[a]

[(a-b)] Values labeled with a different letter in the same column are significantly different (p<0.05).

4.3.2.7. Microbiological results

4.3.2.7.1. Microbiological analysis of non-inoculated samples

Counts of aerobic mesophilic bacteria present in raw vegetarian patties were significantly reduced ~ 1.3 log CFU/g by all cooking methods. Moreover, naturally present coliforms in raw patties were reduced below the minimum detection limit in all cases (table 4.37).

Table 4.37. Counts of aerobic mesophilic bacteria (TSA) and coliforms (MPN in BGBL and VRBA) in non-inoculated raw and cooked vegetarian patties.

Treatments	TSA Count*	BGBL Count**	VRBA Count*
Raw	4.15 ± 0.17^{a}	2.56 ± 0.14	2.76 ± 0.14
IR Laser	2.77 ± 0.20^{b}	n.d.	n.d.
IR Oven	2.98 ± 0.15^{b}	n.d.	n.d.
Flat Grill	2.90 ± 0.06^{b}	n.d.	n.d.

$^{(a-b)}$ Mean (log CFU/g) ± s.d. (n=6). Values labeled with a different letter in the same column are significantly different ($p<0.05$). n.d.: not detected. *Detection limit: <1 log CFU/g. **Detection limit: <0.48 log CFU/g.

Raw samples that were analyzed to investigate the presence of *Salmonella* in meat before inoculation gave negative results.

4.3.2.7.2. Microbiological analysis of inoculated samples

Counts of *S.* Typimurium and *S.* Senftenberg were significantly reduced more than ~ 6.5 log CFU/g by all cooking methods. In the case of samples cooked with Flat Grill, no colonies of the inoculated bacteria were detected, even after the enrichment of the samples (table 4.38).

Table 4.38. Survival of *Salmonella* Typhimurium and *Salmonella* Senftenberg inoculated in vegetarian patties with a contamination level of ~7 log CFU/g and cooked with different methods.

	Salmonella Tyhphimurium		*Salmonella* Senftenberg	
Treatment	Count	Detection[1]	Mean	Detection[1]
Raw	7.34 ± 0,42[a]		7.46 ± 0,54[a]	
IR Laser	0.57 ± 0,51[b]	6 / 6	0.33 ± 0,58[b]	6 / 6
IR Oven	0.47 ± 0,40[b]	6 / 6	0.43 ± 0,40[b]	6 / 6
Flat Grill	n.d.	0 / 6	n.d.	0 / 6

[(a-b)] Mean (log CFU/g) ± s.d. (n=6). Values labeled with a different letter in the same column are significantly different (p<0.05). n.d.: not detected; limit of detection: <1 log CFU/g.
[1] +/6: positive samples after enrichment and growth in selective medium.

In samples inoculated at ~ 3 log CFU/g, all treatments caused the reduction of counts below the detection limit of the plating method (<1 log CFU/g) (table 4.39). *S.* Typhimurium was totally inactivated by all cooking methods since no colonies grew in any plates after enrichment. In the case of *S.* Senftenberg, total inactivation was only achieved by cooking with Flat Grill.

Table 4.39. Survival of *Salmonella* Typhimurium and *Salmonella* Senftenberg inoculated in vegetarian patties with a contamination level of ~3 log CFU/g and treated with different cooking methods.

	Salmonella Tyhphimurium		*Salmonella* Senftenberg	
Treatment	Count[*]	Detection[1]	Mean[*]	Detection[1]
Raw	3,93 ± 0,12		3,90 ± 0,18	
IR Laser	n.d.	0 / 6	n.d.	2 / 6
IR Oven	n.d.	0 / 6	n.d.	1 / 6
Flat Grill	n.d.	0 / 6	n.d.	0 / 6

[*]Mean (log CFU/g) ± s.d. (n=6). n.d.: not detected; limit of detection: <1 log CFU/g.
[1] +/6: positive samples after enrichment and growth in selective medium.

4.3.3. Pizza dough

4.3.3.1. Cooking loss, moisture, proximate analysis and water activity

Cooking losses of pizzas cooked with Convection Oven and IR Oven were significantly higher than those of pizzas cooked with IR Laser (table 4.40). Moisture content decreased significantly after cooking, whereas protein, fat and ashes content increased. Pizzas cooked with Convection Oven had the lowest moisture content, followed by samples cooked with IR Oven. Pizzas cooked with IR Laser kept the highest percentage of moisture ($p<0.05$). Protein, fat and ashes content were affected similarly by cooking methods: pizzas cooked by IR Oven had the highest content of the three components, followed by pizzas cooked by Convection Oven and, finally, by those cooked with IR Laser.

Table 4.40. Cooking loss, moisture and proximate analysis results of raw and cooked Tradizionale pizza dough.

Treatments	Cooking loss (%)	Moisture content (%)	Protein content (%)	Fat content (%)	Ashes content (%)
Raw		35.79 ± 0.16^{a}	6.57 ± 0.02^{d}	6.90 ± 0.05^{d}	1.96 ± 0.02^{d}
IR Laser	13.11 ± 0.52^{b}	25.72 ± 0.78^{b}	7.96 ± 0.15^{c}	8.10 ± 0.13^{c}	2.28 ± 0.03^{c}
IR Oven	18.25 ± 1.19^{a}	18.21 ± 0.94^{d}	9.05 ± 0.13^{a}	8.91 ± 0.11^{a}	2.49 ± 0.01^{a}
Convection Oven	18.18 ± 2.68^{a}	21.08 ± 0.59^{c}	8.69 ± 0.02^{b}	8.54 ± 0.06^{b}	2.42 ± 0.03^{b}

[(a-d)] Mean values ± standard deviations (n=6). Values labeled with a different letter in the same column are significantly different ($p<0.05$).

Water activity was higher in raw pizza dough than in cooked pizza and pizzas cooked with IR Laser had a significantly higher water activity than the rest (table 4.41).

Table 4.41. Water activity of raw and cooked Tradizionale pizza.

Treatments	Water Activity
Raw	0.966 ± 0.002^{a}
IR Laser	0.914 ± 0.003^{b}
IR Oven	0.857 ± 0.037^{c}
Convection Oven	0.874 ± 0.036^{c}

[(a-b)] Mean values ± standard deviations (n=18). Values labeled with a different letter in the same column are significantly different ($p<0.05$).

4.3.3.2. Texture analysis

Samples cooked with Convection Oven and IR Oven presented the hardest force of penetration, although there were not significant differences between the last and samples cooked with IR Laser (table 4.42).

Table 4.42. Force of Penetration in Tradizionale pizza dough samples cooked with different methods.

Treatments	Force of Penetration (N)
Raw	0.14 ± 0.01^{c}
IR Laser	2.41 ± 0.09^{b}
IR Oven	$2.95 \pm 0.31^{a,b}$
Convection Oven	3.45 ± 0.40^{a}

$^{(a-c)}$ Mean values ± standard deviations (n=6). Values labeled with a different letter in the same column are significantly different ($p<0.05$).

4.3.3.3. Color analysis

Color of first cooking side was analyzed separately from color of second cooking side, since there were significant differences between sides (table 4.43).

Regarding color of the first cooking side, lightness (L*) of pizzas cooked by Convection Oven was similar to that of raw pizza ($p>0.05$). L* of pizzas cooked with IR Oven and IR Laser were significantly lower than L* of pizzas cooked with Convection Oven, in accordance with the highest level of browning that could be observed in the former (figures 4.19, 4.20 and 4.21). All cooked samples showed values of chromatic components a* and b* significantly higher than raw pizzas, being the samples cooked with IR Laser and IR Oven the ones with the highest red and yellow component values. These results lead to higher values of ΔE* in pizzas cooked with IR Laser and IR Oven.

Lightness values of the second cooking side were significantly higher in pizzas cooked with IR Oven and Convection Oven than in pizzas cooked with IR Laser. Pizzas cooked with IR Laser and IR Oven showed similar values in the red component a*, which was higher than a* of pizzas cooked with Convection Oven. For chromatic component b*, values were similar in pizzas cooked with IR Laser and Convection Oven and higher than b* values of pizzas cooked with IR Oven ($p<0.05$). External *ΔE** values were significantly different between all samples, being the pizzas cooked with IR Laser the ones that showed more differences with raw pizzas.

Table 4.43. CIE *L**, *a** and *b** values and total color difference (ΔE*) of Tradizionale pizza dough samples cooked with different methods.

		Cooking methods		
	Raw	IR Laser	IR Oven	Convection oven
First cooking side				
L*	86.88 ± 0.77^{a}	78.66 ± 0.76^{c}	75.25 ± 2.75^{c}	83.63 ± 1.45^{a}
a*	0.76 ± 0.15^{c}	6.06 ± 0.40^{a}	8.46 ± 1.74^{a}	3.30 ± 1.00^{b}
b*	14.99 ± 0.17^{c}	29.74 ± 1.00^{a}	31.08 ± 2.23^{a}	25.49 ± 1.98^{b}
Internal ΔE^{*}	-	17.76 ± 4.19^{b}	21.45 ± 6.82^{a}	11.43 ± 3.80^{c}
Second cooking side				
L*		83.19 ± 1.28^{b}	86.07 ± 0.92^{a}	86.46 ± 0.70^{a}
a*		0.99 ± 0.19^{a}	0.75 ± 0.14^{a,b}	0.59 ± 0.02^{b}
b*		21.02 ± 0.49^{a}	17.57 ± 0.71^{b}	20.11 ± 1.57^{a}
External ΔE^{*}		7.25 ± 1.45^{a}	2.90 ± 1.21^{c}	5.19 ± 1.85^{b}

$^{(a-c)}$ Mean values ± standard deviations (n=18). Values labeled with a different letter in the same row are significantly different ($p<0.05$).

4.3.3.4. Images of samples during the cooking process

Images of pizza dough samples were taken before, during and after cooking treatments to illustrate changes and differences in appearance.

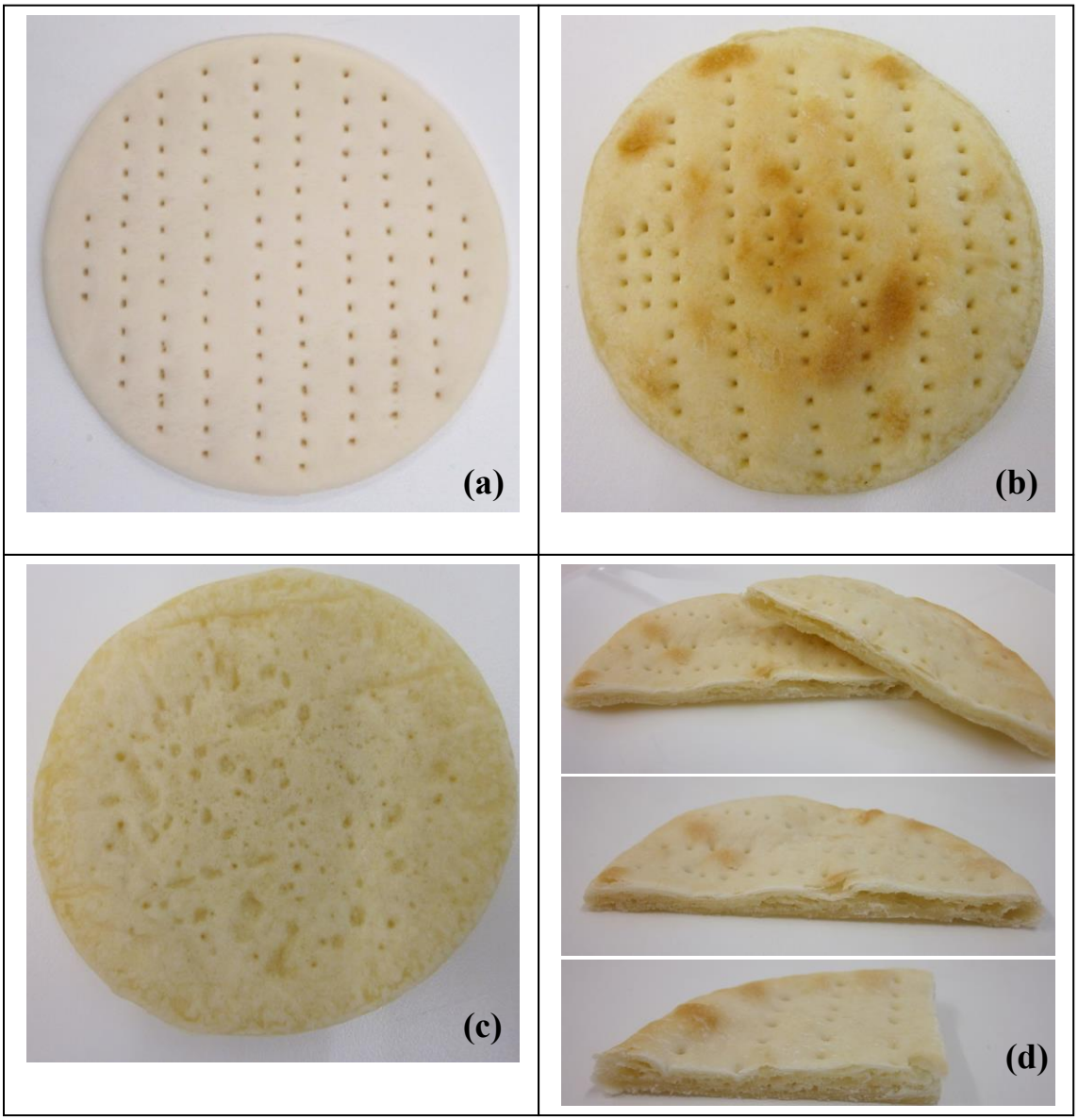

Fig 4.19. Tradizionale pizza dough samples cooked with IR Laser. (a) Raw pizza dough; (b) First side after laser impact; (c) Second side of laser impact; (d) Cooked pizza, vertical cross-section.

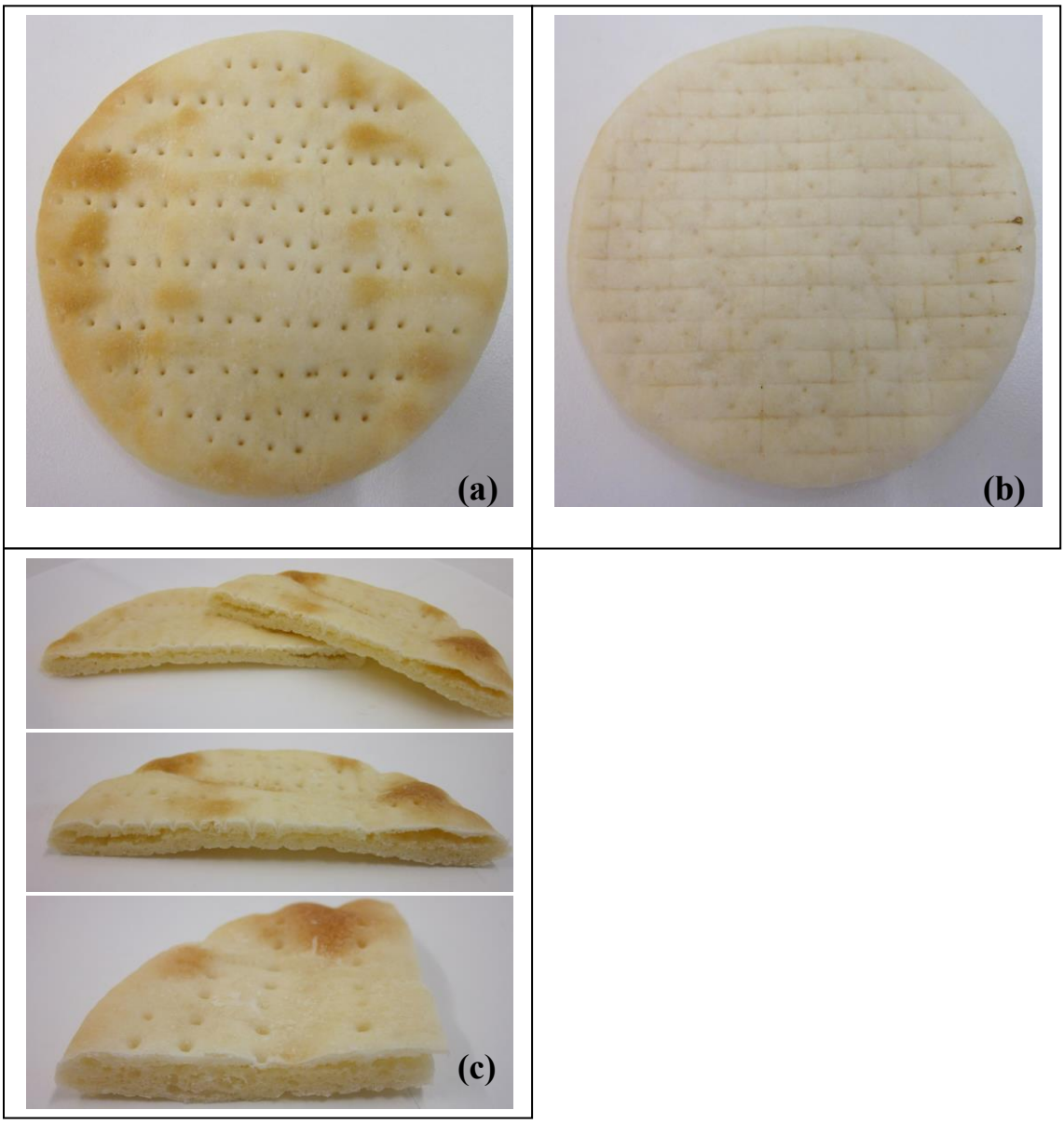

Fig 4.20. Tradizionale pizza dough samples cooked with IR Oven. (a) Top side; (b) Bottom side in contact with the rack grill; (c) Vertical cross-section.

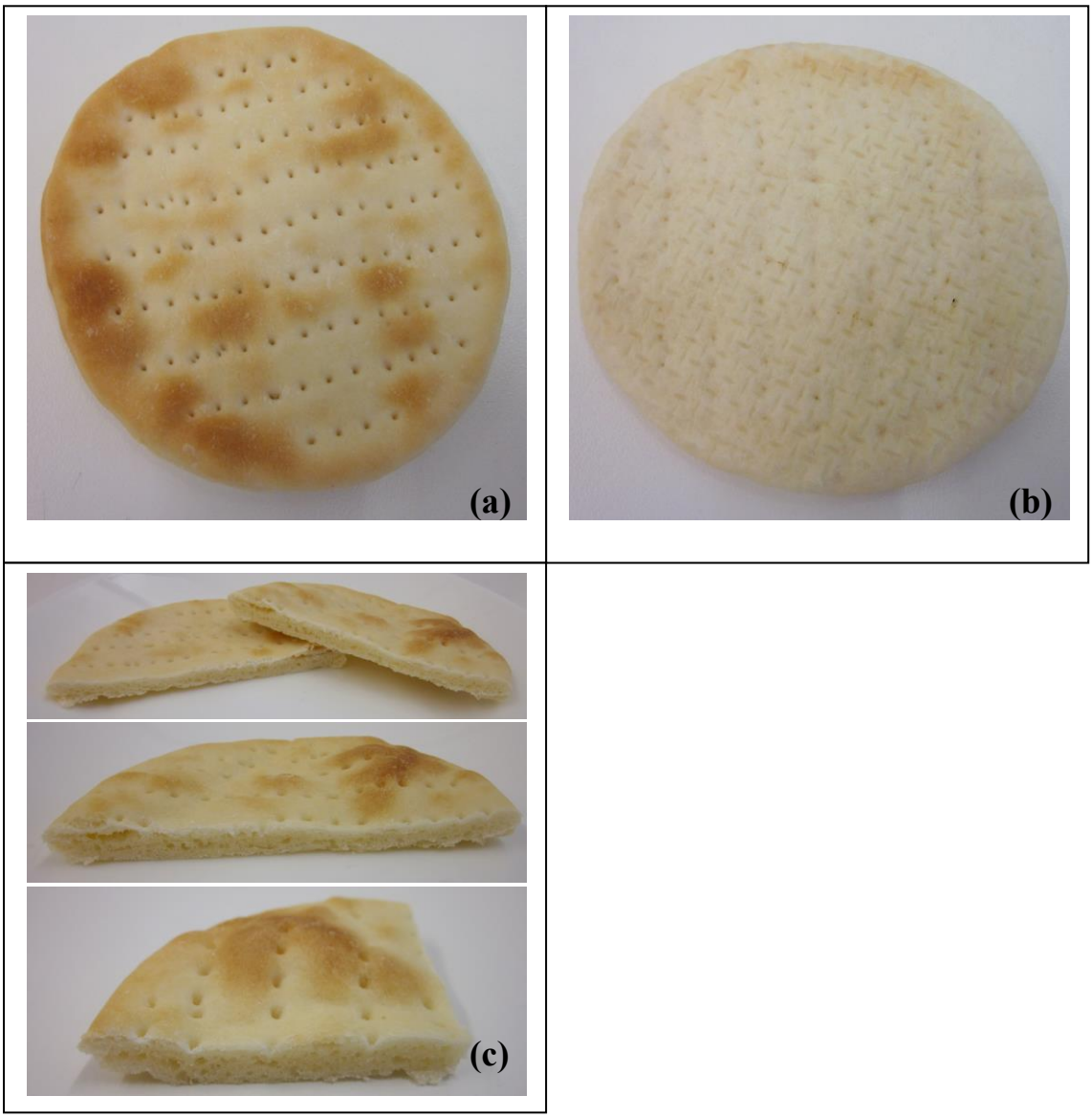

Fig 4.21. Tradizionale pizza dough samples cooked with Convection Oven. (a) Top side; (b) Bottom side, in contact with the rack grill; (c) Vertical cross-section.

4.3.3.5. Sensory analysis

Consumers considered that pizzas cooked with IR Oven had a significantly better general appearance, followed pizzas cooked with IR Laser. Samples cooked with Convection Oven received the lowest general appearance assessment (table 4.44).

Regarding the intensity of sensory attributes, pizzas cooked with IR Oven and IR Laser had the brownest external color, whereas pizzas cooked with the Convection Oven had a lighter color. Pizzas cooked with IR Oven received the highest ratings in the level of doneness, taste and flavor. There were not significant differences between the intensity of these attributes of pizzas cooked with IR Laser and Convection Oven. All cooking methods produced patties with comparable intensity in crunchiness ($p>0.05$).

The evaluation of acceptability of sensory attributes followed the same pattern as the evaluation of their intensity. Attributes evaluated as more intense (*i.e.* external color of pizzas cooked with IR Laser and IR Oven; and doneness, taste and flavor of pizzas cooked with IR Oven) also received the best acceptability ratings, whereas crunchiness acceptability was comparable in all samples.

Consumers preferred the pizzas cooked with IR Oven, followed by pizzas cooked with IR Laser. Pizzas cooked with Convection Oven were ranked in the last position (table 4.45).

Table 4.44. Results of the consumer test for Tradizionale pizza cooked with different methods.

	IR Laser	IR Oven	Convection Oven
General appearance	4.93 ± 1.39[b]	5.66 ± 0.84[a]	4.28 ± 1.32[c]
Intensity			
External Color	4.97 ± 0.70[a]	5.36 ± 0.73[a]	3.36 ± 1.24[b]
Doneness	3.96 ± 1.40[b]	4.75 ± 0.67[a]	3.62 ± 0.99[b]
Crunchiness	3.23 ± 1.09	3.39 ± 1.00	3.05 ± 1.06
Taste	3.76 ± 1.03[b]	4.63 ± 1.25[a]	4.06 ± 1.36[a,b]
Flavor	3.46 ± 1.13[b]	5.01 ± 0.89[a]	3.49 ± 1.27[b]
Acceptability			
External Color	5.10 ± 1.04[a]	5.64 ± 1.03[a]	3.72 ± 1.49[b]
Doneness	3.72 ± 1.26[b]	5.03 ± 0.89[a]	3.95 ± 1.34[b]
Crunchiness	3.20 ± 1.13	3.81 ± 1.59	3.38 ± 1.41
Taste	4.30 ± 1.09[b]	5.29 ± 0.97[a]	4.56 ± 1.35[b]
Flavor	4.02 ± 1.16[b]	5.32 ± 1.19[a]	4.19 ± 1.48[b]

[(a-c)] Mean values ± standard deviations (n=50). Values labeled with a different letter in the same row are significantly different (p<0.05).

Table 4.45. Preference test for Tradizionale pizza cooked with different methods.

	Number of answers for each order of preference (1-3) and multiplied by its order of preference			
	***1**	***2**	***3**	Sum
IR Laser	10	54	39	103[b]
IR Oven	31	22	24	77[c]
Convection Oven	9	24	87	120[a]

[(a-c)] Values labeled with a different letter in the same column are significantly different (p<0.05).

4.3.3.6. Polycyclic aromatic hydrocarbons analysis

Concentration of PAHs for all samples and all treatments were below the minimum detection limit of the chromatographic technique.

4.3.3.7. Differential scanning calorimetry

Peak areas of thermograms from all cooked pizzas were significantly lower than areas of raw pizzas. Between cooking methods, only clear differences between areas of pizzas cooked with IR Laser and Convection Oven could be detected ($p<0.05$). Cooking caused a significant decrease in peak temperatures but there were not significant differences between samples cooked with different methods.

Table 4.46. Peak areas and peak temperatures from DSC analysis of raw and cooked Tradizionale pizza.

Treatments	Area(J/g)	Peak Temperature(°C)
Raw	350.16 ± 21.43^{a}	108.07 ± 1.95^{a}
IR Laser	297.90 ± 14.87^{b}	89.62 ± 2.85^{b}
IR Oven	$267.81 \pm 28.78^{b,c}$	88.80 ± 1.48^{b}
Convection Oven	247.93 ± 22.01^{c}	87.54 ± 1.94^{b}

$^{(a-c)}$ Mean values ± standard deviations (n=12). Values labeled with a different letter in the same column are significantly different ($p<0.05$).

4.4. Numerical simulations: Results of the model validation

The results of the application of the numerical model (detailed in section 3.4) to simulate the behavior of the complete cooking process of beef burger and vegetarian patty, by means of the ray tracing method, are described.

4.4.1. Beef burger

Figure 4.22 shows the evolution of thermal conductivity of beef burger components (considered individually and mixed) with the meat central temperature (*Central T)*, according to the correlations reported in Section 3.4.2.

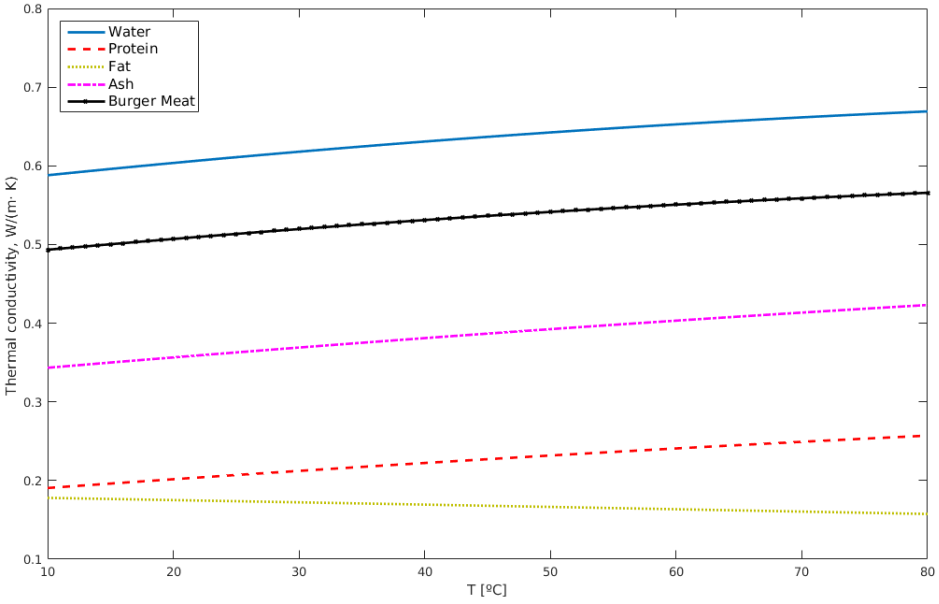

Figure 4.22. Variation of thermal conductivity of beef burger meat with temperature (*Central T*)

The evolution of cooking loss and internal temperatures of beef burgers cooked with the CO_2 IR Laser Foodini system (table 4.47) were measured to compare the experimental results with the numerical simulation of the model.

Table 4.47. Evolution of cooking loss and internal temperatures measured in the center and in the lateral side of beef burgers cooked with the CO_2 IR Laser Foodini system.

Cooking time (min)	Cooking loss (%)	Initial Temperature (°C)	Central Temperature (°C)	Lateral Temperature (°C)
1	1,11 ± 0,10	8,3 ± 0,5	25,8 ± 2,6	25,5 ± 1,4
2	2,3 ± 0,01	8,3 ± 0,5	34,9 ± 2,1	32,9 ± 1,2
3	2,92 ± 0,42	7,4 ± 0,7	38,3 ± 1,6	37,1 ± 2,00
4	4,65 ± 0,16	7 ± 0,1	45,5 ± 3,4	45,1 ± 1,2
5	5,73 ± 0,53	8,2 ± 1,8	49,4 ± 3,9	50,6 ± 1,6
6	6,94 ± 0,37	9,5 ± 0,2	53,7 ± 2,8	53,6 ± 1,9
7	8,61 ± 0,41	8,7 ± 0,1	57,3 ± 3,2	60,6 ± 4,5
8	10,71 ± 0,62	8 ± 0,9	63,0 ± 3,8	63,6 ± 2,2
9	12,45 ± 0,34	7,7 ± 1,1	64,0 ± 3,0	66,7 ± 2,1
10	13,38 ± 0,64	7,5 ± 1,8	64,1 ± 0,9	65,1 ± 1,1
11	15,80 ± 0,72	8,9 ± 0,5	65,9 ± 0,7	67,2 ± 0,6
12	16,64 ± 0,83	8,3 ± 0,2	66,5 ± 1,0	67,9 ± 0,7
13	18,13 ± 0,88	8,2 ± 0,6	67,2 ± 1,0	68,5 ± 1,6
14	19,56 ± 0,70	8,6 ± 0,0	69,2 ± 1,0	70 ± 1,2
15	20,18 ± 0,39	5,8 ± 0,5	70,3 ± 1,2	72,1 ± 2,1
16	20,89 ± 0,69	8,9 ± 0,0	71,3 ± 2,2	74,1 ± 1,6
17	21,36 ± 0,83	8 ± 0,4	72,7 ± 1,6	74,5 ± 1,4
18	22,61 ± 0,80	9,3 ± 1,3	76,0 ± 2,6	76,6 ± 3,3

Mean values ± standard deviations (n=6).

Water cooking losses were taken into account to adjust the calculation of thermal properties along the simulation. Indeed, the water content decreased along the cooking process, leading to the increase of volume and mass percentages for all the other components.

The numerical results for the temperature evolution at the center and lateral position of the burger are depicted in figure 4.23. Lateral temperature was simulated in two different fixed points, which rotated along the axis during the simulation. The first fixed point (named *Lateral T 1*) was calculated at 5 mm depth from the midpoint of lateral side, while the second point (named as *Lateral T 2*) was calculated at 7 mm depth. The

numerical results for both calculated lateral temperatures showed a marked oscillation in time. This behavior could not be observed from experimental data, due to the lower probing frequency and the impossibility of probing at the same exact location.

The experimental data of the internal temperature evolution (*Central Temperature* and *Lateral Temperature* included in table 4.47), was compared with the calculated central and lateral temperatures of the model (*Central T*, *Lateral T 1*, *Lateral T 2*) reported in figure 4.23. The numerical results have shown an overall good agreement with the experimental results, except for the first four minutes where there was a high difference between the experimental data and numerical simulation.

Figure 4.24 represents the iso-lines that show the evolution of the temperature on a vertical cross-section when the model is used to simulate a complete cooking process. In the first seconds of simulation, the burger was heated from the both the top and bottom part. This was due to the fact that the initial burger temperature was lower that the initial plate temperature. At t=480s the burger was reversed. The temperature at the bottom was suddenly lowered by the contact with the plate surface, while the hotter center zone delivered heat to both top and bottom parts. Hence, after this transition process, the heat delivery from the top surface subjected to the ray tracing started again, leading to the complete cooking of the meat.

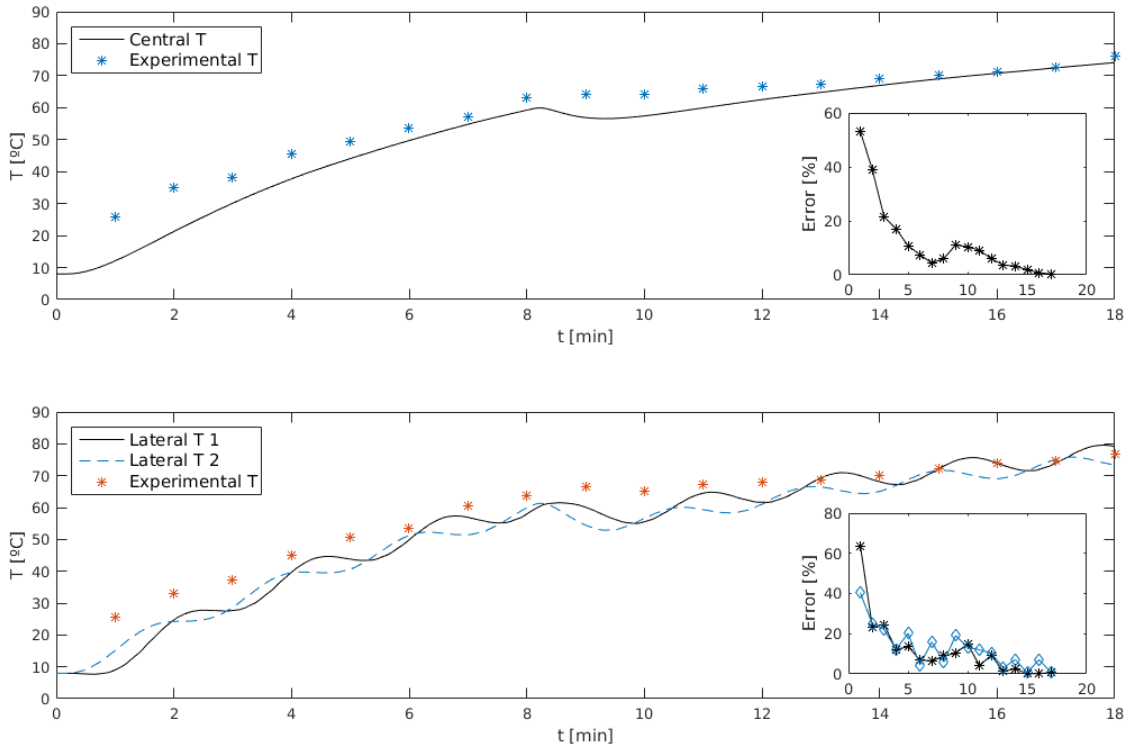

Figure 4.23. Numerical simulation of the complete cooking process of beef burger and comparison to experimental data.

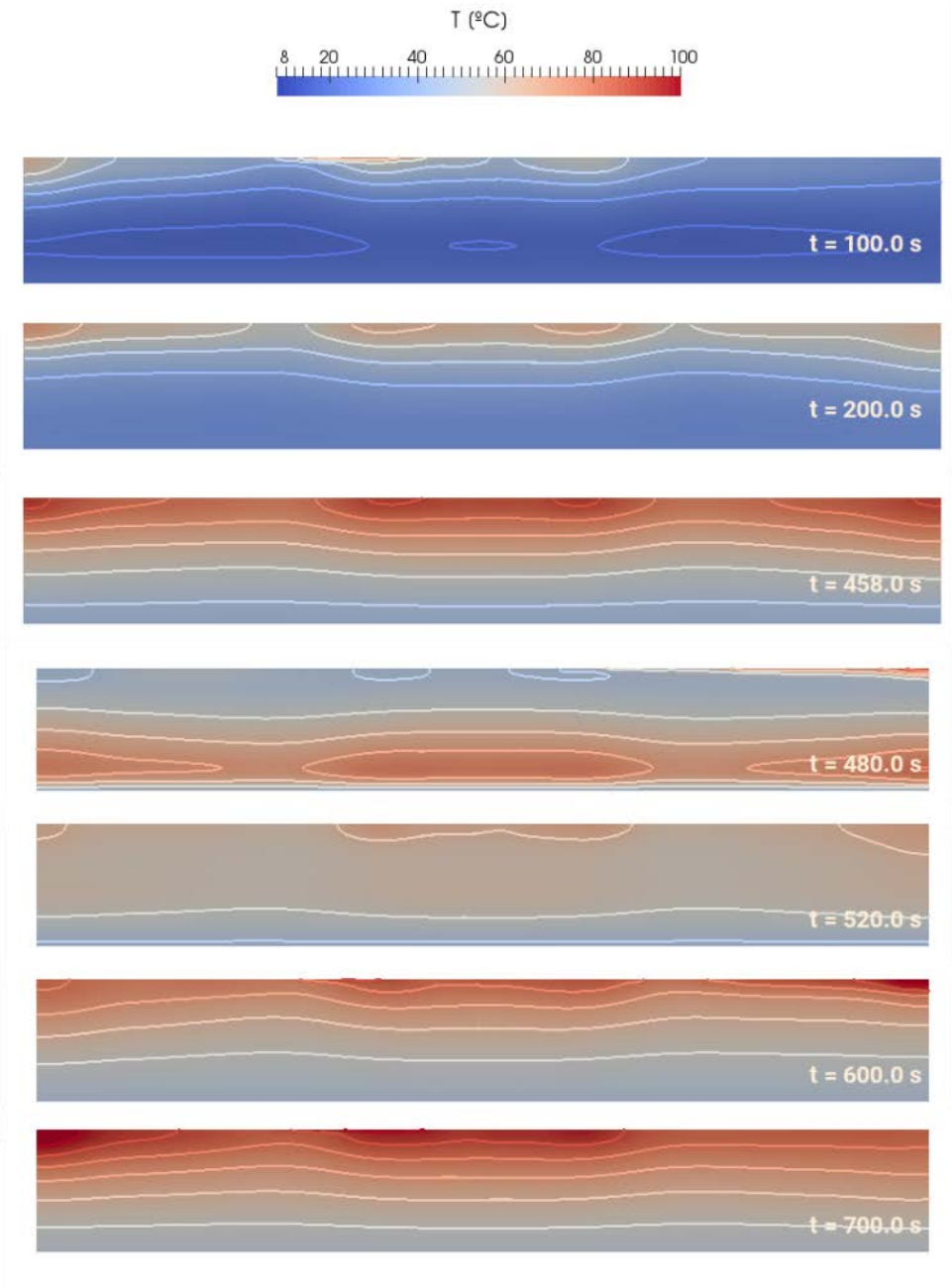

Figure 4.24. Evolution of temperature in a vertical cross-section of the beef burger during cooking simulation.

4.4.1. Vegetarian patty

In the vegetarian patty case, the initial composition was used to calculate the thermal conductivity. In this case, carbohydrates percentage, calculated by difference was taken into account (data not shown).

Figure 4.25 shows the evolution of thermal conductivity of vegetarian patties components (considered individually and mixed) with the central temperature (*Central T*), according to the correlations reported in Section 3.4.2.

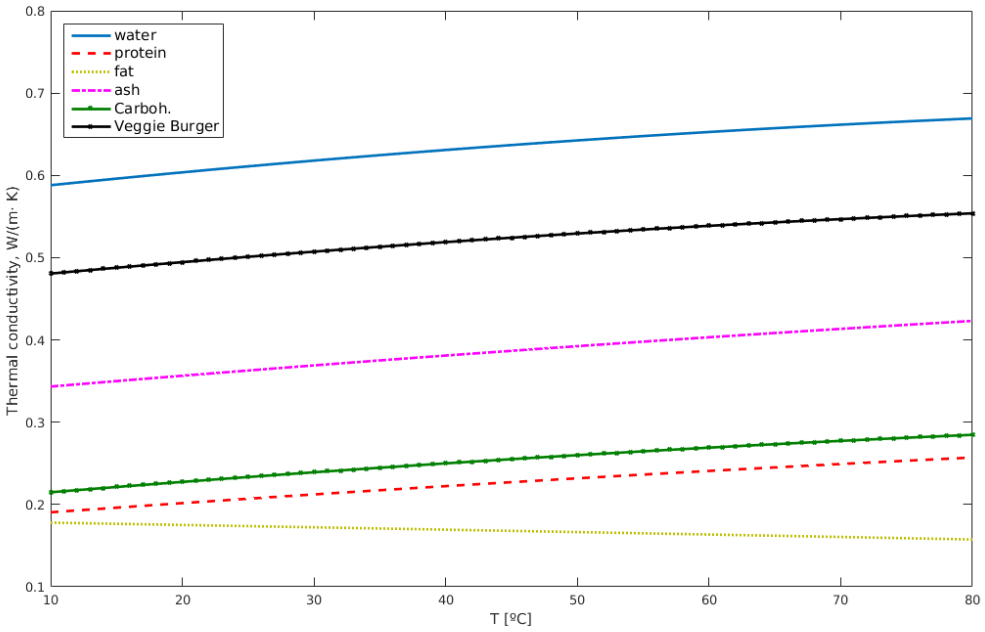

Figure 4.25. Variation of thermal conductivity of vegetarian patty with temperature

Numerical results were compared to the experimental data reported in table 4.48.

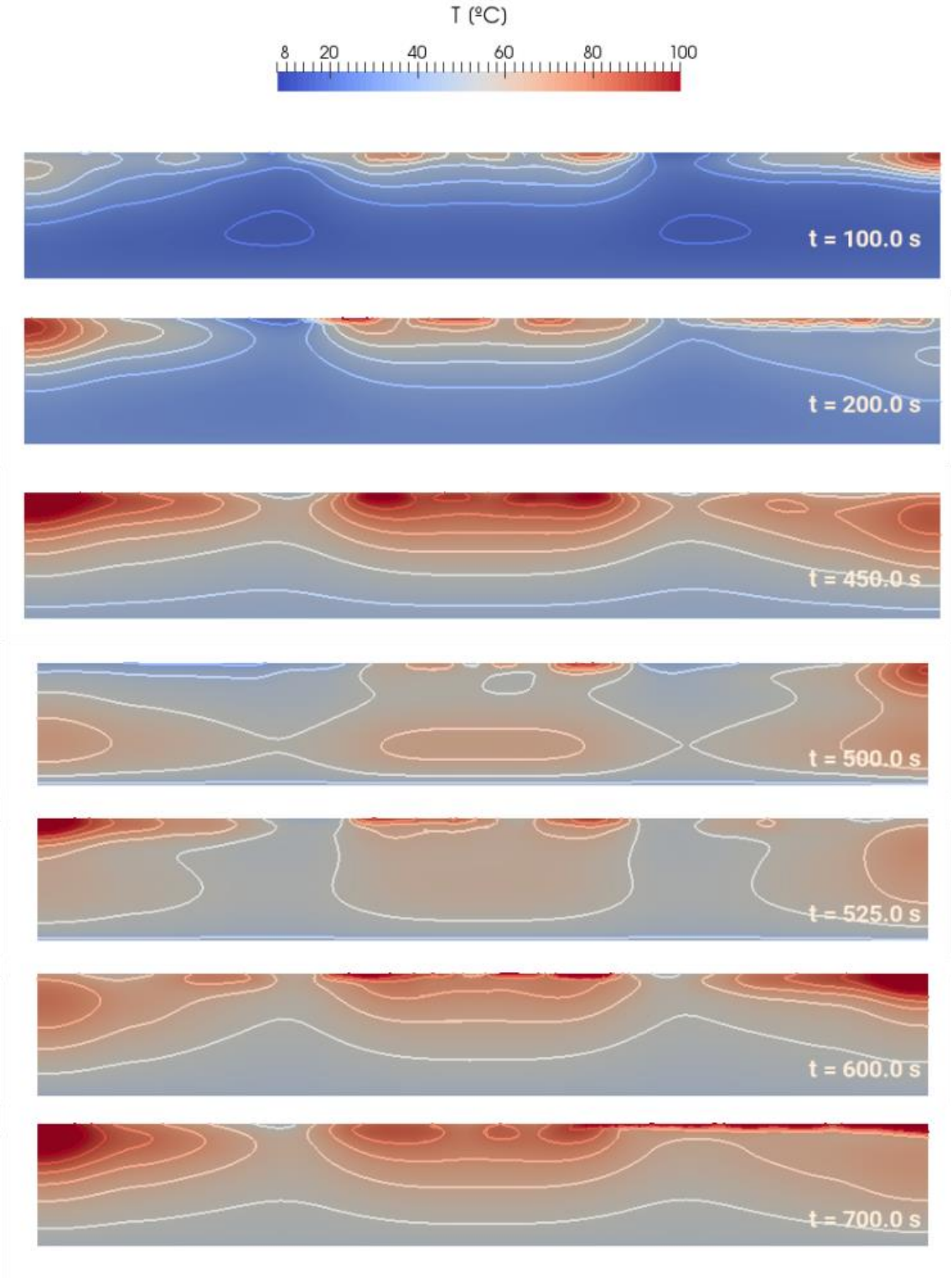

The numerical results for the temperature evolution at the center and lateral positions of the patty are depicted in figure 4.26, showing an overall good agreement with experimental results, except for the first three minutes where there was a high difference

between the experimental data and numerical simulation. Figure 4.27 represents the iso-lines that show the evolution of the temperature on a vertical cross-section of the vegetarian patty, when the model is used to simulate a complete cooking process.

Table 4.48. Evolution of cooking loss and internal temperatures measured in the center and in the lateral side of vegetarian patties cooked with the CO_2 IR Laser Foodini system.

Cooking time (min)	Cooking loss (%)	Initial Temperature (°C)	Central Temperature (°C)	Lateral Temperature (°C)
1	2,27 ± 0,17	7,1 ± 0,3	24,4 ± 1,0	24,3 ± 3,5
2	3,44 ± 0,14	8,1 ± 0,8	30,4 ± 1,0	29,9 ± 1,9
3	3,81 ± 0,07	6,3 ± 0,9	36,1 ± 1,3	36,4 ± 0,9
4	4,83 ± 0,16	6,4 ± 1,3	39,3 ± 2,3	39,7 ± 1,9
5	6,06 ± 0,46	7,5 ± 0,7	43,1 ± 1,7	43,6 ± 1,1
6	7,23 ± 0,36	7,0 ± 1,9	49,2 ± 1,8	49,6 ± 2,0
7	7,90 ± 0,42	8,0 ± 1,6	51,9 ± 1,3	50,8 ± 1,3
8	9,55 ± 0,11	6,9 ± 0,4	55,9 ± 0,9	58,0 ± 3,8
9	10,40 ± 0,37	7,2 ± 0,9	60,1 ± 3,6	61,3 ± 1,5
10	11,07 ± 0,40	8,8 ± 0,2	57,6 ± 0,7	57,5 ± 0,7
11	11,54 ± 0,33	8,9 ± 0,6	59,4 ± 1,3	60,4 ± 0,5
12	12,05 ± 0,03	8,8 ± 0,6	62,6 ± 1,5	64,3 ± 1,9
13	13,35 ± 0,28	7,8 ± 0,4	64,4 ± 1,1	65,9 ± 1,7
14	14,29 ± 0,02	8,3 ± 1,0	66,5 ± 0,6	67,5 ± 0,8
15	15,00 ± 0,41	9,1 ± 0,5	68,0 ± 0,7	69,1 ± 0,3
16	15,27 ± 0,28	8,3 ± 0,4	71,0 ± 0,3	71,4 ± 0,5
17	15,90 ± 0,50	9,3 ± 0,5	73,5 ± 1,2	74,8 ± 2,6
18	16,30 ± 0,60	8,4 ± 0,6	75,3 ± 1,8	77,2 ± 2,2

Mean values ± standard deviations (n=6).

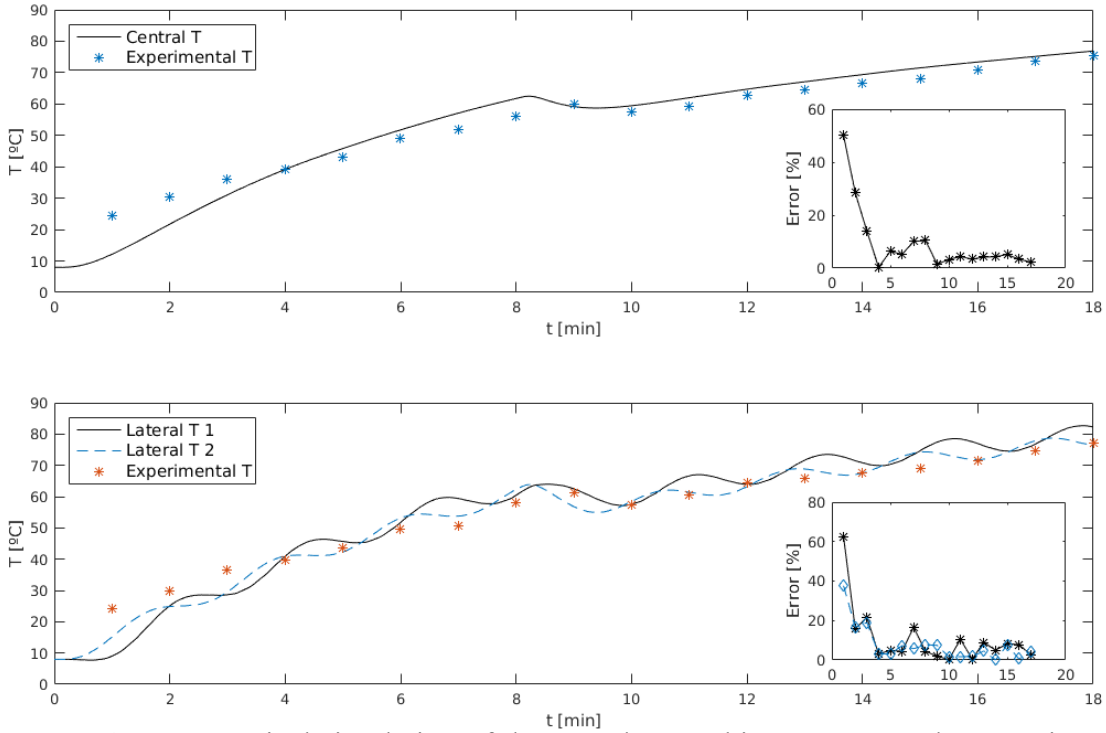

Figure 4.26. Numerical simulation of the complete cooking process and comparison to experimental data (vegetarian patty case).

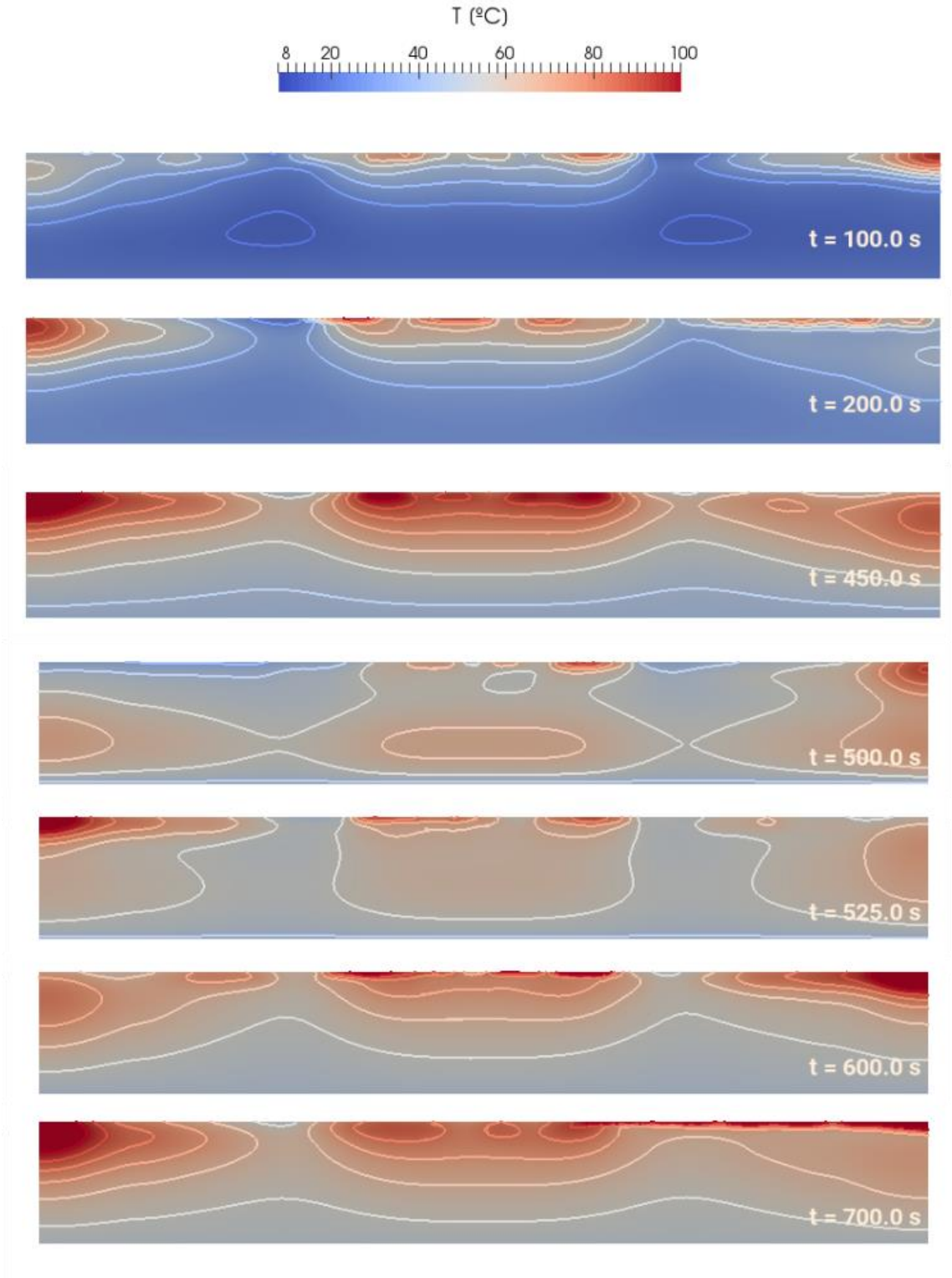

Figure 4.27. Evolution of temperature in a vertical cross-section of the vegetarian patty during cooking simulation.

CHAPTER 5

DISCUSSION

5. Discussion

Discussion of the results has been organized by product type to facilitate the comparison between the cooking effect of the different methods used in this thesis.

5.1. Discussion of beef burgers results

5.1.1. Cooking methods

The main characteristic of each cooking method is given by the heat transfer mechanisms involved in the heating of beef burgers.

CO_2 IR laser cooking can be considered as a purely radiative treatment, comparable to selective heating by IR radiation treatment, with a high electromagnetic IR radiation absorption by water, fats, carbohydrates (starches) and close to an area of maximum absorption peaks (9 μm) for lipids (Krishnamurty, 2008). The CO_2 IR laser Epilog equipments used in the first part of the thesis are industrial engraving and cutting equipments not originally designed for cooking. After a very long trial and error series of experiments, specific conditions of working operation adapted to cooking of food matrices were found. These conditions could be considered as unusual since beef burgers were cooked from upper pole to lower pole of the same side, and the cooking time was very long (12-14 mins per side) to guarantee cooking temperature >72°C inside burgers. Results showed that cooking with CO_2 IR laser Epilog equipments, a high uniformity in physico-chemical characteristics, a high consumer acceptance and the elimination of naturally present coliforms in meat could be achieved. Nevertheless, the level of inactivation of inoculated *Salmonella* was lower than the inactivation attained with other traditional systems.

IR Oven used an IR lamp and can be considered a mixed system as it combines IR radiation with fan convection and, also, some conduction effect from the grid, although with predominance of radiant action (Koutchma, 2017).

The BBQ Grill system can be considered a broiling system, since the meat is cooked by proximity to the radiant heat or "broiler." The meat is placed above the heat source and the heat radiates from one direction, so the meat must be turned during cooking. Broiling

can also be considered a combined system since the grid, where the burger is placed, transmits heat through conduction.

The Flat Grill system (also known as panbroiling system) is a conductive-based method due to the direct heat transmission from the metallic surface to the meat. Burgers must be turned frequently to prevent excessive surface browning or crust formation and to allow an even cooking. The pan or griddle should not be covered during panbroiling (AMSA, 2016).

In the second study, an innovative CO_2 IR laser system was developed and adapted to cook inside Foodini. This system allowed homogeneous cooking over the surface of beef burgers by irradiating a defined area using the fast movement of galvo mirrors, while the plate with the sample rotated to distribute heating. As for the cooking system used in the first study, a very long trial and method strategy was carried out to determine the most appropriate cooking conditions. With the CO_2 IR laser Foodini equipment, the cooking time was considerably reduced in comparison with the Epilog equipment, and it was closer to IR Oven system. Besides, the laser energy was completely focused on the food, hence avoiding the damage of internal mechanics or electronics of the 3D Printer. CO_2 IR laser Foodini system was able to guarantee safe cooking of beef burgers since a 6-log reduction of inoculated *Salmonella* and *E. coli* O157:H7 was achieved (FSAI, 2018), and the levels of analyzed PAHs were under the detection limit. Moreover, physico-chemical results showed that CO_2 IR Laser Foodini system was comparable to the traditional cooking methods used and it received a high level of acceptance from consumers.

5.1.2. Physico-chemical parameters

The decrease in moisture content after cooking was reflected in cooking loss values. Water losses did not result in a decrease in water activity, since the water content of cooked beef burgers was still very high. In both experiments, the protein, fat and ash content of cooked samples were higher than in raw samples because of the concentration effect caused by evaporative water losses.

In the case of the first study (with Epilog system), no differences were observed between cooking loss values or moisture content of cooked burgers whereas in the second study (with Foodini system), higher cooking losses were observed for Flat Grill treatment, in

comparison with IR Laser and IR Oven treatments. In Flat Grill, the highest cooking loss corresponded with the highest moisture content.

Cooking losses cannot be only attributed to water losses since fat is also lost during cooking of beef burgers, as indicated by Sheridan and Shilton (2002) and Ortigas-Marty et al. (2006) who found that cooking losses were mainly caused by water reduction, fat and some suspended solids. In our study, fat content expressed on dry basis of Flat Grill and BBQ Grill samples was lower in comparison with the rest of treatments. This result could be attributed to faster drip loses of fat, since it melts at 40°C, in comparison with water which needs more time to evaporate (Sheridan, 2002). Hence, the shorter cooking time of Flat Grill could lead to higher fat losses and lower moisture losses.

However, Dreeling *et al.* (2000) evaluated the effect of different cooking treatments on low-fat hamburgers (≈ 7.2% fat) and they observed that the cooking method did not affect the fat content of burgers. This fact could be motivated for the biggest size and weight of their burgers, which required a larger cooking time to reach 72°C inside the samples.

Sheridan and Shilton (1999) evaluated the efficiency of cooking burgers using two sources of IR with 2.7 μm and 4.0 μm of maximum wavelength peak and concluded that the samples cooked with 4.0μm had lower losses. Among other factors, they attributed that radiation with a length of 2.7μm penetrated the surface of food samples more efficiently, likely because of the preferential absorption spectrum of water in the surface at this wavelength. The difference in absorption at 2.7μm and 4μm in water is about 2 log units. In our study, we did not found differences in cooking losses caused by IR Oven lamps and IR Laser, and this could be attributed to the high absorptivity bands of water, both in IR Oven (~ 2.2 -3.2 μm) and in IR laser system (10.64 μm).

Sheridan and Shilton (2002) observed that in burgers with low fat content cooked with an IR oven, water was available in enough quantity during the cooking process to cool continuously the surface by evaporation of water. The migration of water through the surface seemed to prevent the formation of the surface crust. This would also be the case of the burgers cooked with IR laser and IR Oven laser, in which a clear formation of a crust was not observed either. Braeckman *et al.* (2009) studied the use of IR barbecue prior to convection cooking to investigate if a combined treatment could help to reduce fat and moisture losses through the formation of a crust. On the contrary to their initial

statement, they observed that losses of the first cooking stage were added to those of the second treatment.

Concerning texture, on one hand, the higher hardness values of samples cooked with IR Oven and IR laser-based systems suggest a possible relationship with the longer time of cooking, which would induce a higher protein denaturation of intramuscular collagen (reported to happen at 60-70°C) and structural changes in myofibrils (reported to happen at 68-80°C in actin) and cause toughening (Berhe *et al.* 2014). The shrinkage due to myofibrillar denaturation has been associated with hardness increase (Zzman, 2013; Domínguez-Hernández, 2018). On the other hand, the lower values of hardness and cutting force of samples cooked with Flat Grill and BBQ Grill could be influenced by a lower cooking time, which would induce less structural changes in proteins. Dreeling et al. (2000) studied the effect of different cooking methods of low-fat burgers, and the results obtained for TPA values (hardness and springiness) were similar to the results in our study, although they obtained higher cutting forces.

In both Epilog and Foodini studies, color of burgers changed significantly and accordingly to the cooking treatment of samples. Ground beef is manufactured from larger cuts of meat or trimmings from primal and sub-primals. When these materials are ground, oxygen is incorporated, and meat becomes bright with cherry red color due to oxymyoglobin formation (Claus, 2007). The internal and external a* color values (~ 15) of raw burgers confirms the oxidation of myoglobin. With an increase in temperature and cooking time the red pigmentation of myoglobin changes to metamyoglobin, thus, the red color of the raw meat becomes brown due the oxidation of the hemo group and the denaturation of globin from 60-75°C (Ranken, 2000; Christensen, 2012).

In Epilog study, comparable L* and a* values of internal color indicate that the cooking treatment had caused similar changes, except in burgers cooked with IR Laser 29, which had lower values of L* and higher values of a* than the rest of samples. This difference might be attributed to a shorter residence time at highest temperatures (>70°C) thus, causing less myoglobin denaturation. In Foodini study, IR Laser cooking rendered burgers with internal L* and a* values comparable to the burgers cooked with the other methods, suggesting that the heat transmission to center of all burger was similar and indicating an appropriate cooking performance of the new laser system.

Regarding the external color, samples cooked by IR Laser in the Epilog experiment were ones with the lowest total color difference with raw samples, whereas the contrary happened in the Foodini experiment. On one hand, this confirms the higher performance of IR Laser Foodini study than IR Laser 29 and 25 from Epilog study. Overall results of both studies showed that measured color values of burgers cooked with IR Laser treatments and IR Oven were close, which indicates that IR radiation on food surface leads to a similar heat process inside and outside beef burgers. Results show that the way or strategy in the application of IR laser is a key factor to control an optimal heating process. Although laser is based on a single beam, the radiation energy must be uniformly distributed over the entire food sample. DSC analysis of cooked and raw samples were performed to provide another indicator of the cooking efficacy of the methods compared in this study since the values of integrated peak areas correspond to the endothermic energy used for protein denaturation in beef burger samples. Results of both Epilog and Foodini studies showed that the energy applied for protein denaturation in raw meat was higher than the energy required for cooked samples, since proteins of cooked meat were already partially unfolded or denatured. No differences could be established between cooking treatments in terms of areas. However, peak temperatures of cooked burgers with IR Laser 29 and IR Laser 25 were closer to raw meat, which could indicate that changes induced by these treatments were less intense. Anyway, the interpretation of this result remains unclear as in Foodini study no differences in peak temperatures were found between raw and cooked samples. A typical thermogram of beef muscle has three endothermic peaks clearly differentiated which correspond to denaturation of myosin (54-58°C), collagen and sarcoplasmic proteins (65-67°C) and actin (80-83°C) (Wright *et al.*, 1977). Other authors place the endothermic peak of actin around 75-79°C (Xiong *et al.*, 1987; Sikes *et al.*, 2010). In the thermograms obtained in the present work only one peak located between 74 to 76°C was observed, which could be attributed to actin denaturation.

5.1.3. Sensory analysis

In the preference tests of the sensory analysis corresponding to Epilog study, consumers preferred indistinctly the burgers cooked with IR Laser 29, IR Laser 25, IR Oven, followed by the burgers cooked with BBQ Grill and the ones cooked with Flat Grill in the last position. In the preference test of Foodini study, burgers cooked by IR Laser were

the most preferred by consumers, followed by the group of burgers cooked by IR Oven and Flat Grill, and the last place was for burgers cooked with BBQ Grill. In general IR cooked burgers were identified as tenderer, juicier, with a lower level of doneness and less brown than BBQ and Flat Grill cooked burgers. The higher evaluation of tenderness and juiciness in intensity tests was translated into a significantly higher acceptability of burgers cooked with IR Laser and IR Oven cooking methods.

Results from instrumental analysis can contribute to explain the results obtained in the sensory tests. On the one hand, the higher fat content in burgers cooked with IR methods could increase the tenderness of the samples. Tenderness can also be associated with a longer cooking time between 60 and 70°C, which increases gelatinization of collagen and favor the solubilization of connective tissue leading to meat tenderization (Davey and Niederer, 1977; Zzaman, 2013). Results from the temperature evolution inside burgers cooked with IR Laser Foodini system show that time from 60 to 72°C took longer than time needed to reach 60°C. . The fact that consumers considered the burgers cooked with Flat Grill as harder and less juicy is probably related with their lower fat content and with crust formation on these burgers, due to the contact with a hot surface at 180°C which could imply overcooking on the surface of the sample.

Considering the results of sensory and instrumental analyses, most notable differences were found between burgers cooked with IR Laser treatments and Flat Grill method. Based on this, it is possible to state that burgers cooked with the IR Laser systems underwent a milder heating process, whereas burgers cooked with Flat Grill were subjected to a more intense treatment. These differences would be mainly related with the heat transfer mechanism, IR Laser being a pure radiative method and Flat Grill being pure conductive.

To understand differences between IR Laser methods used in this study, it must be taken in account that with the CO_2 IR Epilog laser system, CO_2 lamp radiates a very specific area of the sample for each given time, while the rest of the sample remains unheated. On the one hand, this method increases substantially the cooking time to achieve the internal target temperature (72°C) but, on the other hand, there are no overcooked surface areas. Besides, with the CO_2 IR Foodini laser system, the radiated zone is much wider, favoring a more homogeneous thermal treatment that reduces notably the cooking time and avoids overcooked areas.

5.1.4. Microbiological analyses

Microbiology results of the Epilog study indicate that burgers cooked with IR Laser 29 were not kept enough time at high temperature (72°C) to obtain a significant reduction in aerobic mesophilic bacteria counts or to eliminate the naturally present coliforms in meat. For this reason, they were excluded from the tests with inoculated *Salmonella*.

Results from inoculated samples cooked with IR Laser 25 indicate that this method still does not guarantee the safety of cooked burgers because it was not able to reduce the 6 log units stablished as a safety performance standard (FSAI, 2018) Moreover, in the tests with burgers inoculated at ~ 3 log units of *Salmonella*, IR Laser 25 was less effective than other cooking methods. Despite IR Laser 25 provided two more min of cooking time than IR Laser 29, the system of laser application (from upper pole to lower pole) did not provide a homogeneous heating treatment. This means that even if the temperature of 72°C was reached in the center of the beef burger, the time at this temperature was apparently too short.

Burgers cooked with BBQ Grill in the Epilog study did not reach the required reduction standard for both types of *Salmonella*. In both cases, due to the high survival of *Salmonella* in one of the six cooked burgers. This result indicates a high variability in the effects of this method, which could be influenced by the position of the burgers over the rack grill.

Microbiological results from Epilog study indicated two improvements that should be implemented in further studies: improvement of the heating process of IR Laser method to increase microbial inactivation, and reduction of variability associated to BBQ Grill treatment.

In the second study, carried out with the CO_2 IR laser Foodini system, this method caused lethalities in all inoculated pathogens that were comparable to the rest of cooking methods and accomplished the required reduction above 6 log units that guarantees the safety of the burgers.

Moreover, in this study, a tendency that can be also observed in Epilog study was reinforced: in general, IR Oven seemed to cause a higher lethality than the rest of methods. The highest inactivation effect of this method would be explained because

inside an IR Oven the heat flux is distributed and penetrates homogeneously all over the sample surface and it is able to keep constant high temperatures, according to Koutchma (2017).

Some authors have observed a high thermal resistance of *S.* Senftenberg (Mañas *et al.*, 2003). Results of Epilog and Foodini studies with burgers inoculated at ~ 3 log CFU/g, seem to confirm this point as *S.* Senftenberg survived in 37 out of 48 plates from sample enrichment whereas S. Typhimurium survived in 23 out of 48 plates.

5.1.5. PAHs analysis

Results of PAHs content in cooked burgers, which remained under the limit of detection for all treatments, show that CO_2 IR Foodini laser system did not overcook the burger surface. Thus, IR laser radiation was properly applied to cook burgers without surface burning degradation. These results agree with results from other studies with conventional cooking methods (*e.g.* grilling, roasting) where PAHs also remained under the limit of detection (Rose, *et al.*2015; Chen and Lin, 1997; Larsson *et al.*, 1983).

5.2 Discussion of pizza dough results

Pizza dough was cooked using both IR Laser systems studied in the present thesis. In CO_2 IR Laser Epilog system study, Finissima pizza (height: 3 ± 1 mm; diameter: 60 mm) was cooked with cooking conditions named as IR Laser 20. In CO_2 IR Laser Foodini system study, Tradizionale pizza (height: 5 ± 1 mm; diameter: 100 mm) was cooked with cooking conditions named as IR Laser.

In both studies, cooking loss was exclusively due to water evaporation since fat, protein and ashes content expressed on dry basis did not change between raw and cooked pizzas. The changes in moisture content of cooked pizzas caused a decrease in their water activity.

Cooking and water losses of pizzas cooked with both IR Laser systems were significantly lower than the losses of pizzas cooked with the other methods. These differences were caused because of the heating characteristics of the cooking methods used. IR Oven provided a continuous IR heating radiation over the entire surface of pizzas, combined with some convection effect. The deck oven used was an industrial equipment where

pizzas were placed over a heated stone and rapidly cooked by conduction. In Convection Oven, convection heating predominated combined with conduction effect. On the other hand, IR Laser 20 method cooked the Finissima pizza from pole to pole, and the IR radiation was not constantly applied over the whole pizza surface. In the studies with burgers, the effect of IR Laser Epilog and Foodini methods could be compared because cooked samples were identical. In the case of pizzas, performance of both methods could not be compared because of differences in the thickness of pizzas.

Regarding color results from Epilog study, L* values of first cooking side of pizzas cooked with IR Laser 20 were the lowest, indicating a darker surface. This browning surface effect was searched during the trial-error methodology applied to determine the cooking conditions for Finissima pizza. The objective was to use the laser beam to imitate the brown color and black spots found in traditionally cooked pizzas. In general, color values of Finissima pizzas cooked with the IR Laser 20 were significantly different with other treatments.

In Foodini study, L* values indicate that the browning effect obtained with IR Laser was comparable to the browning effect with IR Oven. The cooking methodology previously described in the material and methods section (with four Lissajous equations) was a strategy that searched two objectives: to bake the Tradizionale pizza and to provide surface browning. Indeed, the color values of the first cooking side of the Tradizionale pizza were very similar for IR Laser and IR Oven treatments whereas the color of the second side of samples cooked with IR Laser was different from the other cooking treatments.

Sensory analyses showed differences between the first and second study and between the IR laser treatments applied. Although, as stated, the results cannot be directly compared as pizza characteristics were quite different. In the first experimental study, Finissima pizzas cooked by IR Laser 20 were well evaluated in terms of the general appearance, which somehow indicated the acceptability of the external color by consumers.

The results of the sensory analysis of Foodini study were completely different. The most accepted and preferred samples where Tradizionale pizzas cooked with IR Oven. In this study, a conventional convection oven was used instead of the deck oven due to operational reasons. Low acceptability values and ranking position in preference test for

IR laser and Convection Oven might indicate that Tradizionale pizza were not appropriately baked with these methods, at least from the organoleptic point of view.

DSC analysis, which could be considered as an indirect measure of starch gelatinization and protein denaturation, show that Finissima pizzas cooked with IR Laser 20 treatment were well baked since the average peak area was highly reduced (>50%) in comparison with the raw pizza, and it was comparable to peak area obtained for IR Oven. In Foodini study, although the peak area of Tradizionale pizza cooked with IR Laser was significantly lower than the area of raw dough, its high values might indicate that the baking process was not complete.

Hence, considering sensory results, cooking losses and DSC peak areas of Tradizionale pizzas cooked with IR Laser treatment in Foodini study, it is possible to state that samples were not cooked as well as expected. Improvement of IR Laser cooking conditions to bake Tradizionale pizzas will be considered for future work. Probably, better results could have been obtained by baking a thinner and smaller pizza as Finissima with IR Laser Foodini system with, but the exploration of the current limits of the system is required in order to make improvements.

Anyway, Finissima pizza samples were well cooked using the CO_2 IR Epilog laser system, which demonstrate that CO_2 IR laser systems could be a new cooking method for baking pizzas and, also, other bakery products comparable to pizza dough.

5.3. Discussion of mashed potatoes bites results

Cooking losses experienced by mashed potatoes prepared with the different cooking methods changed accordingly to their moisture content. Moreover, since fat, protein and ashes content expressed on dry basis did not change between methods, it can be confirmed that samples were only subjected to water losses. Cooking losses of bites prepared with IR Laser 62 were above the 50% of cooking losses of bites prepared by IR Laser, and slightly higher than those of bites prepared with Traditional Method (cooked in microwave). Again, these differences might be explained by considering the heating characteristics of different cooking methods. On the one hand, IR radiation inside the oven covered completely the mashed potatoes surface, thus favoring a more intense surface evaporation transfer. Moreover, mashed potatoes bites were cooked over a dish,

which was also heated during the cooking process, providing a heat conduction flux through the glass which could increase cooking losses. On the other hand, the unusual cooking conditions provided by CO_2 IR Epilog laser, which heated from upper pole to lower pole of the sample, did not supply a constant heat flux over the whole surface. Additionally, the laser beam did not heat the glass where mashed potatoes bites were placed. Hence, cooking losses were lower. Finally, cooking losses in Traditional Method were driven by the water evaporation during the boiling process inside the microwave and remained low because it was the fastest method of preparation.

Results of compression force showed clear textural differences between treatments. Texture of mashed potatoes is mainly related to the starch gelatinization degree of dehydrated potatoes, where ungelatinized and gelatinized starch are usually present due to thermal energy input during the drum drying process. Both types of starch facilitate the pasting process between 50°C (gelatinized starch) and 60-65°C (Shiotsubo, 1984). The higher compression force of mashed potatoes bites cooked with the IR Oven could be related to the gelatinization of the initially ungelatinized starch and to a better hydration of the already gelatinized starch, due to the constant heat treatment conditions inside the oven. In the case of IR Laser-cooked samples, which had a higher compression force than those cooked with Traditional Method, gelatinization and hydration processes were also achieved, but with less intensity in comparison with IR Oven.

Color analyses also showed clearly the influence of each cooking method. Bites prepared with Traditional method were lighter since no surface treatment was applied. Bites cooked with IR Laser 62, had the lowest values of L*, which indicate a darker surface. This was due to small black spots found on the surface, which were considered a desired attribute when the laser cooking conditions were fixed, in order to imitate the browning effect of grilling inside an oven. IR Oven also showed a surface browning effect although fewer black spots were obtained.

Sensory analysis showed that consumers preferred mashed potatoes cooked by IR surface treatments. This preference was not based on the external color, since no significant differences were observed on the general appearance neither in the acceptability of the external and internal color (although consumers did observe differences in their intensities). Preference for IR radiation methods was probably related to the harder texture and the higher taste intensity. Increase in the intensity of both parameters would be due

to higher water losses, which caused a higher concentration of solid components. In the case of taste, probably an increase of salty taste was perceived. Although consumers did not found differences in flavor, likely due to an unclear comprehension or to an inappropriate explanation of the attribute, the perceived better taste was probably linked to flavors from Maillard reactions generated by radiation heating.

To sum up, IR Oven and IR Laser 62 caused similar cooking effects, according to perception of consumers. Nevertheless, there were differences in physico-chemical instrumental parameters between both methods. It can be hypothesized that if mashed potatoes bites were cooked with CO_2 IR Laser Foodini system they would have shown physico-chemical characteristics closer to bites cooked with IR Oven. The high amount of water and starch in mashed potatoes facilitates the IR surface heating process, due to the high absorbance of water and starch at both IR wavelengths applied.

5.4. Discussion of vegetarian patty results

Proximate analysis showed that differences in the final composition of cooked vegetarian patties were due to water loss. IR Oven caused the highest cooking and water losses but the fat, protein and ashes contents on dry basis of samples cooked by this method were not different from those of samples cooked by other methods. This data indicated that IR Oven was the most intense treatment, favoring a large surface evaporation. Flat Grill caused around 50% fewer losses than IR Oven did, probably because conduction is a faster heating process and it generated less water loss. Cooking losses caused by IR Laser were between those of previously mentioned treatments. Hence, IR Laser could be considered a less intense radiative treatment due to the cooking conditions, as burgers were cooked side per side and IR radiation, even it was applied homogeneously, did not cover the entire surface simultaneously.

Values of cutting force were not affected by cooking methods. Probably, the fact that the main ingredients (*i.e.*, chickpeas and lentils) were already cooked, reduced the influence of cooking methods on textural attributes. Nevertheless, the cooking process could still affect other ingredients in the patty (*e.g.*, raw vegetables, egg, flour, potato) but it seems that heat provided by the different cooking methods induced similar effects on them (*e.g.*, egg protein denaturation and starch gelatinization). This hypothesis is reinforced by the

results of internal color of patties, because no differences were found between samples subjected to different cooking treatments.

On the contrary, the external color of vegetarian patties did show the influence of the heat flux due to radiative or conductive methods. External vegetarian patties cooked with Flat Grill had a higher L* which indicated that the surface was darker. Moreover, it was possible to observe some degree of overcooking due to the high temperature of the grill surface (180°C). IR Oven and IR Laser also generated a slight, and more homogeneous, surface browning.

Sensory tests showed that consumers preferred vegetarian patties cooked with Flat Grill and IR Laser, followed by IR Oven. Differences between treatments came from two attributes already described in the discussion of physico-chemical analyses: water content and external color. Consumers found that burgers cooked with Flat Grill were juicier. Besides, the darker color of their surface was better accepted. Maybe, the overcooked areas in vegetarian patties influenced consumers positively due to its similarity with cooked meat burgers. IR Laser rendered an external color in patties that was better accepted than the external color caused by IR Oven cooking, likely, because the way of application of IR laser system was less intense and the drying surface effect was lower. Absence of differences in intensity and acceptability of doneness and crunchiness would confirm that heating processes affected the textural attributes in a similar way.

Microbiological results showed that IR Laser cooking provided a safe cooking temperature inside vegetarian patties (>72°C) because, in samples inoculated with ~7 log CFU/g of *S.* Typhimurium and *S.* Senftenberg, the level of count reduction was above 6-log for both types of *Salmonella*. The inactivation achieved by IR Laser was comparable to the inactivation achieved by IR Oven. Complete inactivation, even of *S.* Senftenberg, was only accomplished by cooking with Flat Grill. As in the case of burgers, survival results from samples inoculated at ~ 3 log CFU/g seemed to indicate a slightly higher resistance of *S.* Senftenberg compared with *S.* Typhimurium.

Overall results showed that the CO_2 IR Laser Foodini system was able to cook properly the vegetarian patties, rendering physico-chemical characteristics and sensory attributes comparable, or even more accepted by consumers, to standard cooking systems.

Moreover, the laser system guaranteed an appropriate thermal treatment to eliminate pathogens, thus ensuring a high degree of food safety.

5.5. Discussion of the numerical simulation results

Numerical method was in a high accordance with the experimental values for burgers and for vegetarian patties (figures 4.23 and 4.26). Different variable cooking parameters, such as, food components, the different radiative, conductive and convective heating processes and the fact that burgers were turned to cook both sides consecutively, were well integrated in the model.

Simulated temperatures of the first three or four minutes were lower than experimental measures. This could be related with the initial fat and water loss dripping from the areas near the heated surface towards the centre of food samples (where the experimental temperatures where measured). Liquefied beef fat (which melts at 40°C) mixed with water would descend from the heated top surface to the center of burgers through the cavities that were observed in the cross-sectional burger images (figure 4.14). This dripping effect would affect the experimental measures mainly during the first three or four minutes, and this effect would decrease once the sample was already more homogeneously heated, losses were mainly due to water evaporation through the surface, and there was an overall temperature increasing inside the cooked sample. Actually, differences between the model and experimental data during the first cooking minutes were more clearly observed in beef burgers, maybe mainly due to fat dripping, since raw vegetarian patty was viscous dough and almost no losses of liquid water or liquefied fat were observed in any cooking treatment.

We can considerer also this model as a conservative approach since simulation values are usually lower or slightly above the experimental temperature, especially from 60°C. This fact has been used as an initial statement for the numerical model, with the objective that simulated pasteurization temperatures will be close to the experimental values. Hence, it was possible to better evaluate a simulated thermal effect, for example, regarding count reduction or survival of pathogenic bacteria. The iso-lines of the temperature evolution of a cross-section sample during the heating process (figures 4.24 and 4.27) could be use to evaluate several physico-chemical, sensory, microbiological and toxicological aspects.

The numerical simulation tool will be used to optimize and develop the CO_2 IR laser system. The model will be used to simulate the cooking process with different parametric conditions that will help to improve the design and equipment of the cooking method. Simulations would simplify and guide the experimental work and would also save time and material costs.

CHAPTER 6

CONCLUSIONS

6. Conclusions

The CO_2 IR laser Epilog equipment demonstrated that food could be cooked using a CO_2 IR laser if the overall cooking conditions allowed an appropriate radiation over the food surface. Physico-chemical and sensory characteristics of beef burger, pizza dough and mashed potatoes bites cooked with CO_2 IR Epilog laser were comparable to standard cooking methods, but microbiological results showed that this method must be improved to guarantee food safety.

The CO_2 IR laser Foodini system was specially designed to increase the delivery of infrared radiation to the food surface. Results of physico-chemical, sensory, microbiological and toxicological analyses of beef burger and vegetarian patties cooked with this new CO_2 IR laser Foodini system were comparable to those of beef burger and vegetarian patties cooked with standard methods. However, conditions to cook pizza must be improved.

CO_2 IR laser cooking system shares some cooking characteristics with the IR oven used in the present study, as both are based on an IR radiation heating process using wavelengths which are highly absorbed by water.

The numerical results for temperature evolution given by the model coincide with the experimental data, except for the first minutes of cooking. The numerical simulation model is a powerful tool to optimize the cooking process of the CO2 IR laser system developed in the present study. This model will be used to simulate the cooking process with different parametric conditions and will help to design the future experimental work and improvements.

IR CO_2 laser Foodini system can be integrated in a 3D printer to cook during the printing process or to cook once the food is printed.

CHAPTER 7

REFERENCES

7. References

AMSA. 2016. Research guidelines for cookery, sensory evaluation, and instrumental tenderness measurements of meat. Chicago, IL: American Meat Science Association and National Live Stock and Meat Board

ASHRAE. (2006). ASHRAE Handbook of Refrigeration SI.

Abdul-Kadir, Bargman, T., Rupnow, J. 1990. Effect of infrared heat processing on rehydration rate and cooking of Phaseolus vulgaris (var. Pinto). J. Food Sci. 55(5), 1472–1473.

Abe, T., Afzal, T.M., 1997. Thin-layer infrared radiation drying of rough rice. J. Agric Eng. Res. 67, 289–297.

Afzal, T.M., Abe T., 1998. Diffusion in potato during far infrared radiation drying. J. Food Eng. 37(4), 353–365.

Arntfield, S.D., Scanlon, M.G., Malcolmson, L.J., Watts, B.M., Cenkowski, S., Ryland, D, Savoie, V. 2001. Reduction in lentil cooking time using micronization: comparison of 2 micronization temperatures. J. Food Sci. 66(3), 500–505.

Berhe, D. T., Engelsen, S. B., Hviid, M. S., & Lametsch, R. (2014). Raman spectroscopic study of effect of the cooking temperature and time on meat proteins. Food Research International, 66, 123–131.

Blutinger, J.D., Meijers, Y., Chen, P.Y., Zheng, C., Grinspun, E., Lipson, H., 2018. Characterization of dough baked via blue laser. J. Food Eng. 232, 56-64.

Burgheimer, F., Steinberg, M.P., Nelson, A.I. 1971. Effect of near infrared energy on rate of freezedrying of beef spectral distribution. J. Food Sci. 36(l), 273–276.

Chen, B.H., Lin, Y.S., 1997. Formation of polycyclic aromatic hydrocarbons during processing of duck meat. J. Agric. Food Chem. 45, 1394–1403.

Christensen, L.M. 2012a. Evaluation of textural properties of cooked beef batters. California Polytechnic State University. San Luis Obispo, CA, USA.

Chua, K.J., Chou, S.K. 2005. A comparative study between intermittent microwave and infrared drying of bioproducts. Int. J. Food Sci. Technol. 40, 23–39.

Claus, J.R. 2007. Color Changes in Cooked Beef. University of Wisconsin-Madison, Beef Research, USA.

Dagerskog, M. 1979. Infra-red radiation for food processing II. Calculation of heat penetration during infra-red frying of meat products. Lebens. Issen. Technol. 12(5), 252–257.

Das, I., Das, S.K., Bal, S. 2004. Drying performance of a batch type vibration-aided infrared dryer. J. Food. Eng. 4, 129–133.

Davey, C. L., & Niederer, A. F. (1977). Cooking tenderizing in beef. Meat Science, 1, 271–276.

Decareau, R.V. 1985. Microwaves in the food processing industry. Orlando, Fla.: Academic Press.

Dostie, M., Seguin, J.N., Maure, D., Tonthat, Q.A., Chatingy, R. 1989. Preliminary measurements on the drying of thick porous materials by combinations of intermittent infrared and continuous convection heating. In: Mujumdar, A.S., Roques, M.A., Ed. Drying'89. New York: Hemisphere Press.

Dreeling, P., Allen, P., Butler, F. (2000). Effect of cooking method on sensory and instrumental texture attributes of low-fat beefburguers. Lebensmittel Wissenschaft und Technologie, 12, 325-329

Fisher, J. C., 1993. Qualitative and quantitative tissue effects of light from important surgical lasers. Laser Surgery in Gynecology: A Clinical Guide. 58–8

FSAI (Food Safety Authority of Ireland). 2018. An investigation of the most appropriate z-value to be used in calculating "equivalent cooks" for beef burgers in food business establishments. Dublin: Food Safety Authority of Ireland.

Gabel, M.M., Pan, Z., Amaratunga, K.S.P., Harris, L.J., Thompson, J.F. 2006. Catalytic infrared dehydration of onions. J. Food Sci. 71(9) E ,351–357.

Galindo, F.G., Toledo, R.T., Sjoholm, I. 2005. Tissue damage in heated carrot slices. Comparing mild hot water blanching and infrared heating. J. Food Eng. 67, 381–385.

Hagen, W., Drawert, F. 1986. Determination of water content by infrared. Monatsschrift Brauwissenschaft 40(6), 240–246.

Halford, R.S. 1957. The influence of molecular environment on infrared spectra. Ann New York Acad. Sci. 69, 63–69.

Hashimoto, A., Takahashi, M., Honda, T., Shimizu, M.,Watanabe, A. 1990. Penetration of infrared radiation energy into sweet potato. Nippon Shokuhin Kogyo Gakkaishi. 37(11), 876–893.

Hashimoto, A., Sawai, J., Igarashi, H., Shimizu, M. 1992b. Far-infrared irradiation effect on pasteurization of bacteria on or within wet-solid medium. J Chem Eng Japan 25(6),666–671.

Hashimoto, A., Sawai, J., Igarashi, H., Shimizu, M. 1993. Irradiation power effect on pasteurization below lethal temperature of bacteria. J Chem Eng Japan 26(3), 331–333.

Hashimoto, A., Yamazaki, Y., Shimizu, M., Oshita, S. 1994. Drying characteristics of gelatinous materials irradiated by infrared radiation. Drying Technol, 12,1029–1052.

Hideki, Asano "Food Cooking Apparatus" Japanese Patent Publication No. JP2002147762A2, published on May 22, 2002.

https://en.wikipedia.org/wiki/List_of_laser_types (Accessed: 6 May 2018)

Huang, L., Sites, J. 2008. Elimination of *Listeria monocytogenes* on hotdogs by infrared surface treatment, Journal of food science, 73(1), 27-31

Hunter, J.D. 2007. Matplotlib: A 2D graphics environment. Computering in science & engineering. 9(3), 90-95

Jun S. 2002. Selective far infrared heating of food systems [PhD dissertation]. Pa.: The Pennsylvania State Univ.

Kebes. 2008. https://commons.wikimedia.org/wiki/File:Absorption_spectrum_of_liquid_water.png (Accessed: 9 August 2018)

Khan, M.A., Vandermey, P.A. 1985. Quality assessment of ground beef patties after infrared heat processing in a conveyorized tube broiler for foodservice use. J. Food Sci., 50, 707–709.

Kiyoshi, Terakubo "Laser Cooking Device" Japanese Patent Publication No. JP63003131A2, published on Jan. 8, 1988.

Koutchma, T., Application of infrared and light-based technologies to meat and meat products. In: Emerging Technologies in Meat Processing: Production, Processing and Technology. Ed. Cummins, E.J. and Lyng, J.G. JohnWiley and Sons, Ltd. 2017

Kramer, A., Kahan, G., Cooper, D., Papavasiliou, A. 1974. A nonparametric ranking method fort the statistical evaluation of sensory data. Chem Senses Flavor.,1, 121–133.

Krishnamurthy, K., Khurana, K.H., Jun, S., Irudayaraj, J., Demirci, A. 2008. Infrared Heating in Food Processing: An Overview. CRFSFS. 7: 2-13.

Krishnamurty, K., Khurana, H. K., Jun, S., Irudayaraj, J. M., Demirci, A. Infrared Radiation for Food Processing. In: Food Processing Operations Modeling: Design and Analysis. (2nd Ed.). Ed. Jun, S., Irudayaraj, J.M. CRC Press. Taylor & Francis Group, LLC. 2009

Larsson, B.K., Sahlberg, G.P., Eriksson, A.T., Busk, L.A., 1983. Polycyclic aromàtic hydrocarbons in grilled food. J. Agric. Food Chem. 31, 867–873.

Lentz, R.R., Pesheck, P.S., Anderson, G.R., DeMars, J., Peck, T.R., inventors; The Pillsbury Co., assignee, April 16 1995. Method of processing food utilizing infra-red radiation. U.S. patent 5, 382,441.

Luikov, A.V. 1975. Systems of differential equations of heat and mass transfer in capillary-porous bodies. International journal of heat and mass transfer, 18, 1-14

Mañas, P., Pagán, R., Álvarez, I., Condón, S, 2003. Survival of Salmonella senftenberg 775W to current liquid whole egg pasteurization treatments. Food microbiology, 20(5), 593-600

Masamura, A., Sado, H., Nabetani, H., Nakajima, M. 1988. Drying of potato by far-infrared radiation. Nippon Shokuhin Kogyo Gakkaishi 35(5), 309–314.

McCurdy, S.M. 1992. Infrared processing of dry peas, canola, and canola screenings. J. Food Sci. 57(4), 941–944.

Midilli, A., Kucuk, H., Yapar, Z.. 2002. A new model for single-layer drying. Drying Technol. 20(7), 1503–1513.

Mongpreneet, S., Abe, T., Tsurusaki, T.. 2002. Accelerated drying of welsh onion by far infrared radiation under vacuum conditions. J. Food Eng. 55, 147–156.

Muchnik, Boris. "Laser Cooking Apparatus" U.S. Pat. Publication No. US 20080282901, published on Nov. 20, 2008.

Muriana, P., Gande, N., Robertson, W., Jordan, B., Mitra, S. 2004. Effect of prepackage and postpackage pasteurization on postprocess elimination of Listeria monocytogenes on deli turkey products. J, Food Prot. 67(11), 2472–2479

Navari, P., Andrieu, J., Gevaudan, A. 1992. Studies on infrared and convective drying of nonhygroscopic solids. In: Mujumdar AS, editor. Drying 92. Amsterdam: Elsevier Science. p 685–694.

Nowak, D., Levicki, P.P. 2004. Infrared drying of apple slices. Innov. Food Sci. Emerg. Technol., 5, 353–360.

Olsson, E.E.M., Tr¨ag°ardh, A.C., Ahrn´e, L.M. 2005. Effect of near-infrared radiation and jet impingement heat transfer on crust formation of bread. J. Food Sci. 70(8), E 484–491.

Ortigues-Marty, I., Thomas, E., Prévéraud, D.P., Girard, L.C., Bauchart, D., Durand, D.,Peyron, A. 2006. Influence of maturation and cooking treatments on the nutritionalvalue of bovine meats: Water losses and vitamin B12. *Meat Sci.,* 73: 451-458.

Patankar, S. (1980). *Numerical Heat Transfer and Fluid Flow.* CRC Press.

Patel, C. K. N., 1964. Continuous-Wave Laser Action on Vibrational-Rotational Transitions of CO2. Physical Review. 136 (5A): A1187–A1193

Perez, M.G.R., Calvelo, A. 1984. Modeling termal conductivity of cooked meat. Journal of food science, 49, 152-156.

Phang, HO.S., Bruhn, C.M. 2011. Burger Preparation: What Consumers Say and Do in the Home. J. Food Protect., 74: 1708–1716.

Pope, R.M., Fry, E.S., 1997. Absorption spectrum (380e700 nm) of pure water II Integrating cavity measurements. Appl. Optic. 36 (8710).

Ranjan R, Irudayaraj J, Jun S. 2002. Simulation of three-dimensional infrared drying using a set of three-coupled equations by the control volume method. Trans ASAE 45(5), 1661–1668.

Rose, M., Halland, J., Dowding, A., Petch, S., White, S., Fernandes, A., Mortimer, D. (2015). Investigation into the formation of PAHs in foods prepared in the home to determine the effects of frying, grilling, barbecuing, toasting and roasting. Foods and chemical toxicology, 78, 1-9

Rosenthal I. 1992. Electromagnetic radiations in food science. Berlin, Heidelberg: Springer-Verlag.

Sakai, N., Hanzawa, T., 1994. Applications and advances in far-infrared heating in Japan. Trends Food Sci. Technol., 5, 357–62.

Sandu, C. 1986. Infrared radiative drying in food engineering: a process analysis. Biotechnol Prog 2(3), 109–19.

Sargolzaei, J., Abarzani, M., Aminzadeh, R., 2011. Modeling and Simulation of Hamburger Cooking Proces using Finite Difference and CFD Methods. Int. J. Chem., 2(1), 52-62.

Sawai, J., Nakai, T., Hashimoto, A., Shimizu, M. 2004. A comparison of the hydrolysis of sweetpotato starch with b-amylase and infrared radiation allows prediction of reducing sugar production. Int. J. Food Sci. Technol. 39, 967–974.

Sharma, G.P, Verma, R.C., Pathare, P.B. 2005. Thin-layer infrared radiation drying of onion slices. J. Food. Eng., 67, 361–366.

Sheridan, P., Shilton, N. 1999. Application of far-infrared radiation to cooking of meat products. J. Food Eng., 41, 203–208.

Sheridan, P., Shilton, P. (2002). Analysis of yield while cooking beefburguer patties using for infrared radiation. Journal of food engineering, 51, 3-11

Sheridan, P., Shilton, P. (2002). Determination of the thermal diffusivity of ground beef patties under infrared radiation oven-shelf cooking. Journal of food engineering, 52, 39-45

Shewchuk, J. R. (1994). An introduction to the conjugate gradient method without the agonizing pain. Pittsburgh, Pa. :School of Computer Science, Carnegie Mellon University, 1994. Print. https://www.cs.cmu.edu/~quake-papers/painless-conjugate-gradient.pdf (Accessed: 20 December 2018)

Shilton, N., Mallikarjunan, P., Sheridan, P. (2002). Modeling of heat transfer and evaporative mass losses during the cooking of beef patties using far-infrared radiation. J. Food Eng., 55, 217-222

Shiotsubo, T. 1984. Gelitinization temperature of potato starch at the equilibrium state. Agric. Biol. Chem., 48 (1), 1-7

Sikes, A., Tornberg, E., Tume, R. 2010. A proposed mechanism of tenderising post-rigor beef using high pressure–heat treatment. Meat Sci., 84: 390-399.

Silfvast, William T. Laser fundamentals, Cambridge University Press, 2004. ISBN 0-521-83345-0

Singh, Inderjit "Method and apparatus for plasma assisted laser cooking of food products". US Pat. Publication No. 20130344208 A1, published on Mar. 11, 2013.

Skjoldebrand, C. 1979. Some aspects on frying of meat products in a forced convection oven. Lebensmittel Wissenschaft und Tecnologie, 12, 325-329

Skjoldebrand, C. 2001. Infrared heating. In: Richardson P, editor. Thermal technologies in food processing. New York: CRC Press.

Tanaka, F., Verboven, P., Scheerlinck, N., Morita, K., Iwasaki, K., Nicolaı, B. 2007. Investigation of far infrared radiation heating as an alternative technique for surface decontamination of strawberry. J. Food Eng., 79, 445–452

Togrul, H. 2005. Simple modeling of infrared drying of fresh apple slices. J. Food Eng. 71, 311–323.

Turner, I.W., Perre, P. 1996. A synopsis of the strategies and efficient resolution of techniques used for modeling and numerically simulating the drying process. In: Mathematical modeling and numerical techniques in drying technology. New York: Marcel Dekker Inc. p 1–82.

Vogel, A., Venugopalan, V., 2003. Mechanisms of pulsed laser ablation of biological tissues. Chem Rev. 103 (2), 577–644. doi:10.1021/cr010379n. PMID 12580643.

www.aesculight.com/why-aesculight/wavelength/ (Accessed: 21 October 2018)

www.engineeringtoolbox (Accessed: 15 November 2018)

www.fda.gov/Food/ResourcesForYou/HealthEducators/ucm082294.htm (Accessed: 15 January 2019)

www.laserproject.es (Accessed: 20 December 2018)

www.naturalmachines.com (Accessed: 14 September 2018)

www.perten.com/Publications/Articles/Potato-flakes/ (Accessed: 21 January 2019)

www.rp-photonics.com/co2_lasers.html (Accessed: 20 January 2019)

Wright, D. J., Leach, I. B., Wilding, P. 1977. Differential scanning calorimetric studies of muscle and its constituents. J. Sci. Food Agric., 28: 557.

Xiong, Y.L., Brekke, C., Leung, H.K. 1987. Thermal Denaturation of Muscle Proteins From Different Species and Muscle Types as Studied by Differential Scanning Calorimetry. Food Sci., 20: 357-362.

Yildiz, T.G., Icier, F., Kor, G. 2016. Influence of infrared final cooking on color, texture and cooking characteristics of ohmically pre-cooked meatball. Meat Sci, 114, 46-53

Zzaman, W., Chantrong, P., Idrus, N.F.M., Yang, T.A., (2013). Effect of different cooking methods on the quality attribute of beef burguers. Journal of applied sciences research, 9 (4), 2538-2547.